CHARACTERIZATION AND HYDROGEOCHEMISTRY OF AQUIFER SYSTEMS IN CRYSTALLINE BASEMENT WITHIN LILONGWE, MALAWI

MASTER OF SCIENCE DEGREE IN WATER RESOURCES MANAGEMENT AND DEVELOPMENT THESIS

DANIEL FRED KILEMBE

MZUZU UNIVERSITY

JULY 2024

CHARACTERIZATION AND HYDROGEOCHEMISTRY OF AQUIFER SYSTEMS IN CRYSTALLINE BASEMENT WITHIN LILONGWE, MALAWI

DANIEL FRED KILEMBE
Bachelor of Science (Earth Science)

A THESIS SUBMITTED TO THE FACULTY OF ENVIRONMENTAL SCIENCES OF MZUZU UNIVERSITY IN FULFILMENT OF THE REQUIREMENTS FOR THE AWARD OF A MASTER OF SCIENCE DEGREE IN WATER RESOURCES MANAGEMENT AND DEVELOPMENT

MZUZU UNIVERSITY

JULY 2024

DECLARATION

I hereby declare that this thesis titled, "*Characterization and Hydrogeochemistry of Aquifer Systems in Crystalline Basement within Lilongwe, Malawi*" has been written by me and is a record of my research work. All citations, references, and borrowed ideas have been duly acknowledged. It is being submitted in fulfilment of the requirements for the award of the degree of Master of Science Degree in Water Resources Management at Mzuzu University. None of the present work has been submitted previously for any degree or examination in any other University.

Daniel Fred Kilembe Date……

Name of STUDENT

Signed……. Date……

CERTIFICATE OF COMPLETION

We, the undersigned, certify that this thesis is a result of the author's work and that to the best of our knowledge, it has not been submitted for any academic qualification within Mzuzu University or elsewhere. The thesis is acceptable in form and content, and that satisfactory knowledge of the field covered herein was demonstrated by the candidate through an oral examination held on…….....

Signature:

…….……...Date…….

Major Supervisor and Postgraduate Coordinator: Dr. Russel Chidya (Ph.D.)

Signature:

……...……...Date……...

Co-Supervisor: Associate Professor Maurice Monjerezi (Ph.D.)

Signature:

……...……...Date……...

Head of Department: Dr. Brighton Chunga (Ph.D.)

DEDICATION

This accomplishment is dedicated to Berness Mary Chisumira (my late mum) and My Dad Darwin Fred Stanford Kilembe, my wife, daughters Tehillah and Talia, my dear sisters (Olive, Mary, Fayinala, Costance, Grace and Linnie), Major Harry Soko (Retired) and Diana Soko (Nee Chisumila) and Family, Chawanangwa Soko and Family, cousins, and friends whose financial and moral support has pushed me to achieve all I have today. I am truly grateful. I also thank the rest of my family for always being there for me.

ACKNOWLEDGEMENT

First, I thank the Almighty God for the gift of life, strength and wisdom that enabled me to accomplish my research project. With profound gratitude and great humility, I would like to acknowledge my supervisors Dr. Russel Chidya and Associate Professor Maurice Monjerezi who took their time to provide me with valuable information, guidance and mentorship towards the completion of this work. I am thankful to the Lilongwe Water Board (LWB) particularly Project Assistant Engineer Emma Mwale, for offering me the technical assistance to my research work.

Special thanks to the technical expertise of Blessings Mudzingwa and Ngonidzashe Isaac Tobani of Groundwater Mineral Services (GMS) and Eng. Thomas Mkangama of HydroConsult.

Lastly, I thank my family members, fellow course mates and friends for their patience and moral support throughout my academics. I owe you a large debt of gratitude and I love you so much.

ABSTRACT

Ever-increasing population and the rapid increase in the development of Lilongwe City has led to high increase in water demand. Understanding the complexity of the hydrogeochemical process, which controls the variability of the groundwater composition, is vital in groundwater resource management for both scientific community and policy makers. This study characterized deep aquifers and defined hydrogeochemistry with hydrogeological settings within crystalline basement complex rocks of Lilongwe. Study is an quantitative research design which used an experimental research approach using both purposive sampling in 21 deep wells and simple random sampling on 50 shallow wells to collect groundwater samples. Due to microbial analysis requirement only shallow well samples were used for microbial analysis since deep wells could meet the required time of sampling duration of within 24 hours of collection. Statistical analysis was done using IBM SPSS, chemical plots was done using Aquachem 14 and spatial maps was done using ArcGIS. Aquifers were characterized into fractured aquifers and weathered aquifer. Fractured aquifers have of low to high yield and transmissivity of low to medium. Weathered aquifers have very high yield and very high transmissivity. Aquifers are defined by the concentration of Ca^{2+}-$HCO3^{-}$, indicating influence of recharge through rainfall. Presence of Na^{+} and SO_4^{2-} shows mixing of this fresh groundwater with older water. Aquifer chemistry is controlled by the precipitation of oversaturated minerals with increasing TDS, ion exchange and simple dissolution. Deep fractures are spatially related to the dominance of Na+ and SO_4^{2-}, shows presence of deep percolation and dominance of Ca^{2+}, Mg^{2+} and HCO_3^{-} relates to shallow fractures. Ca-HCO_3 is the most dominant water type among; Na-K-Cl-SO_4, Na-K-Cl-SO_4 and Ca-SO_4. Dominance Ca-HCO_3 water shows presence of recently recharged groundwater within basement aquifers. Groundwater flow system within the basement aquifers occurs in; local, intermediate and regional. Local groundwater flow system is associated with weathered zone. Intermediate system occurs in both the weathered and fractured zones. Regional groundwater flow system is deep, occurring mainly in the deep fractured basement aquifer. All groundwater chemical parameters were within the recommended standard of MBS 2017 and WHO 2018 standard for domestic use. Basement aquifers are within the FAO 1994 irrigation water index requirement for irrigation use.

Key Words: Basement, aquifer, dissolution, transmissivity and fractured.

LIST OF ABBREVIATIONS AND ACRONYMS

ANOVA	Analysis of Variance
DEM	Digital Elevation Model
FAO	Food and Agriculture Organization
GCS	Council for Geosciences
HCA	Heirchical Cluster Analysis
ITCZ	Intertropical Convergence Zone
IWRM	Integrated Water Resource Management
MAR	Magnesium Adsorption Ratio
MBS	Malawi Bureau of Standards
MH	Magnesium Hazard
NA%	Sodium Percentage
PCA	Principal Component Analysis
PI	Permeability Index
RSC	Residual Sodium Carbonate
SAR	Sodium Adsorption Ratio
SADC	Southern Africa Development Community
UTM	Universal Transverse Mercator
WHO	World Health Organization
WRA	Water Resource Area
WRU	Water Resource Unit

TABLE OF CONTENTS

LIST OF TABLES

LIST OF FIGURES

CHAPTER ONE: INTRODUCTION

1.1 Background

Groundwater represents 30% of the world's freshwater resource (Poeter et al. 2020) and provides almost 36% of drinking water, 40% of agricultural irrigation, and 24% of industrial use worldwide (Berghuijs et al. 2022). In Africa, groundwater is the largest, most reliable, and convenient source (Alilouch et al. 2017) of potable water to supplement the ever-increasing demand for water supply. In Malawi, 61.7% of the total population and 71.03% of the population of the Capital City, Lilongwe, depends on groundwater for domestic use (National Statistical Office 2019).

Groundwater occurrence and flow in basement complex rocks are confined in the weathered and fractured zone in phreatic conditions and semi-confine conditions (Fetter 2018). The weathered zone contains aquifers with different variation of yields and occurs in shallow depth, however fractured aquifers are high yielding and mostly associated with deep seated fault (Lachassagne et al. 2021). The heterogeneous nature of these basement aquifers requires a better characterization and quantification at local and regional level for better groundwater management (Makungo et al. 2021). Though weathered aquifers have been the most reliable rural groundwater supply, over exploitation due to rapid population has affected their reliability for rural water supply (González et al. 2021). According to Kang et al. (2019), due to their high yield, the deep fractured aquifers are an increasingly valuable resource in arid areas, during droughts, and in water-stressed regions but studies of this resource are limited. As such it is vital to evaluate deep groundwater quality and quantity for the purposes of protection and potential use.

Groundwater compositional properties are defined by hydrogeochemical processes of solutions or precipitation of solid minerals, reduction and oxidation compounds, solution or evolution of gases, sorption or ion exchange, pollution, leaching fertilizers or manure, and mixing of different waters (Tikhomirov 2016). Hydrogeochemical processes depend on water and rock interaction, atmospheric inputs, inputs of chemicals by human activities, precipitation, geological structure, and mineralogy of aquifers (Blanchette et al. 2013). Wali, Alias & Harun (2020) describe geochemical reactions as the main contributors to variation in elemental concentrations in the groundwater.

The concentrations of major ions of groundwater are key in finding out the intensity of water-rock interaction as well as chemical reactions (Apollaro et al. 2021). Hence understanding water-rock interaction and associated reactions are vital in defining the variability of groundwater chemistry (Blanchette et al. 2013). Some studies have found that a high salinity in the groundwater comes from mineral dissolution and cation exchange, both in the water-rock interaction during water infiltration and groundwater horizontal flow within the aquifers in Southeast China (Liu, Li & Hu 2013). Blanchette et al. (2013) found that recharge plays a vital role in carbonate dissolution as well as ion exchange in groundwater. A review of groundwater resources within Sub–Saharan Africa shows that, weathered crystalline basement rocks forms a good source of groundwater in Malawi and has three major aquifers. These have been distinguished as: the extensive but low yielding weathered Precambrian basement complex aquifer of the plateau area, the high yielding alluvial aquifer of the lake shore plains and the lower Shire valley and the lake Chilwa - Phalombe plain and the medium yielding aquifer of the fracture zone in the rift valley escarpment (Chavula et al. 2018).

Studies in Nkhotakota and Salima concluded that water-rock interaction can potentially influence the character of aquifers, which could affect groundwater quality (Nyirenda et al. 2015). Addison et al. (2020) found that lithological composition is the main control in fluoride occurrence. The presence of Augen gneiss of granitic composition in the weathered basement of Nathenje and the surrounding area is the main factor in the distribution of fluoride in the weathered aquifers in the area (Kalin et al. 2020). Mkuwu (2019) studies shows that the extent of fluoride in groundwater within Nkhotakota is due to mica minerals which are weathered from biotite gneiss and muscovite rocks present in the area. Kamoto and Mussa (2022) assessed the groundwater quality within Lilongwe urban areas and concluded that bacteria possess a risk in the boreholes within the Lilongwe Urban particularly Area 25. This shows how urbanization has affected the alluvial aquifers within Lilongwe urban and recommended provision of basic treatment before consumption.

This research investigated the characteristics of the aquifer and define the hydrogeochemistry with the hydrogeological settings within the crystalline basement complex rocks of Lilongwe, Malawi. This was accomplished through defining characteristic of crystalline basement aquifers and delineate hydrogeochemistry characteristics of deep aquifers within the basement complex rocks.

This enables the study to evaluate the spatial relationship of geological structures on groundwater geochemistry and groundwater flow within the deep basement aquifers.

1.2 Problem statement

Characterization and hydrogeochemical of deeper aquifers are vital in defining the hydrogeological conditions of the aquifers system for implementing sustainable integrated groundwater resource management (Ahmad & Al-Ghouti 2020). The current ever-increasing population and the rapid increase in the development of Lilongwe City has led to high increase in water demand (World Bank 2017). This has the potential to affect groundwater recharge and flow pattern within the river basin such as Lilongwe plain (Hao et al. 2020). Currently Lilongwe Water Board is abstracting groundwater as an alternative source of supply within Lumbadzi and Air Wing areas (Lilongwe Water Board 2019). Lumbadzi aquifers produces very low yield in the pick of dry season which affects the sustainability of supply within the area (World Bank 2017). As such proper characterizing and hydrogeochemistry of aquifers in crystalline basement will define the drastic changes within aquifer system and groundwater flow pattern which is vital in implementing sustainable groundwater management (Lapworth et al. 2018). Kang et al. (2019), due to high yield deep fractured aquifers are valuable resource during in water-stress time but studies of this resource are limited.

Presently, several studies of groundwater in Lilongwe have not related the characterization and hydrogeochemistry of the aquifer with the hydrogeological settings. Among them, Nyirenda et al. (2013), defined the water type of groundwater from shallow aquifers in the Salima and Nkhotakota districts. Addison et al. (2020) identified the source of fluoride in aquifers within the Nathenje area. Bank & Joloza (2019) focused on assessing the hydrogeological and hydrogeochemistry of shallow groundwater aquifers based on shallow wells and Afridev-pumped boreholes. Kamoto & Mussa (2022) assessed the groundwater quality of Lilongwe Urban Areas.

Despite these studies there is still lack of knowledge on characteristics and hydrogeochemistry of deep aquifers. This will be vital in sustainability and management of groundwater resources within the area. Therefore, this study seeks to characterize the aquifer and define the hydrogeochemistry of the aquifer with the hydrogeological settings within the Lilongwe crystalline basement complex.

1.3 Study objectives

1.3.1 Main objective of the study

The main aim of this study is to characterize the aquifer and define the hydrogeochemistry with the hydrogeological settings within the crystalline basement complex rocks of Lilongwe.

1.3.2 Specific objectives

The study had the following specific objectives:

a) To determine the characteristic of crystalline basement aquifers within Lilongwe.
b) To delineate the hydrogeochemistry characteristics of the deep aquifers within the basement complex rocks.
c) To evaluate the spatial relationship of geological structures on groundwater geochemistry and groundwater flow within the deep basement aquifers.
d) To determine the groundwater quality within Lilongwe River Basin for irrigation and domestic use.

1.3.3 Research questions

The study was guided by the following questions;

a) What are the characteristics of crystalline basement aquifers within Lilongwe?
b) What are the hydrogeochemistry characteristic of the aquifers within the basement complex?
c) Does the geological structure have influence on the groundwater distribution and movement within the Lilongwe River Basin?
d) What is the quality of groundwater within basement aquifers of Lilongwe in relation to domestic use and irrigation?

1.4 Justification of the study

Understanding the complexity of the hydrogeochemical process, which controls the variability of the groundwater composition, is vital in groundwater resource management (Li et al.2018). The hydrogeochemical process defines the natural evolution and variation of the aquifers within a geological environment through an understanding of the groundwater systems (Sidibé, Lin & Koné 2019).

This enhances the understanding of the characteristics and hydrogeochemistry of the aquifers within the basin contributes to the management of the quality and quantity of groundwater resources (Bank & Joloza 2020).

According to Chen et al. (2019), understanding the hydrogeochemical process is essential in determining the use of groundwater for various purposes by revealing zones and quality of water within the ecosystem. Understanding factors and changes influencing groundwater chemistry such as rock-water interactions and anthropogenic activities is vital to prevent its pollution (Li et al.2018). Hence the study will be crucial in understanding groundwater interactions within the basin in supporting how the groundwater resource can be utilized within the ecosystems.

1.5 Ethical consideration

The study ethical clearance was obtained from MZUNIREC protocol number MZUNIREC/DOR/22/01. Lilongwe Water Board who is the owner of the exploration boreholes drilled within Lilongwe City and some rural areas granted the permission for the study to use the deep wells data (Appendix 1).

1.6 Study limitations

This study only focused on Lilongwe which has deeper well at present but the government should also focus on having deeper well for future research in other parts of the areas with basement aquifers as well as karoo aquifer in Malawi to properly understand the aquifers and make decisions in groundwater resource management. The study had also a limitation on the finance to support the quick transportation of samples and better laboratory facilities to fast track the groundwater sample analysis.

CHAPTER TWO: LITERATURE REVIEW

2.1 Overview

In recent years, there is an increasing demand for water resources in the sub-Saharan Africa due to the rapid population increase (United Nation 2020). Climate change within the region has limited the availability of surface water sources as such there is need for increase in exploitation of groundwater source to meet the demand (Worthington 2022). The aquifers which host groundwater resource in sub-Saharan Africa occur in weathered and fractured crystalline basement aquifers which occupies 40% of the region (Mapoma and Xie 2013). However, supply in the basement aquifers is limited which is strained by global climate change which limits the potential of recharge (Woessner at al. 2023). As such, with these constraints basement aquifers as groundwater sources is complex and present a challenge in the characterization of the aquifers.

2.2 Characteristics of the aquifers within the basement complex

The basement aquifers are characterized by the hydraulic parameters which define the transmission and storage of groundwater within the water-bearing zones (Dewandel et.2012). Such properties are porosity, permeability, hydraulic conductivity, transmissivity and storativity. According to Woessner at al. 2023, crystalline rock has low hydraulic properties due to dense nature. However fresh metamorphic and intrusive rocks have lower porosity and permeability which is mostly below 1.0percent porosity (n) and permeability between 10-5 and 10-8. Weathered basement rocks can have an increased porosity up to 45% and permeability of up to 70m/day, Table 2.1. But porosity in fractured basement is lower than the overlying regolith it ranges between 5 -10% (Worthington 2022). According to Mkandawire 2004; Mapoma and Xie 2013, most weathered aquifer within the Malawi crystalline basement complex rocks have transmissivity in the range of 5 to 35 m2/day.

Specific gravity (Sy)or the effective porosity refers to the actual amount of water which is release under influence of gravity to the nearby well or spring by water-bearing zones (Sharp 2014).

Crystalline basement aquifers have effective porosity less than total porosity of the medium due to unconnected fractures being not relevant for groundwater flow. It is only connected fractures that transmit effectively groundwater within basement aquifers.

Table 2.1 Representative values of hydraulic properties in selected geological formations (modified after Worthington 2022)

Geological formation	**Porosity (n %)**	**Specific yield/effective porosity (S_y) %**	**Hydraulic Conductivity (K)m/s**	**Relative Groundwater Potential**
Gravel	28-34	15-30	$1\text{-}10^{-3}$	Very high
Sandstone	15-50	5-30	$10^{-2}\text{-}10^{-7}$	Very high to moderate
Clay	40-60	1-5	$10^{-6}\text{-}10^{-9}$	Moderate to low
Fresh Crystalline rock	0-5	0-3	$10^{-9}\text{-}10^{-13}$	Low to Very low
Weathered basement rock	20-40	10-20	$10^{-4}\text{-}10^{-9}$	Moderate to low
Fractured Basement rock	5-10	2.5	$10^{-4}\text{-}10^{-9}$	Moderate to low

The effective porosity in basement complex is usually less than the total porosity of the medium due to groundwater flow being depend on connectivity of fractures (Lachassagne et. 2021). The estimated hydraulic conductivities within the weathered aquifers within Malawi basement complex rocks range from 0.01 to 1 m/d (Council of Geosciences 2013).

Hydraulic conductivity (K) the measure of the ability of a formation to transmit water. It is a crucial aquifer property which is used to characterize aquifers. The hydraulic conductivity (K) in crystalline basement rocks depends on the density, size and fracture interconnections (Worthington 2022). The values of K in Table 2.1 indicate that fresh crystalline basement rocks have $10^{-9}\text{-}10^{-13}$m/s classified with low to very low groundwater potential.

But weathered and fractured crystalline basement are characterized with moderate groundwater potential with K values of 10^{-4}-10^{-9}. Malawi weathered basement aquifers have a storage coefficient ranging from 0.01 to 0.001 (Woessner at al. 2023). Reliable estimates of hydraulic parameters are essential for the management and protection of groundwater resources (Woessner et al. 2023). This is more so in crystalline basement terrains, where the uniformities of the geo-hydrological properties of rocks are expected to be large as a result of spatial changes in geological/structural features (Dewandel et al.2012). This has been effective through estimation of the depth variations of hydraulic properties in the weathered-fractured components of crystalline basement terrains of Malawi and part of sub-Saharan Africa (Chilton & Foster 1995).

2.3 Hydrogeochemistry of the aquifers within the basement complex rocks.

Hydrogeochemistry of the aquifers within the basement rocks is well explained through geochemical evolution and recharge processes occurring within the aquifer system. These are all factors of groundwater chemistry within the aquifer system which is influenced by the chemical weathering of different minerals as silicate minerals and rock-water interaction (Aisha et al.2022). The changes in hydrogeochemical facies defines the recharge and discharge processes within the basement aquifers. As such it reflects the amount of recharge through rainfall and amount of discharge through abstraction within the aquifer system (Luo et al. 2018).

The hydrogeochemistry of aquifers can also define the groundwater flow direction within the basement aquifers through interactions within the aquifer system of different types of rocks. This is demonstrated by geochemical evolution through different chemical constituents within the groundwater flow directions (Apollaro et al.2021). The mineral rock composition of the rock through which groundwater flows is essential geochemical properties of groundwater. As such hydrochemical properties of aquifers along the groundwater flow path is defined by the concentration of chemical species within the geological environment (Blanchette et al. 2013). According to Aghazadeh, Chitsazan & Golestan 2016, these will depend on the properties of the bedrock within geological environment base on the climatic, biological and physicochemical properties. The hydrogeochemical can be used in determining recharge and sources of groundwater. The recharge zone can be assessed physical through stable isotopes and radiogenic isotopes of groundwater (Apollaro et al.2021).

2.3.1 Evaluation of hydrogeochemistry in basement aquifers

Concentrations of cations (Ca^{2+}, Mg^{2+}, Na^{+} and K^{+} and anions (HCO^{3-}, CO_3^{2-}, SO_4^{2-} and Cl^{-}) are used to evaluate groundwater in terms of its alkalinity, salinity, recharge, flow path and residence time in the groundwater system (Chegbeleh et al.2020). This is done by projecting the concentrations of these ions on Tri- and Quadi- diagrams using Piper and Durov diagrams. The plots resulting in grouping of the concentrations in certain parts of the diagrams, enabling characterizing the groundwater based on these plots. The plots enable visualization of the components and hydrochemical types of groundwater and hence importance of hydrogeological processes controlling the water quality (Apollaro et al. 2021). In the Piper plots, the data are plotted on two ternary triangles, for cations and anions that is projected to a third diamond shaped diagram. The plots on the two ternary triangles and projection to the diamond shaped diagram can result in characterization of the groundwater into the following major classes.

- Samples that plot at the top of the diamond is high in cations Ca^{2+} and Mg^{2+} and anions Cl^{-} and SO_4^{2-}. This water has permanent hardness.
- Samples that plot near the left corner are rich in Ca^{2+} and Mg^{2+} and anions of CO_3^{2-} and HCO_3^{-} and show water with temporary hardness.
- Samples that plot at the lower corner of the diamond is primarily composed of alkali carbonates (Na^{+} and K^{+} and HCO_3^{-} and CO_3^{2-}).
- Samples lying near the right hand side of the diamond may be considered saline (Na^{+} and K^{+} and Cl^{-} and SO_4^{2-}).

The double triangular diagram as proposed by Durov in 1948, the major ions are plotted as percentage of mill equivalent concentrations in two base triangles and total cations (top triangle, $Na^{+}+K^{+}$, Ca^{2+}, Mg^{2+}) and total anions (left triangle, Cl^{-}, HCO_3^{-}, SO_4^{2-}). The data points in the two base triangles are projected into a square (combined field of $Na^{+}+K^{+}$ and HCO_3^{-}) of the main field which lies perpendicular to the third axis in each triangle. The Durov plot shows clustering of groundwater quality data points and finally displays some possible geochemical processes, such as ion exchange, reverse exchange and simple dissolution or mixing (Chegbeleh et al.2020).

The composition of groundwater chemistry is controlled by several factors which are chemical composition of recharge water, water-rocks interactions, dissolution/precipitation of mineral phases, evaporation, mixing processes and human activities (Sidibe et al.2019).

2.4 Spatial relationship of geological structures on groundwater geochemistry and groundwater flow within the deep basement aquifers

Groundwater recharge and groundwater flow is processes are controlled by climate, morphology and structure lineaments (geological conditions) (Verspasiano et al. 2021). An assumption regarding groundwater recharge and flow processes that are applicable to porous media such as weathered regolith are not relevant in fractured rocks (Flores et al. 2023). As such the spatial relationship of the structures on groundwater geochemistry and groundwater flow within the deep basement aquifers is vital in define the characteristics of recharge and flow processes (Sikakwe & Eyong 2022).

Structures or lineament can control the spatial and temporal geochemical distribution of groundwater type within a catchment area. The concentration in the deep aquifers is usually defined by the deep fracture conduit within the catchment area (Verspasiano et al. 2021). The groundwater types show the nature of recharge and the spatial variation of groundwater types follow within the trend of regional lineaments orientation. Most shallow aquifers in basement complex are characterized by Ca-HCO_3. Ca+Mg-HCO_3 water type while the deep fractured aquifer is characterized by Na-K-HCO_3 and Ca-SO_4/Ca-Mg-SO_4 water type. The dominance of Ca-HCO_3 indicates an active groundwater recharge area. The presence of groundwater types also shows the trends in the regional fault within the geological environment since it controls the regional groundwater flow. The groundwater types also show the presence of processes within the aquifers such as mixing which can be show by the presence of Ca-SO_4 and Ca-Mg-SO_4 groundwater type. This shows the mixing of fresh recently recharge groundwater with older and more saline groundwater. The presence of fractures characterizes the regional groundwater flow within the aquifer system through the spatial variation of groundwater types within the aquifer system.

Basement aquifers, understanding the groundwater evolution, flow path, and recharge processes mechanisms are very much needed for the optimal usage of groundwater resources (Blanchette et al. 2013).

The chemical plots such as Gibbs plot explains the natural mechanism controlling in basement aquifers. The basement aquifers can be controlled by the rock, evaporation and precipitation dominance. The geochemical properties of groundwater are essentially a function of the mineral composition of the rock through which it flows. In addition, the concentration of chemical species varies along its flow path, and several hydrogeochemical processes impact groundwater geochemistry. According to Chegbeleh et al.2020, chemical plots such as the piper plots are very useful in understanding the geochemical evolution as well as chemical relations of groundwater. It also used to assess the recharge flow path.

The chemical characterization of aquifers is based on its alkalinity, salinity, recharge, flow path and residence time in the aquifer system through concentrations of cations (Ca^{2+}, Mg^{2+}, Na^{+} K^{+}) and anions (HCO_3^{-}, CO_3^{2-}, SO_4^{2-}, Cl^{-}). The groundwater movement is mainly controlled by deeply fractured zones. The changes happening within the deep aquifers is determined through understanding relationships among major ions (Sunkari et al. 2022). The abundance of Ca^{2+} ions in the basement aquifer system shows the presence of deep lying fractures which are conduits to groundwater flow which influences percolation of recent water within the system. High recharge also shown through the abundance of Ca^{2+} in groundwater chemistry which indicate the presence of fresh or recently recharge water which has little residence time and has not undergone the full chemical evolution from Ca^{2+} dominant (fresh water) to Na^{+} dominant (old water).

2.5 Groundwater quality

Groundwater quality is concerned with health risks, ecological impacts, impacts on ecosystem services and impacts on aquifer properties (Eid et al.2023). Chemical characteristics include; inorganic constituents such as salts and nutrients; trace elements such as metals and organic constituents such as benzene, pesticides and organic carbon. A combination of the composition of water that enters the aquifers and the reactions with minerals present in the rocks results in the chemical composition and characteristics of groundwater (Zhu et al. 2020). The physicochemical parameters of groundwater water quality include, among others; temperature, turbidity, colour, taste and odor while biological characteristics include the pathogen indicators organisms such as protozoa, bacteria and viruses (Chen et al. 2019). Though groundwater is often viewed as the cleanest water source, it is also contaminated by several sources.

The most common groundwater contaminants are naturally occurring, point sources and non-point of sources (Khatri & Tyagi 2015). Examples of naturally occurring contaminants are arsenic and seawater intrusions, whereas point sources include leaking underground storage tanks (gas stations), industrial spills, landfills, septic systems, sewer lines, animal feedlots, manure lagoons and leach fields, and non-point sources include urban runoff and agricultural activities (Aral & Taylor 2011).

Groundwater assessments are done for several reasons including the need to assess its suitability for use in industries, irrigation and domestic purposes (Konikow & Bredehoeft 2020). Furthermore, in recent times, groundwater assessment has been done to generate hydrochemical data of an area, to understand the hydrogeology of an aquifer. The understanding of the recharge, flow, water-rock interactions and discharge processes (Zhu et al. 2020). Groundwater assessment is also done to investigate groundwater pollution through identification and quantification of the occurrence of pollutants as well as processes around events. Assessment can also be undertaken to identify changes in the aquifers occasioned by pollution, climate change and over-exploitation, through regular observations (Konikow & Bredehoeft 2020).

2.6 Irrigation groundwater quality

Groundwater is increasingly used for irrigation by smallholder and commercial farmers globally (Jafary & Bradley 2018). However, most often, hand-dug wells and treadle pumps, particularly in dambo areas, are used by smallholder farmers while the motorized pump is used by commercial farmers (Council of Geosciences 2018). Siebert et al. 2010, report that globally, 43% of the groundwater is used for irrigation. In the SADC region, the total use of groundwater is 7.7% and irrigation uses 82% of it. In Malawi, the total usage of groundwater for domestic supply is 29%, as such irrigation is the major user with 87% (SADC-GMI 2019). But according to National Statistical Office 2020, the total area fully equipped with groundwater irrigation in Malawi is at 0.02 per cent. Groundwater use for irrigation purposes faces a number of challenges such as infrastructure development, groundwater quality and over-exploitation of aquifers (Carrard et al.2019). The status of groundwater quality has a major impact on the soil and crop yield. Hence it is vital to manage the quality of this water to reduce the effects. The quality of groundwater varies based on the nature and geological environment of the aquifer (Kalantar 2020).

As such application of groundwater quality standards is adopted to ensure that suitable water is applied to the soil and crop for better yields.

The irrigation water quality indices are a fast, effective and verifiable tool for the suitability of groundwater quality for irrigation (Wanda et al. 2013). These indices are obtained through a number of mathematical processes that can convert a large amount of water quality data to a single number to enable the decision-maker to make an appropriate judgment on water quality and appropriate uses. These indices are described below:

2.6.1 Sodium Absorption Ratio

Sodium Absorption Ratio (SAR) is the measure of the relative ratio of sodium ions (Na^+) to Ca^{2+} and Mg^{2+} present in the water sample (Rawat, Singh & Gautam 2018). SAR measures the estimated potential of Na^+ to accumulate in the soil due to water movement at the expense of Ca^{2+}, Mg^{2+} and K^+, as a result of regular use of sodic water using equation 2.1.

$$SAR = \frac{Na^+}{\sqrt{\frac{(Ca^{2+}+Mg^{2+})}{2}}} \quad \text{.....Equation 2.1}$$

where the concentrations are expressed in meq/L. According to Kaur et al (2016), SAR is classified into four classes:

SAR: <10 (Ideal or Excellent), 10−18 (Good), 18−26 (Doubtful), >26 (Unsuitable).

2.6.2 Permeability Index

Permeability Index (PI) is the measure of the concentration of salt for long-term use of irrigation water which influences water movement capability (Rawat, et al. 2018). Most water movement capability is affected by Na^+, Ca^{2+}, Mg^{2+} and HCO_3^- ions in the soil. PI assess water movement capability in the soils as the suitability of waters in the basement aquifers for irrigation as used by, Narsimha *et al*., (2013) using the formula equation 2.2:

$$PI = \left[\frac{Na^+ + \sqrt{HCO_3^-}}{Ca^{2+}+Mg^{2+}+Na^+}\right] \times 100 \quad \text{.....Equation 2.2}$$

where all concentrations are expressed in meq/L. PI is categorized into three classes, based on Doneen 1964: Class I (> 75% suitable), Class II (25−75% Good) and Class III (<25% Unsuitable). Water under Class I and II is recommended for irrigation.

2.6.3 Sodium Percentage

Sodium percentage (Na%); is a tool used to access the concentration factor of sodium ion (Na+) in irrigation water sources, which can react with any ion in the soil and affects its permeability (Rawat et al., 2018).

The formula and classifications; Narsimha, Sudarshan & Swathi (2013) using equation 2.3, can be used to estimate and categorize the sodium percentage in a basement aquifer:

$$\%Na = \left[\frac{Na^{+}}{Ca^{2+}+Mg^{2+}+Na^{+}+K^{+}}\right] \times 100$$ ..... Equation 2.3

where the all concentrations are expressed in meq/L.

The classification, based on %Na, is as follows: excellent (<20%), good (20−40%), permissible (40−60%), doubtful (60−80%) and unsuitable (>80%).

2.6.4 Residual sodium carbonate

Residual sodium carbonate (RSC) is the amount of sodium carbonate (Na_2CO_3) and sodium bicarbonate ($NaHCO_3$) present in irrigation water if the concentration of carbonate and bicarbonate ions surpasses the concentration of Ca^{2+} and Mg^{2+} ions (Rawat, et al.2018). The RSC measures the potential causes of soil precipitation, impairing the soil structure as well as potentially activating soil sodium. The RSC can be calculated using the formula and classification equation 2.4, according to Narasimha et al. (2013).

$$RSC = \left[\left(HCO_3^{-} + CO_3^{2-}\right) - \left(Ca^{2+} + Mg^{2+}\right)\right]$$ .....Equation 2.4

Based on the RSC range, sodium hazard has been classified into three classes as follows: RSC<1.25 (low), 1.25−2.5 (medium) and>2.5 (high). RSC is expressed as milliequivalents per litre (meq/L) of $NaCO_3$

2.6.5 Magnesium Hazard or Magnesium Adsorption Ratio

Magnesium Hazard (MH) or Magnesium Adsorption Ratio (MAR) measures the effects of magnesium in the irrigation water source. Calcium (Ca^{2+}) and Magnesium (Mg^{2+}) ions maintain the state of equilibrium in groundwater.

According to Narasimha et al. (2013), magnesium hazard (MR) or Magnesium Adsorption Ratio can be calculated using the formula, equation 2.5:

$$MAR = \left[\frac{Mg^{2+}}{Ca^{2+}+Mg^{2+}}\right] \times 100$$ ……. Equation 2.5

where the concentration of each cation was expressed in meq/ L

The MH or MAR value is classified as follows:

If the MAR value < 50, the groundwater may be used for irrigation purposes, otherwise, if the MAR value > 50, the groundwater is unsuitable for irrigation purposes.

2.6.6 Kelly Ratio

According to Rawat et al. (2018), Kelly Ratio (KR) focuses on the concentration levels of Na^+ against Ca^{2+} and Mg^{2+} in groundwater and it can be calculated using the formula equation 2.6:

$$KR = \frac{Na^+}{Ca^{2+}+Mg^{2+}}$$ ……...Equation 2.6

where the ion concentrations are expressed in meq/L.

The KR value is classified as follows: KR>1 indicates an excess level of Na^+ in waters and is not suitable for irrigation and KR≤1 means less Na^+ and is suitable for irrigation.

2.6.7 Corrosivity Ratio

This measures the state of the supply of groundwater through pipes. Supplying through pipes is based on the ratio of corrosivity (Kaur et al.2016). The Corrosivity Ratio can be calculated using the following formula equation 2.7:

$$CR = \frac{\left(\frac{Cl^-}{35.5}+2\left(\frac{SO_4^{2-}}{96}\right)\right)}{\left(2\left(\frac{HCO_3^- + CO_3^{2-}}{100}\right)\right)}$$ ……...Equation 2.7

Corrosivity is classified as:

CR < 1 can be conveyed through any kind of pipe. The CR > 1 shows the corrosive nature of water and cannot be conveyed through metal pipes.

2.6.8 Total Hardness

According to Rawat et al. (2018), Total Hardness (TH) measures water hardness due to the presence of divalent metallic cations (Ca^{2+} and Mg^{2+}). It is calculated as the sum of Ca^{2+} and Mg^{2+} concentration as meq/L equivalent to $CaCO_3$, using the formula equation 2.8:

$TH = 2.5 \times Ca^{2+} + 4.1 \times Mg^{2+}$ ……...Equation 2.8

Total hardness (TH) is usually classified as soft (0−60 mg/L), moderately hard (60−120 mg/L), hard (120−180 mg/L) and very hard (>180 mg/L) (EPA, 1986).

2.6.9 Total Dissolved Solids

The total dissolved solids (TDS) measure the amounts of minerals and nutrients that have dissolved in water, and also major ions, i.e., Ca^{2+}, Mg^{2+}, Na^{+}, K^{+}, CO_3^{2-}, HCO_3^{-}, Cl^{-}, SO_4^{2-} and PO_4^{3-} in groundwater which is used for irrigation (Rawat et al.2018). Mostly, these ions are caused by weathering dissolution of soil and rocks in the water. According to Narsimha et al. (2013), TDS for irrigation is classified as TDS<450 mg/l (Suitable for irrigation), TDS>450–2000 mg/l (slight to moderate) and TDS>2000 mg/l is unsuitable for agricultural purposes.

CHAPTER THREE: MATERIALS AND METHODS

3.1 Description of the study area

3.1.1 Location

The study was conducted in Lilongwe district, in the central region of Malawi. It specifically covers the area within the Lilongwe River Basin. The district lies within 3°58'0.91"S, 33°47'14.1"E (520000-640000 Easting and 838000-850600 Northing) (Figure 3.1). According to the National Population Census of 2018, the district has a total area of 5,808 km^2, with a population of 1,637, 583 in the rural, while the urban has a total area of 403 km^2, with a population of 989,318 (National Statistical Office 2019). Access to improved water service has been a long-time challenge in Lilongwe city. This is due to the increase in socioeconomic activities and population growth. There is a need for studies on how to properly manage water resources within the area (World Bank 2017).

3.1.2 Weather and Climate

The study area climatic conditions are influenced by the dominant wind shift caused by the Intertropical Convergence Zone (ITCZ), which oscillates north and south between seasons in the African continent (Kaonga et al. 2015). The wet season occurs from November to April, when the ITCZ moves southward, bringing rainfall, and the dry season occurs from May to October when the ITCZ retreats northwards. The climate of the study area can be categorized as sub-tropical, with a distinctive, winter (May to August), hot season (September to October) and wet (November to April). Annually, minimum temperatures range from 5°C to 22°C, whereas maximum temperatures range between 25°C and 35°C. The rainy season contributes approximately 95% of the annual rainfall, being the most humid, at a range of 600 mm and 1,200 mm (Department of Climate Change and Meteorological Services 2022.

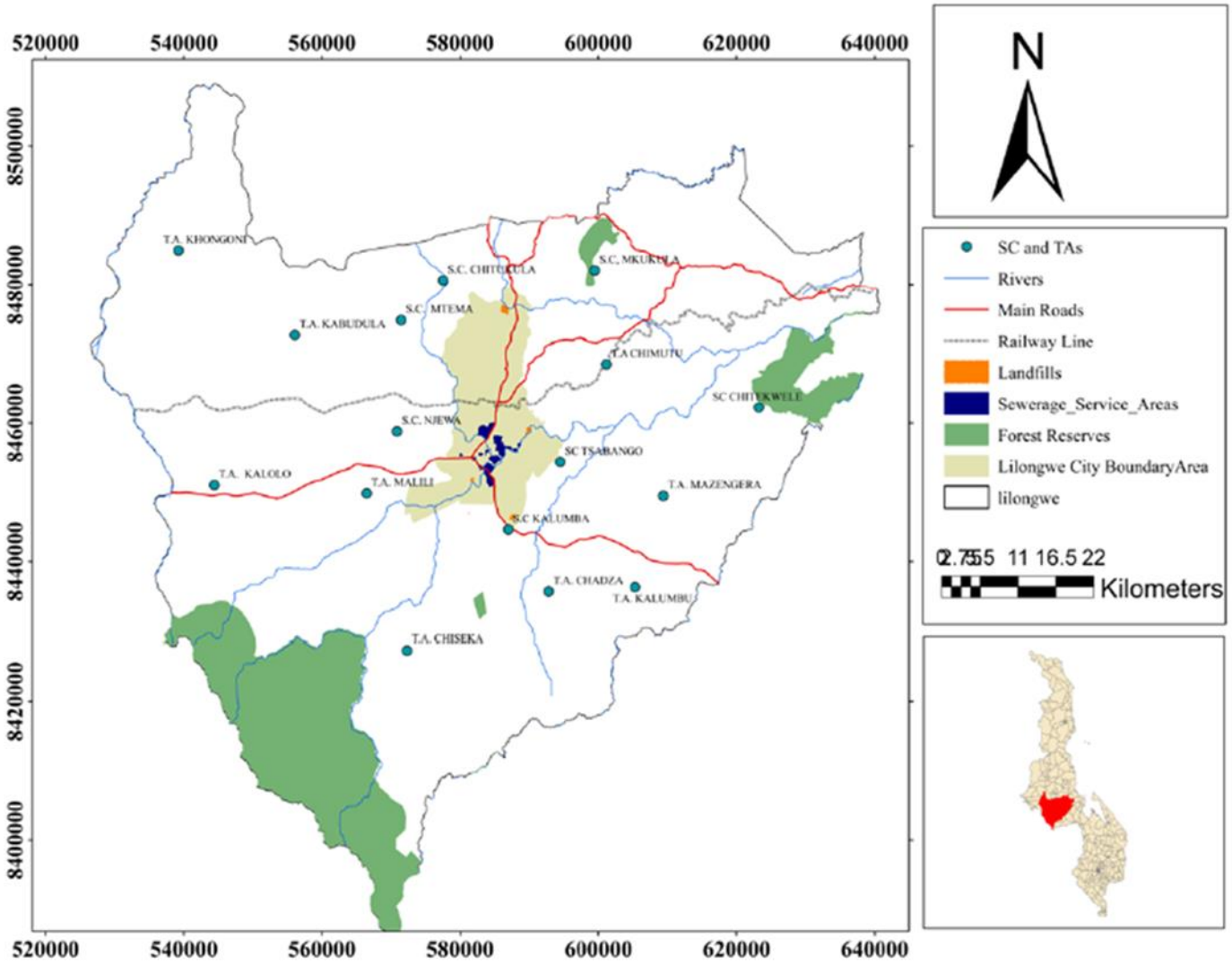

Figure 3.1: Map of the Study area, Lilongwe

3.1.3 Land use and land cover

Lilongwe city and district is classified into five major land use classes, based on the Land-use Classification of 1995, namely, rock outcrops, cultivated land, plantations, grassland and Dambos (UN-HABITAT 2011). Rock Outcrops are mainly large swaths of granite domes and inselbergs occurring within the plain, the notable one being Bunda Hill. Cultivated Land covers more than 80% of all land cover in the plain, which is represented by subsistence agricultural or community land which depends on rain−fed agriculture. Plantations occur mainly to the southeast and southwest of Lilongwe district (Lilongwe City Council 2010). Grasslands are limited as most of the vegetation has been cleared for cultivation. Dambos are wet areas, characterized by depressions, with an impermeable clay base layer. The clay results in perched water or perched aquifers, leading to perennial wet soils. The dambos are mainly found in the headwaters of streams and in the western part where recent sand and clay cover the underlying rock (Government of Malawi 2017).

3.1.4 Topography and geomorphology

Plateau and upland areas are more prevalent in the study area, with the escarpment occurring just outside the plain to the east. Plateau areas are also characteristically covered by a compounded mantle of recent alluvial sediments and with relatively thick weathered regolith, presumably from a prolonged period of stability, allowing for deeper advancement of the weathering front into the underlying geological formations (Council of Geosciences 2018). The upland areas can be described with an elevation range of 2000 to 3000 meters above mean sea level to the west, east and north such as Chitupa, Bunda and Chikhoma. These are categorized as remnants of the Gondwana surface. Most of these areas comprise of intrusions of granitic and syenitic plutonic rocks (Hodges et al.2015). Similarly, inselbergs and granitic tors stand out above the local plains in the study area, such as the top of the Dzalanyama Range to the south of Lilongwe (Government of Malawi 2017). The peneplains occur in the South Lilongwe plain, which stretches northwest to the north of Lilongwe and comprises several wide valleys that are separated from each other. These areas have an elevation ranging from 900 to about 1300 m (Council for Geoscience 2018).

3.1.5 Geology of the study area

The study area is overlain with a crystalline metamorphic basement complex intruded by igneous rocks. The basement complex rocks consist mainly of gneisses and granulites, formed as a result of medium to high-grade metamorphism and various phases of deformation. The lithologies include syenitic granites, charnockitic and ultra-basic gneisses, schists, granulites and quartzites. The basement complex is intruded by dolerite dykes of the Chilwa Alkaline Province of Jurassic to cretaceous and overlain by quaternary deposits **(Figure 3.2 and Table 3.1).** Quaternary deposits including alluvium, lateritic soils and sandy clays cap the geological sequence in the eastern parts of the area.

Table 3.1 Chromo stratigraphy of the study area (Modified after Council for Geoscience 2018)

Era	Formation	Groups	Member	Lithology
Quaternary				Alluvium
				Lateritic Soils
				Sand Soils
				Red brown Sandy Clays soil
Cretaceous-Jurassic	Chilwa Alkaline	So"lvsbergites	Dolerite Dykes	Dolerite
Paleozoic	Basement Complex	Orthogneisses & intrusive	Migmatites and Migmatization	Venites, granitize schist and perthitize gneisses
			Intrusions	Pegmatites
			Dzalanyama Granite	Porphyritic biotite-granite,leucogranite and micro-granite
			Perthite-augen gneiss	Augnen Gneiss
			Meta-pyroxenites	Meta-pyroxenites
			Amphibolites	Amphibolites
		Charnockitic Granulites, Paragneisses & Schist	Mchinji Group	Pelitic Schist,Quartzite and Quartzo ferspathic
			Calc-mgnesian	Marble, Calc-silicate granulite and gneiss
			Calc-psammitic gneiss, granulite & schist	Quarzo-feldspathic, Calcereous quartzites and quartz-schists
			Psammitic gneiss, schists and granulites	Muscovite-quartz-schist, Kyanite, Quartz-feldspathic granulites and gneiss
			Pelitic gneiss and schists	Kyanite-mica-gneiss, schists and graphite gneisses, calcareous pelitic schists
			Semi-pelitic and psammo-pelitic biotite-gneisses, schists & granulites	Biotite gneiss and granulites, garnetiferous kyanite-biotite-gneiss and epidotic biotite quartz
			Granulites and cafemic gneiss	Biotite gneiss and granulites

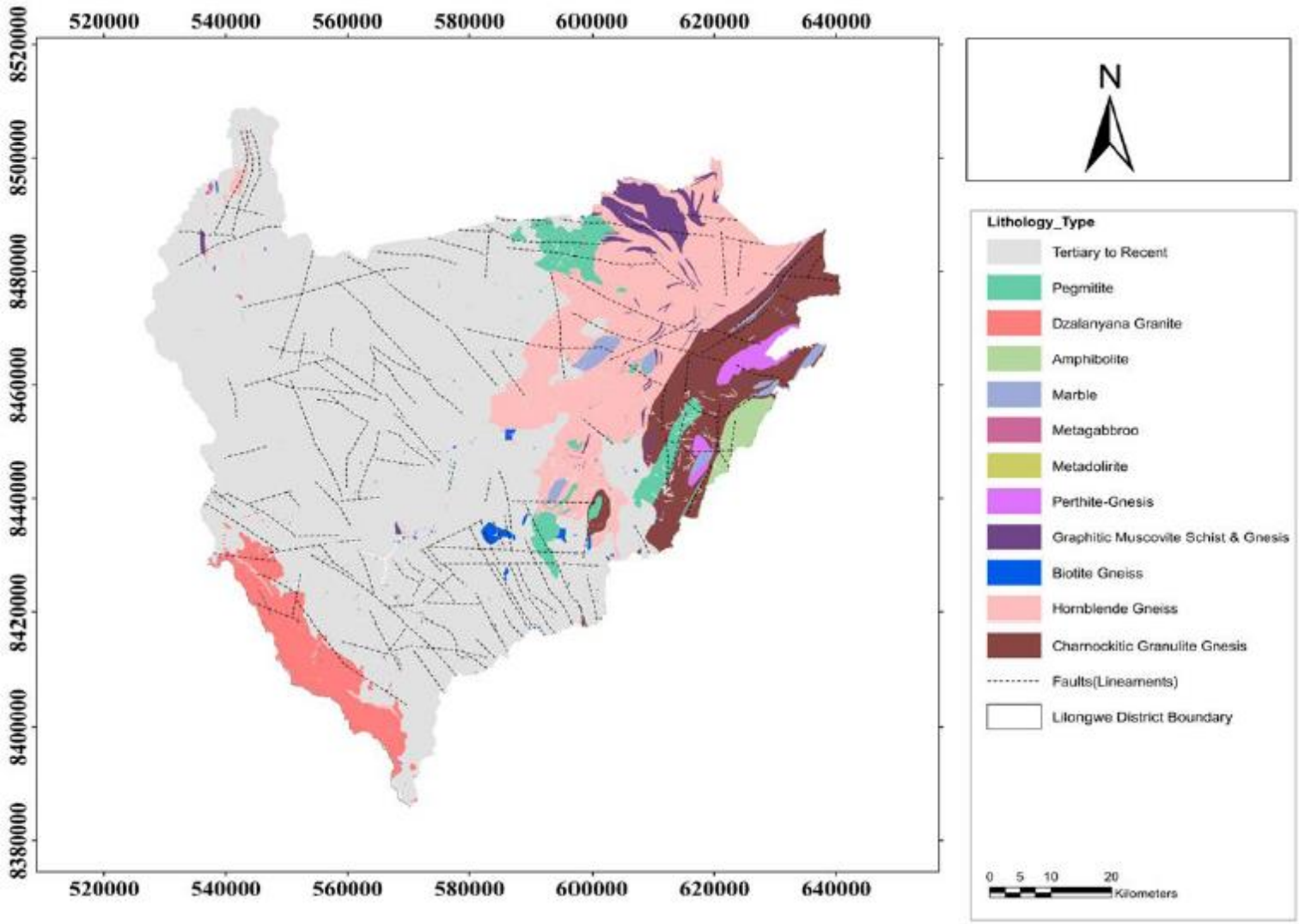

Figure 3.2 Geology of the study area

3.1.5.1 Geological Facies of the study area

The Basement Complex of the Proterozoic era is the most widespread group of rocks within the study area and comprise mainly of weathered and fractured gneisses (Figure 4.2). However, highly metamorphosed and deformed make them high groundwater prospects or aquifer host rocks. Biotite-hornblende gneisses are mostly found within Lilongwe and comprise rocks that are regionally metamorphosed under amphibolite and granulite facies. These varies from felsic to mafic containing hyperstene, pyroxene, hornblende, biotite, quartz, and plagioclase. K-feldspar, cordierite and sillimanite are also found. Biotite-hornblende gneiss also occurs with garnet sillimanite and diopside. Pelitic schists and gneisses form part of the Mchinji groups whereas in some parts pelites are graphitic with muscovite and kyanite but also interbedded with quartzites. Orthogneisses and intrusive rocks consist of amphibolites, pyroxenite, meta pyroxenite, meta-anorthosite and metagabbro (Carter 1973). Dzalanyama granite is a porphyritic microcline granite with epidote found in southwest Lilongwe. Syenites, consisting of perthite augen-gneisses, perthitic syenite monzonites and minor granite found between Lilongwe City.

3.1.6 Water resources areas within the study area

The study area forms a major part of the Linthipe Water Resources Area, one of the seventeen Water Resources Areas (WRA) in Malawi, divided based on the river basins (Japan International Cooperation Agency (JICA 2017). It covers a major part of the Linthipe River Basin, which has a total catchment area of 8884.8 km^2. The basin is drained by the following stream; Lifisi, Diamphwe, Lifidzi, Lilongwe, Linthipe, Msunduzi, Namitete, Nanjiri, Chaulongwe, Lingazi, Lumbadzi, Mtedza and Likuni (Government of Malawi 2017). It also partly covers the Lilongwe-Kasungu plain. Most of the streams within the basin drain from this plain (JICA 2017).

3.1.6 Drainage of the area

The main drainage system of rivers locally flows towards north to northeast and eventually east towards Lake Malawi. The most common river patterns in the area consist typically of dendritic and trellis river patterns (Council for Geosciences 2018). Lilongwe river is the major river in the basin which has the following significant tributaries: Nanjiri, Chaulongwe, Katete, Likuni, Lingadzi and Lumbadzi.

3.2. Research design

Quantitative research design has been used to characterize the hydrogeochemistry of the aquifer in relation to the hydrogeological settings and to ascertain the quality of groundwater for irrigation and domestic use in the Lilongwe River Basin. An experimental type of primary quantitative research design was employed, where the goal of the study was to examine the cause-effect relationships of aquifers within the basement complex (Leedy & Ormrod 2015). Quasi-experimental type of experimental research design has been employed in this research to characterize the aquifers system within the Lilongwe River basin. This design suits the study since groundwater samples have been collected from all the twenty drilled deep weels (exploration boreholes) and simple random sampling on fifty shallow wells (Afridev-pumped boreholes) within the study area.

3.3. Sampling framework and methods

Non-probability sampling method was used in determining the number of deep wells to be sampled within the Lilongwe Plain catchment area (Lohr 2022). Purposive sampling was used to allocate the twenty-one (21) deep wells within the study area (Figure 3.3) where groundwater sampling, lithological logs and pump testing were done. Simple random sampling was used in collecting fifty (50) samples from shallow wells (Afridev boreholes) within the study area which targeted all Afridev boreholes near an exploration borehole.

3.4. Data Collection

The research used both secondary and primary data sources to meet the objective of the study.

3.4.1 Secondary Data

Secondary data was collected from all relevant previous studies and reports. Secondary data included geological maps, water quality, hydrogeological and log data sets of hand-dug wells, shallow boreholes, and monitoring boreholes. The data were collected from different organizations such as Lilongwe Water Board (LWB) and the Department of Water Resources, in the Ministry of Water and Sanitation. Remote sensing was also used to extract geology and structural data from the geophysical data (magnetics and uranium).

Landsat Images and satellite (google earth images) data from 2017 to 2021 were used to collect information on geology, land use and drainage pattern within the plain.

3.4.2 Primary Data

The Primary data collection involved collection of groundwater sampling from twenty-one (21) exploration boreholes, lithological data from the rock chips at every 1m deep, collection of hydrogeological information of the boreholes (borehole yield, water strike and water level) and collection of well parameters during pumping test. Microbial samples require that they be analyzed within 24 hours of collection and be kept in a cool/ice container or refrigerated. Sampling and analyses for microbial was not possible during drilling and test pumping. Transporting a single sample per borehole would have been too costly to make 37 to and from trips to collect and send a sample to the laboratory each time a borehole was completed. Microbial analysis was therefore only carried out for the 50 samples collected using stratified random sampling to only boreholes near to exploration boreholes. A total of 10 samples would be brought back from the field each day for analysis rather than one sample at a time from drilling and test pumping.

3.4.3 Sample Treatment and Transportation

The samples were collected according to the Standard Methods for Examination of Water and Wastewater (APHA 2017) and by the Malawi Standard (MS) sampling protocol (MS 682-11:2012). The groundwater samples from the deep wells were collected in the two litres bottles after well-developed using the drill rig air compressor to pump water from deep aquifers. Two replicate samples were collected for laboratory analysis, duplicate samples were collected after the fifth borehole and four duplicate samples were collected from Lumbadzi and Lilongwe rivers. Fifty (50) shallow wells (Afridev) were sampled purposively selected to coincide with areas where deep wells (exploratory borehole) were drilled. Sample collection involve manual pumping of borehole and collecting two replicate samples per site. Sampling bottles were pre-washed three times with distilled water and rinsed with sample water, before collecting the sample for laboratory analysis. The borehole locations and elevations were noted and recorded using a Garmin handheld GPSMAP 64s (S/N:3BP205983).

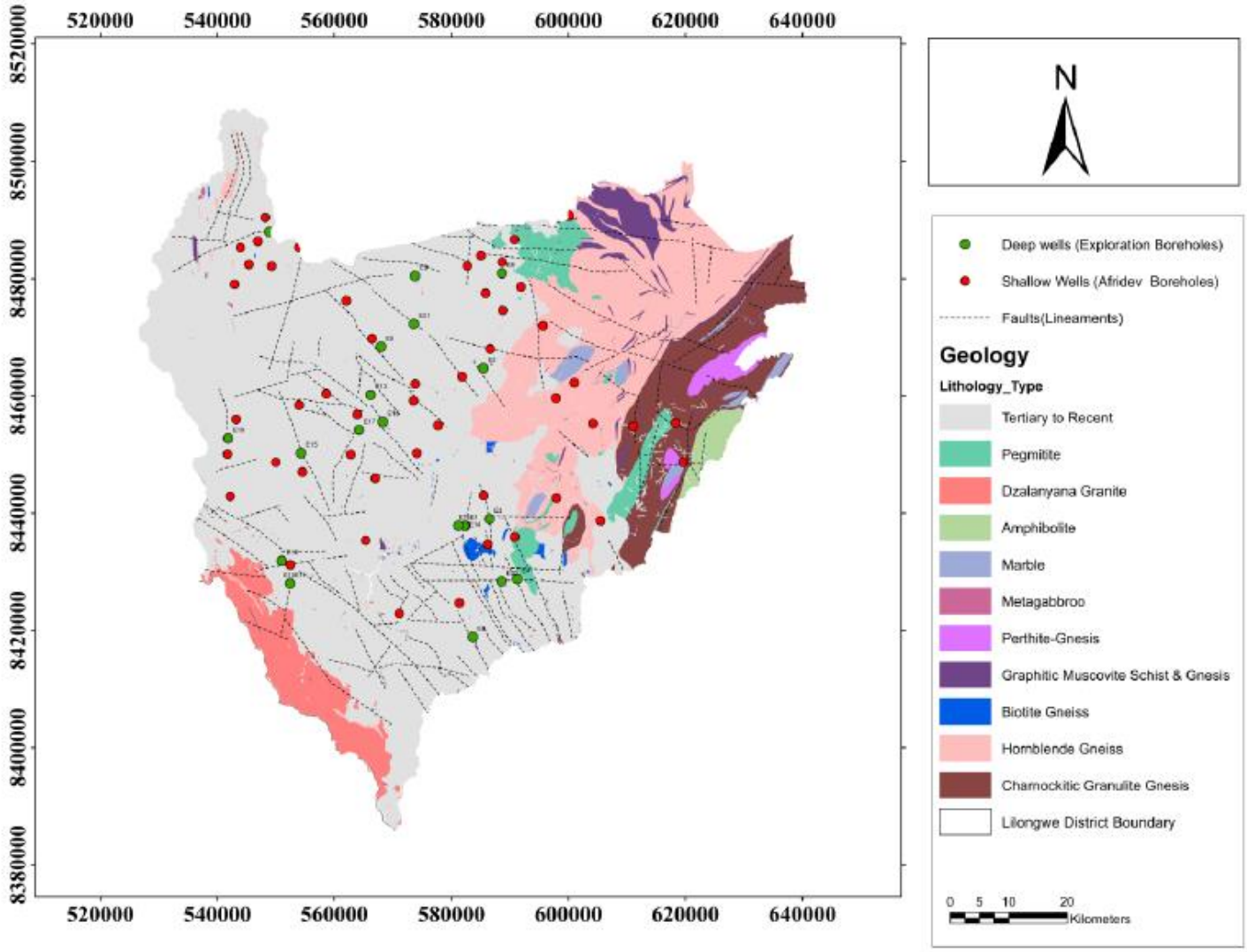

Figure 2.3: Map of the study area showing sampling points

Each sample bottle was labelled using a black permanent marker with a specific code. Anion and cation samples were collected separately in 2-litre bottles. However, all samples for cation and trace element analysis were acidified to a pH less than 2 using a reagent of concentrated nitric acid to minimize cation adsorption and precipitation. Collected samples were transported to the laboratory using a clean cooler box filled with ice packs. The groundwater samples were collected soon after borehole development using the compressor air to pump water from deep aquifers. One set of samples were collected with duplicate samples collected after every fifth borehole.

3.5. Water quality analyses

3.5.1 In-situ analysis

The in-situ analysis of groundwater samples involved the analysis of the physicochemical parameters of pH, EC and TDS. The measuring instruments or meters were calibrated prior to taking measurements. Samples for in-situ analyses were transferred into beakers and measurements were done in triplicate. EC, pH, and TDS were measured using a Hanna Meter (Hanna Instruments, USA) from the collected samples, before being put into sampling bottles for further laboratory analysis.

3.5.2 Laboratory analysis

The representative groundwater samples were collected for laboratory analysis of physical parameters, cations, anions, metals using standard methods and instruments. The laboratory analysis was done at Central Water Laboratories. Several instruments were used in determining the chemical parameters in the groundwater samples (Table 3.4). Two set of samples were collected which were used for all analytes.

3.5.2.1 Determination of stock solutions

3.5.2.1.1 Determination of Potassium and Sodium

For analytical-grade sodium chloride, stock solutions were made using sodium and potassium analytical reagent grade. Then, using the metal cation stock solutions as a starting point, serial dilution was used to create standards of 0, 2, 4, 6, and 10 ppm. Unknown samples were similarly prepared from the fields.

A flame spectrophotometer's direct reading was used to determine trace quantities of potassium and sodium ions at max = 766.5 nm and max = 589.0 nm, respectively. The sample was diluted by a factor if it was extremely concentrated, which was shown by the sample's high conductivity. Each sample was examined, and the equipment was standardized. Then, the flame atomic spectrophotometer was set up in accordance with the instructions in the manual. Any unknown sample(s) were diluted if the measured absorbance or emission was off the scale, for instance outside the range of the standards (APHA 2017).

Table 1.2 Summary of groundwater quality parameters and laboratory equipment used

Equipment	Groundwater Quality Parameter Analyzed	Methodology	Serial Number
Hanna Meter (HI|99300)	Temperature. EC, pH, and TDS	Probe	F0053656
Turbidimeter	Turbidity	Photometric	60045687
Atomic absorption spectrometer (AA500, Pg. instrument)	Copper (Cu), Zinc (Zn), Cadmium (Cd), Lead (Pb), Calcium (Ca^{2+}) magnesium (Mg^{2+}) Manganese (Mn^{2+}) and Iron (Fe^{2+})	Atomic Absorption Spectrometry (AAS)	25-0930-21-0013
Titration unit	(CO_3^{2-}), bicarbonate (HCO_3^-) and chloride Cl^-	Acid Titration	
UV-Vis Spectrophotometer	fluoride (F^-) sulphates (SO_4^{2-}) and nitrates (NO_3^-)	UV-Vis Spectrophotometry	2013010162
Sherwood Flame Photometer	sodium (Na^+), and potassium (K^+)	Flame Spectrophotometry	27780
Filtration unit (Aquaflex MFX50)	faecal coliform and E. coli	Membrane filtration Technique (Culturing)	

3.5.2.1.2 Determination of Iron

A solution of 1000 mg/L of iron metal ions was properly diluted to create solutions of 0.50, 1.50, 2.50, 3.50, 4.50, and 5.00 mg/L.

They served as the basis for the Atomic Absorption Spectrophotometer calibration. 5.00 ml of nitric acid was added to each conical flask, which was then covered with a watch glass. Following this, the prepared water samples were placed to a slow boil. 100 ml of well-mixed samples for iron were then transferred into each conical flask. The samples were placed on a heated plate with boiling chips added to them to prevent acid from boiling and reduce splatter. The samples were slowly boiled before being evaporated to yield 10.0 ml. After that, the room temperature was allowed to reach for the water samples. To 10.0 ml, distilled water was added to make 100 ml in a conical flask. The levels of Fe^{2+} in the blank and worked-up samples were then determined using an Atomic Absorption Spectrophotometer (AAS).

3.5.2.1.3. Determination of Chloride

Argentometric titration was used to determine chloride concentration in the samples.
The reagents were prepared as follows:

3.5.2.1.3.1 Potassium Chromate Indicator

Annular grade potassium chromate (5.00g) was dissolved in 20.0 ml distilled water, followed by the addition of three drops of silver nitrate solution. The mixture was then allowed to stand for one night before filtering, and the filtrate was then diluted to a volume of 100 ml with distilled water in a volumetric flask. After that, it was labeled, corked, and preserved for use as an indicator in chloride determination.

3.5.2.1.3.2 Silver Nitrate Solution

In order to create a 0.01 M solution, 2.40 g of dried silver nitrate was dissolved in 1000 ml of distilled water in a volumetric flask. After that, it was labeled, corked, and stored for use in calculating chloride.

3.5.2.1.3.3 Sodium Chloride Solution

The stock solution for sodium chloride was prepared by dissolving 0.83 g of NaCl in 100 ml of distilled water in a volumetric flask to make a solution of 0.014 M. This was starked and labeled. The working solution was prepared by diluting the 100ml of stock solution to 1000ml with distilled water in volumetric flasks.

Standardizing silver nitrate was done by placing 25.0 ml of diluted NaCl solution in one conical flask and adding 25.0 ml of distilled water. 50.0 ml of distilled water was added to another conical flask, and 1.00 ml of chromate indicator was added to each conical flask. $AgNO_3$ solution was placed in the burette and added drop by drop to the NaCl solution in one of the flasks until the reddish brown color was observed. The amount of $AgNO_3$ used was recorded and corrected for error due to the increase in the volume of NaCl solution resulting from the addition of $AgNO_3$. The correction was done through dilution factor which is (0.003× volume of $AgNO_3$ at the end of titration) +0.02. 50 ml of the sample. This was placed in one conical flask and 50 ml of the distilled water in another conical flask. However, 1.00 ml chromate indicator was added to each conical flask, standardized $AgNO_3$ solution in the burette was added to the sample drop by drop until reddish coloration appeared. A comparison for this was made with the original color of the distilled water and chromate mixture in the second conical flask. As such the amount of $AgNO_3$ solution used was recorded, and this procedure was repeated for all the water samples. The amount of chlorides (mg/l) was calculated using equation 3.1(APHA 2017).

Chloride Ion Concentration (mg/L) = $\frac{(Volume\,(Ml)\ of\ (AgNO3-0.2)\times 500)}{Volume\,(Ml)\ of\ the\ sample\ taken}$ ……. Equation 3.1

3.5.2.1.4 Determination of Fluoride

Preparation of fluoride standards was done in the range of 0.0 to 1.40 mg F-/L by diluting appropriate quantities of standard fluoride solution to 50ml with distilled water.10 ml of SPADNS reagent was pipetted and mixed with each standard. The calibration of photometer was calibrated using 0.5, 1.0, 1.5 and 2.0 mg/l of fluoride standard solution, together with SPADNS reagent. 10.0 ml of the water sample was pipetted into a dry round sample cell and 10.0 ml of distilled water was pipetted into a second dry sample cell (this was the blank). 2.0 ml of SPADNS reagent was pipetted into sample cells containing the sample and the blank. The spectrophotometer was allowed to run for 1 minute at a wavelength of 570nm. The blank was used to zero the spectrophotometer. The prepared water sample was placed into the cell holder, and the concentrations of fluorides were read in mg/l (APHA 2017).

3.5.2.1.5 *Determination* of Calcium and Magnesium

Determining the concentrations of calcium (Ca) and magnesium (Mg) in groundwater samples using Atomic Absorption Spectroscopy (AAS) will be prepared from a stack solution of 601.2 ppm calcium and 10,000ppm magnesium. Four different concentration standards were prepared within the range of linearity (1-10ppm) for calcium and (0.1-1ppm) of magnesium with minimum volume of 250ml using the Atomic Absorbance Spectrometer (AAS).

The absorbance was measured for each calcium and magnesium standard using calcium cathode lamp for calcium and magnesium cathode lamp for magnesium. The absorbance was plotted against the concentration in excel to confirm the linear relationship to show the calibration curve of calcium and magnesium in a graph.

3.5.2.1.6 Determination of nitrate

The preparation of nitrate calibration standards was done in the range of 0 to 7mg NO_3^- N/L by diluting to 50 ml in the following volumes of intermediate nitrate solution: 0, 1.00, 2.00, 4.00, 7.00, 35.0 ml. As such NO_3^- standards were treated in the same pattern as samples. Absorbance was read against redistilled water set at zero absorbance or 100% transmittance. Due to dissolved organic matter, to determine interference a wavelength of 220 nm was used to obtain NO_3^- reading and a wavelength of 275 nm. In both samples and standards; two times the absorbance reading was subtracted at 275 nm from the reading at 220 nm to obtain absorbance due to NO_3^-. A standard curve was constructed by plotting absorbance due to NO_3^- against NO_3^- concentration of standard. Using corrected sample absorbencies, sample concentrations were obtained directly from the standard curve (APHA 2017)

3.5.2.1.7 Determination of concentration of carbonate and bicarbonate ions

Determination of bicarbonate and carbonate ions was done by titrating the water samples with a standard sulphuric acid solution of 0.02 N using phenolphthalein indicator, till the pink color disappeared. The titrate volume was recorded (P) then two drops of mixed indicator (5:1, Bromocresol green: methyl red) were added to the resulting solution. Titration continued till color changed from blue to red. The second titrate volume was recorded (T).

Table 3.3 Relationship of OH Alkalinity, CO_3^{2-} Alkalinity, and HCO_3^- Alkalinity Titration

	Alkalinity due to;		
Value of P & T	**OH^-**	**CO_3^{2-}**	**HCO_3^-**
P=0	0	0	T
P< 1/2 T	0	2T-P	T-2P
P=1/2 T	0	2P	0
P> 1/2T	2P-T	2P-T	0
P=T	T	0	0

The titration was repeated for concordance values and the procedure repeated in all the samples. The carbonate and bicarbonate ion content of the water, samples, which was expressed as milligrams calcium carbonate per litre were determined from the relationship given (Table 3.2)

3.5.2.1.8 Determination of Sulphate Ions

In the determination of the sulphate ions the buffer solution was prepared by dissolving 30 g magnesium chloride, 5g sodium acetate, 1.0 g potassium nitrate and 20 ml acetic acid, CH_3COOH (99%), in 500 ml distilled water and topping up to 1000 ml. The preparation of standard sulphate solution was done by dissolving 0.1479 g anhydrous Na_2SO_4 in distilled water and made up to 1000 ml. 100ml sample was then measured and transferred into a 250-ml Erlenmeyer flask. 20 ml of the buffer solution were added and mixed in stirring apparatus. While stirring, a spoonful of $BaCl_2$ crystals was added and timing began immediately. Stirring was done for 60 s at a constant speed. After stirring, the resulting solution was poured into absorption cell of photometer and turbidity measured at 5 ± 0.5 min. Estimated SO_4^{2-} concentration in the sample were then determined by comparing turbidity reading with a calibration curve prepared by carrying SO_4^{2-} standards through the entire procedure. Standards were spaced at 5-mg/L increments in the 0 to 40 mg/L SO_4^{2-} range. Reliability of calibration curve was checked by running a standard with every three or four samples. Correction for sample color and turbidity was done by running blanks to which $BaCl_2$ had not been added. SO_4^2 concentration was determined directly from the calibration curve after subtracting sample absorbance before adding $BaCl_2$ (APHA 2017).

3.5.2.2 Ionic Balance Error

Percent charge-balance error analyses were also executed to assess the accuracy of the chemical analysis data of groundwater samples. Ion balance Error or Electroneutrality (E.N.) was calculated using equation (3-4).

$$\text{E.N. [\%]} = \frac{(\Sigma\text{cations} + \Sigma\text{anaions})\, meql}{(\Sigma\text{cations} - \Sigma\text{anaions})\, meql} \times 100 \quad \text{..... Equation 3.4}$$

The acceptable ion balance error should be below ±5% in many cases (Johnson 2016).

3.7 Data Management and Statistical Analysis

3.7.1 Statistical Analysis

Data were analyzed using IBM SPSS statistical packages. Hierarchical Cluster Analysis (HCA) and Principal Component Analysis (PCA) was used in interpretation of the results. PCA was used to extract principal components (PCs) using varimax rotation and only PCs with eigenvalue >1 was retained and p-value < 0.05 at 95 % confidence interval of the parameters were retained. Relationships for the test of parameters were detected through the Pearson correlation coefficient (one tailed at 95%). HCA was undertaken on the chemical parameters using Ward linkage method and based on the squared Euclidean distance between groups). Cluster analysis classifies the set of observed hydrochemical data within two or more groups based on combination of interval hydrochemical variables (Bu et al. 2020). The data was transformed or standardized prior to performing multivariate statistical analysis to ensure; data normality, changes in the weights of different species or variables as well as removing the effect of measurement units. All the variables were standardized to their standard scores (z-scores) according to Equation 3-1:

$$Zi = \frac{Xi - \mu}{S}$$ where, Zi is the standard score of the sample i, XI is the value of the sample i, μ is the mean, and S defines the standard deviation. The standardization process assigns each variable equal weight.

3.7.2 Chemical plots

Chemical variables for the sampling data were plotted and interpreted using the Piper, Durov, Wilcox and Scatter plot to demonstrate the groundwater facies for the study area using the software Aquachem and Microsoft Excel.

Aquachem is a software package developed specifically for graphical and numerical analysis and modelling of water quality data. Gibbs, Durov and Piper's plots were employed to explain the major geochemical processes controlling groundwater quality and to identify the hydrochemical facies in this aquifer. Wilcox plot was used to classify the salinity in groundwater within the boreholes for irrigation use.

3.7.3 Aquifer Characterization

The aquifer characterization utilized integration of lithological data and pump testing data from the boreholes. IBM SPSS was used to define the spatial graphs for the aquifer yield, water level and water strikes to classify the aquifers. Aquifer Test pro software was used to define the hydraulic parameters within the basement aquifer such as transmissivity, hydraulic conductivity and aquifer thickness.

3.7.4 Lineament mapping and geological maps

Spatial distribution and well's location maps were prepared using the ArcGIS v10.5 software. The inverse distance weighted (IDW) method was applied to prepare spatial maps. The high-end software ArcGIS was used for spatial mapping of the groundwater quality data and production of geological as well as hydrogeological maps. The maps were overlain on geology to understand the relationship between geology, topography and groundwater quality. Rockworks 17 was used to define the lithological section of each drilled borehole to define the lithological units per every drilled meter. Satellite image such as LANDSAT ETM of the area was downloaded from global land cover facility site to delineate the lineament of the study area. The automatic lineament extraction was carried out with the aid of the Line module of the PCI Geomatica software. The overlying of the filtered lineament was overlain on the geology of the area using Arc GIS software.

3.7.5 Water Quality Assessment

3.7.5.1 Domestic Use

The water quality parameters analyzed in the laboratory and in the field from groundwater samples were compared with international guidelines on drinking water (WHO 2018) and MS733:2013

standards set for boreholes and shallow well water. Filtration was done in the field as developing of microbial cultures and analysis was done in the laboratory.

3.7.5.2 Irrigation use

The concentrations of different parameters were interrelated, and irrigation indexes such as sodium adsorption ratio (SAR), Salinity Hazard, Exchangeable (ESR) Sodium Ratio, and magnesium Hazard (MH) were calculated to assess groundwater quality using FAO 1994 Irrigation Water Quality Index (Appendix 4). Wilcox plot was drawn using Aquachem 14 software also help in assessing the quality of basement aquifers for irrigation use.

CHAPTER FOUR: RESULTS

This chapter gives the results of the samples that were collected and analyzed from the deep boreholes (wells) in Lilongwe plain.

4.1 Determining the characteristics of the aquifers within the basement complex

The borehole analysis involved collection of data during drilling such as lithological logs, water strikes, and yield during drilling, collection of parameters test pumping parameters. This defines the characteristics of the aquifer within the basement complex.

4.1.1 Delineation of lithology within deep wells area

The delineation of borehole lithological logs Figure 4.1 describing lithological units encountered at 200m depth borehole.

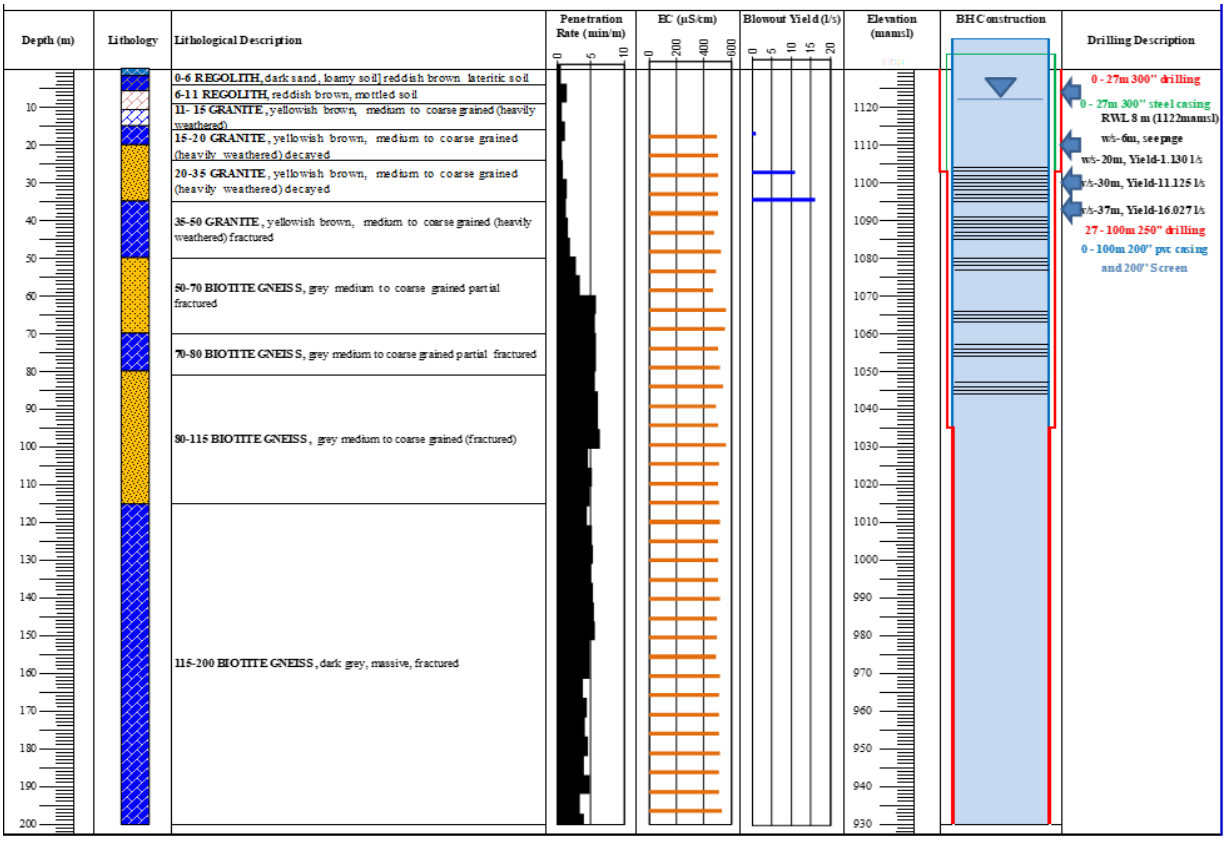

Figure 3.1: Lithological log of a borehole within the study area

The lithological data interpretation indicates the thickness of overburden, weathered zone, fractured zone and depth to fresh bedrock within the Lilongwe basement rock. This is essential for determining aquifer characteristics. The lithological log indicated a variation of the thickness of weathered regolith zone to 34m and fractured biotite gneiss was intercepted from 34m to 200m.

4.1.2 Hydrogeological properties within the wells

4.1.2.1Water strikes

The water strikes within the study area varies from as shallow as 2m to 198m.The shallowest water strikes are within the latosol and deeper water strikes are in fresh fractured basement gneiss (figure 4.2). The trend of most strikes in most boreholes occurs mostly occur at the following:

- Contact between weathered and fractured rock
- Close to the base of weathered aquifer or close to top of fractured aquifer
- Contact between two lithological units, with contacts between granite and another unit being the most productive

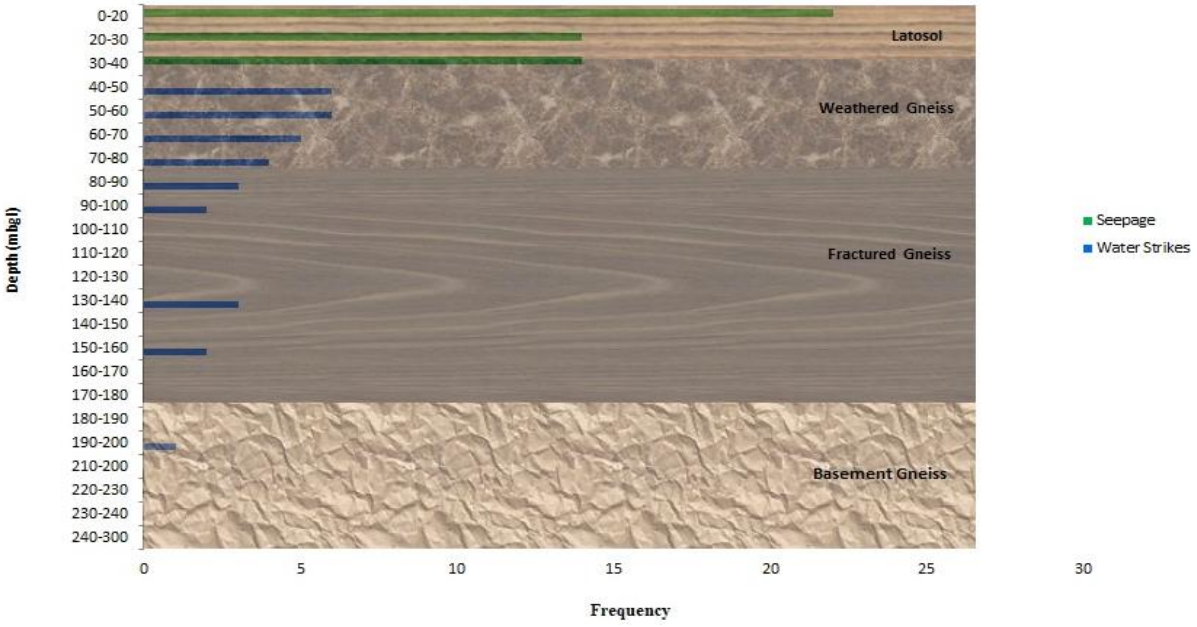

Figure 4.2: Frequency distribution of water strikes within lithological unit

The frequency distribution of the water strikes by depth and depth category show that 25% of water strikes occur at less than 20m depth and these are usually in the weathered rock and mostly latosol.

The borehole depth between 20m and 50m has the majority of water strikes within the drilled boreholes with 43% of the water strikes, 25% of the water strikes occurring between 50m and 100m, Figure 4.2. These water strikes occurring between 20m and 100m occur mostly at the contact or close to the contact between weathered rock and fractured rock. The depth of 100m to 300m has 7% of the water strikes which are associated with deep fracturing within the fractured rock. The data shows that the study area has high yielding, associated with vertical structures associated with deep fractures.

4.1.2.3 Borehole Yields

A frequency distribution of borehole yields from the study area shows that 74% of the deep boreholes have a yield of >1 l/s (>3.6m^3/hr), Figure 4.3.

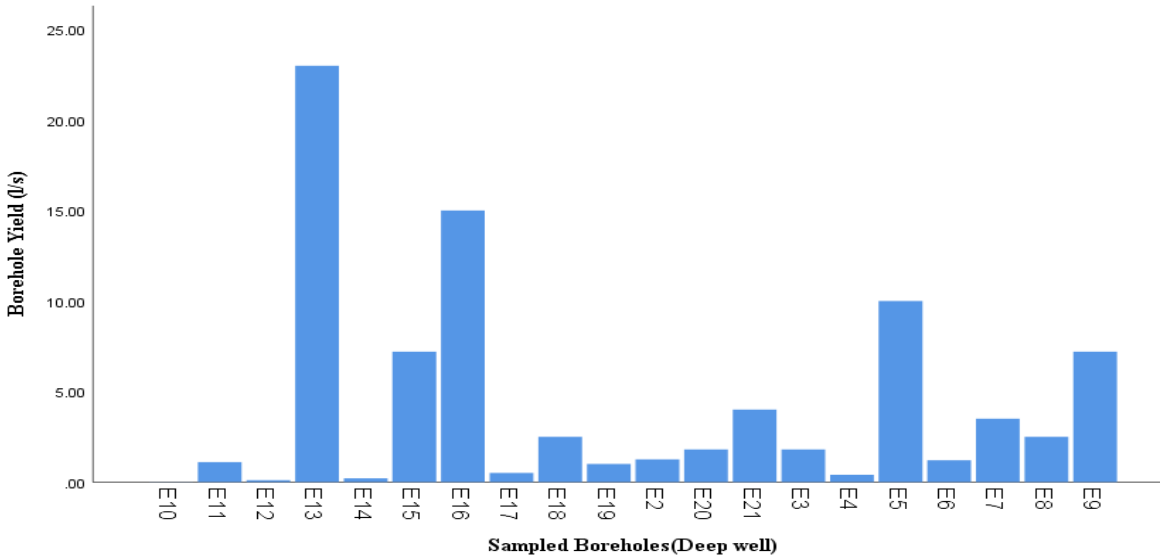

Figure 4.3: Borehole yields among deep wells (Exploration boreholes)

4.1.2.2 Groundwater levels

The groundwater levels reading was collected after drilling and before pumping test. The groundwater levels soon after drilling varied from 3.7m to 25m among the drilled deep wells within the study area, Figure 4. 4. The of groundwater levels from the deep boreholes indicates that most of the water levels after drilling are less than 20m, Figure 4.5.

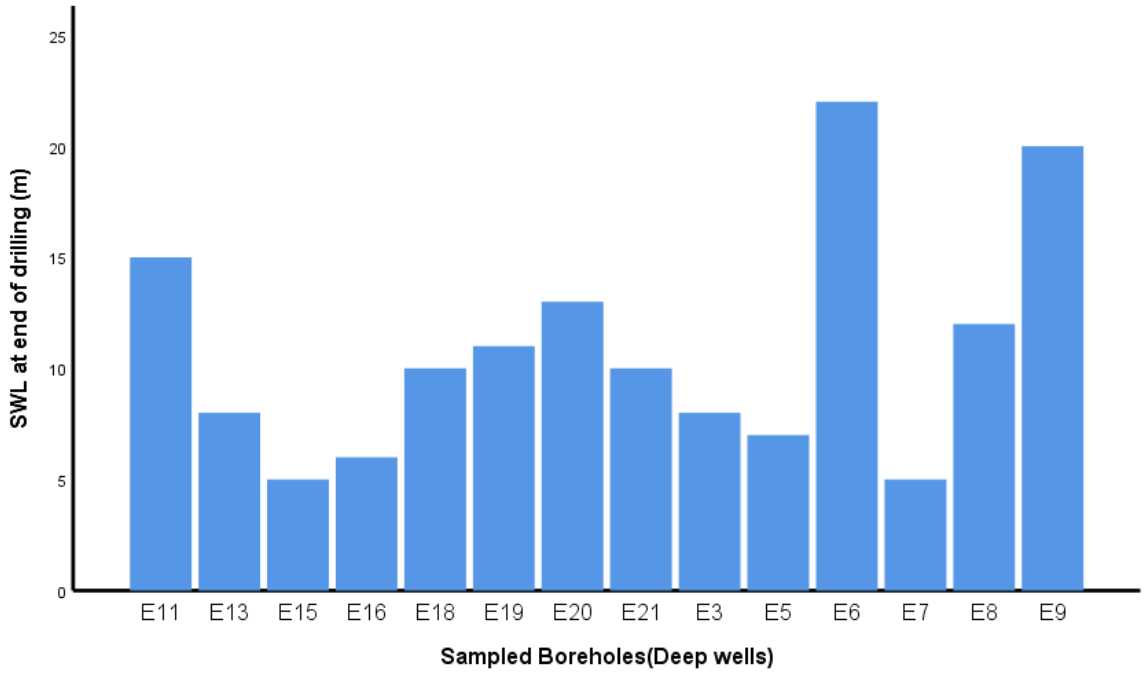

Figure 4. 4: Static water level at the end of borehole drilling

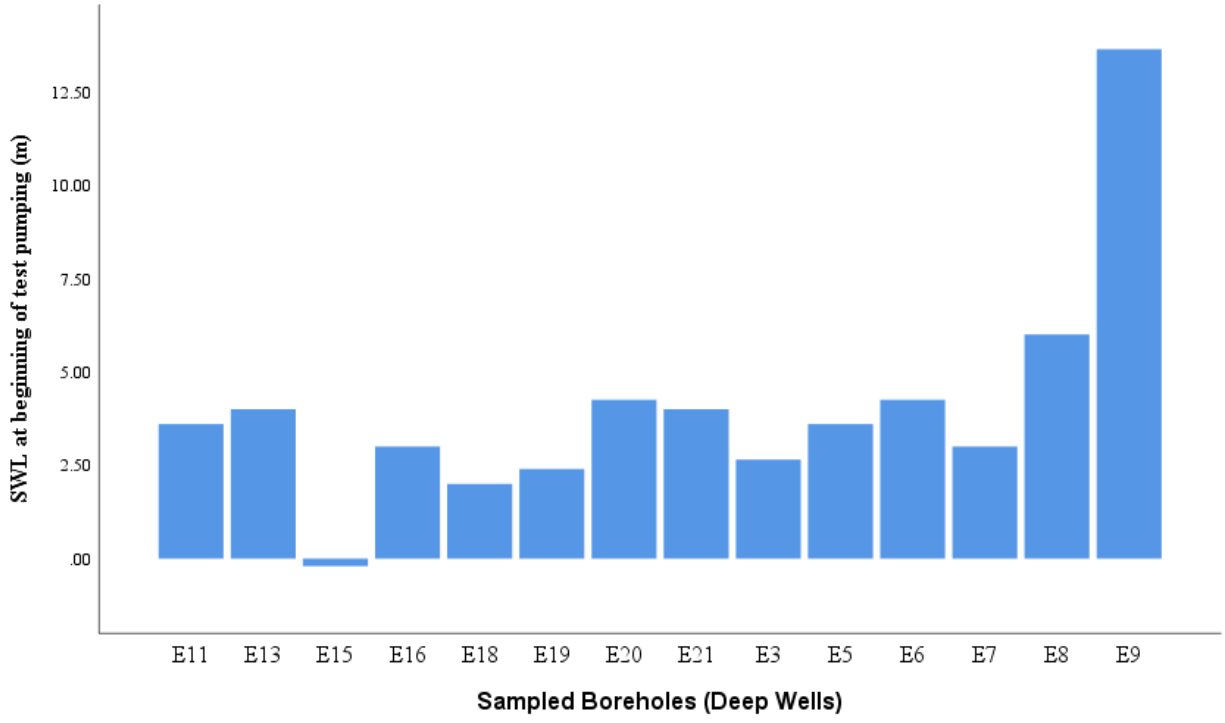

Figure 4.5: Static water level at the beginning of Pump testing

Table 4.1: Comparison of water Levels after drilling and before test pumping

BH	Easting	Northing	Elevation (m)	Depth (m)	SWL at end of drilling (m)	Static water level at beginning of test pumping (m)	Rise in water level (m)
E3	586508	8438985	1105	200	8	2.65	5.35
E5	567970	8468369	1140	200	7	3.6	3.4
E6	588649	8480894	1121	200	22	4.25	17.75
E7	548925	8487982	1176	262	5	3	2
E8	586508	8438985	1210	185	12	6	6
E9	573786	8480461	1219	200	20	13.64	6.36
E11	552431	8427961	1165	250	15	3.6	11.4
E13	566202	8460155	1130	200	8	4	4
E15	554284	8450227	1176	200	5	-0.2	5.2
E16	581189	8437858	1081	245	6	3	9
E18	568303	8455562	1124	299	10	2	8
E19	541844	8452726	1149	200	11	2.4	8.6
E20	588584	8428313	1161	200	13	4.25	8.75
E21	573593	8472233	1156	200	10	4	6

The groundwater level at the beginning of test pumping shows that it had risen above the depth to groundwater recorded soon after drilling in all of the tested boreholes, Figure 4.5. The rise in water levels among the deep boreholes is between 2m and 18m.

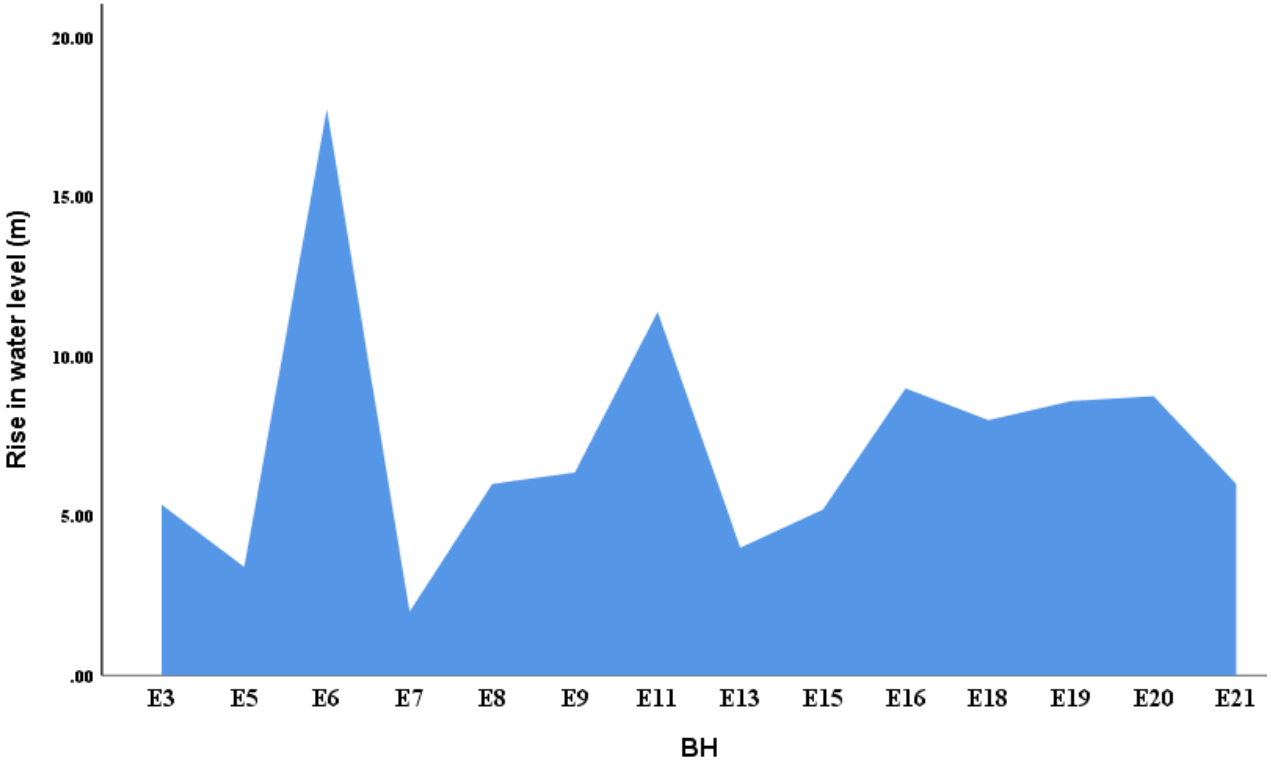

Figure 4.6: Rise in water level (m) in the boreholes

The most significant rise is in E6 and E11, with the least rise of 2m in E7. In borehole E15, the water level rises to 0.2m above the ground, showing the borehole is artesian, Figure 4.6 and Table 4.1.

4.1.3 Hydraulic characteristics of the deep wells

The results show that high specific capacity is associated with boreholes with high transmissivity, whereas lowest specific capacity in boreholes is associated with lowest transmissivity, (Table 4.2). Boreholes, E16, E9 and E21 in Table 4.2 indicate medium to high aquifer potential with transmissivity of 4m2/d to 8m2/d, boreholes E5, E13 and E15 have transmissivity of 10m2/d to 60m2/d with tested rates of 13 L/s to 20 L/s. The results indicate that high specific capacity is associated with boreholes with high transmissivity, whereas lowest specific capacity in boreholes is associated with lowest transmissivity, (Table 4.2)

Table 4.2: Calculated aquifer hydraulic parameters

Site	Depth	Test Duration (hrs.)	Test Pumping rate (m^3/hr.	Drawdown	Specific Capacity(m^3/hr./m)	Aquifer Transmissivity			
						Step test	Constant test	Recovery	Adopted
E3	200	72	3.60	32.40	0.10	4.50	4	2	4
E5	200	72	48	20.42	2.40	48	56	33	60
E6	200	72	9	101.90	0.09	1	1	0.50	1
E7	262	72	7.20	170.14	0.04	0.60	1	1	1
E8	185	72	3.60	54.37	0.14	6	1	1.20	1
E9	200	72	9	20.10	0.45	6.50	6	6	6
E11	200	72	3.60	206.24	0.02	1	2.60	3	2
E13	200	72	72	46.67	1.50	35	35	35	35
E15	200	72	9	20.14	0.45	11	8	10	10
E16	245	72	24	150.50	0.16	2	4	4	4
E18	299	72	7.20	204.50	0.35	0.46	1	1	1
E20	200	72	7.20	43.90	0.15	3	1.40	1.60	1.50
E21	200	72	9	10.85	0.90	14	8	8	8

4.2 Delineation of the hydrogeochemistry of the basement aquifers within the basement complex rocks

4.2.1. Hydrochemical parameters

The statistical summary of the result of the physical parameters, anions, cations, trace metals, and heavy metals are presented in Table 4.3. The physical chemical parameter within the basement aquifers, temperature ranges from 22°C to 29.1°C with an average 24.88 ±1.69°C, pH ranges from 6.6 to 7.9 with an average 7.35±0.37, EC ranges from 175 µS/cm to 795 µS/cm with an average of 436.12±172.96 µS/cm.

Table 4.3: Summary of descriptive statistics of chemical parameters

Parameters	Minimum	Maximum	Mean	Std. Deviation
Temp (°C)	22	29.1	24.88	1.69
pH	6.6	7.9	7.35	0.37
EC	175	795	436.12	172.96
TDS	112	520	253.3	104.06
HCO_3^-	75.6	349	184.97	79.62
SO_4^{2-}	9.1	56.8	28.6	12.53
Cl^-	8.4	47	22.61	9.9
CO_3^{2-}	0	13	2.32	3.73
F^-	0.08	0.92	0.43	0.24
NO_3^-	0.01	0.17	0.07	0.04
Ca^{2+}	14.4	72.9	41.8	17.39
Na^+	7.8	43	18.96	8.64
Mg^{2+}	6.7	31.9	16.68	7.4
K^+	0.5	6.7	2.56	1.56
Fe^{2+}	0.001	0.3	0.11	0.07
Mn^{2+}	0	0.19	0.07	0.06
Cu^{2+}	0	0.02	0.01	0.01
Zn^{2+}	0.01	1.46	0.09	0.31
Cd^{2+}	0.09	0.37	0.28	0.09
Pb^{2+}	0	0	0	0
Cr^{2+}	0	0	0	0
V^{2+}	-58	16	-15.1	22.27

Note: All concentrations in mg/l and EC in µS/cm

NA= Not applicable

The major anions within basement aquifers; HCO_3^-, SO_4^{2-}, Cl^-, CO_3^{2-}, F^- and NO_3^- range from 75.6 to 349mg/l, 9.1 to 56.8 mg/l, 8.4 to 47mg/l, o to 13mg/l, 0.08 to0.92mg/l and 0.01 to 0.17mg/l respectively. The average concentrations of anions; HCO_3^-, SO_4^{2-}, Cl^-, CO_3^{2-}, F^- and NO_3^- are 184±79.62mg/l, 28.6±12.53mg/l, 22.62±9.9 mg/l, 2.32±3.73, 0.43±0.24mg/l and 0.07±0.04mg/l respectively. The major cations within the basement aquifers; Ca^{2+}, Na^+, Mg^{2+} and K^+ range from14.4 to 72.9mg/l, 7.8 to 43 mg/l, 6.7 to 31.9mg/l and 0.5 and 6.7 mg/l respectively. The average concentration of the major cations within the basement aquifers; Ca2+, Na+, Mg2+ and K+ 41.8±17.39mg/l, 18.96±8.64mg/l, 16.68±7.4mg/l and 2.56±1.56mg/l respectively. The trace elements; Fe^{2+}, Zn^{2+}, Mn^{2+} and Cu^{2+}range from 0.001 to 0.3 mg/l, 0.01 to 1.46mg/l, 0 to 0.19mg/l and 0.02mg/l respectively and an average of 0.11±0.07mg/l, 0.09±0.31mg/l, 0.07±0.06mg/l and 0.01±0.01 mg/l respectively. The order of relative abundance of the major anions, cations and trace element are HCO_3^-> SO_4^{2-}> Cl^- >CO_3^{2-}>F^->NO_3^-, Ca^{2+}> Na^+> Mg^{2+}>K^+ and Fe^{2+}> Zn^{2+}> Mn^{2+}> Cu^{2+} respectively (Figure 4.7).

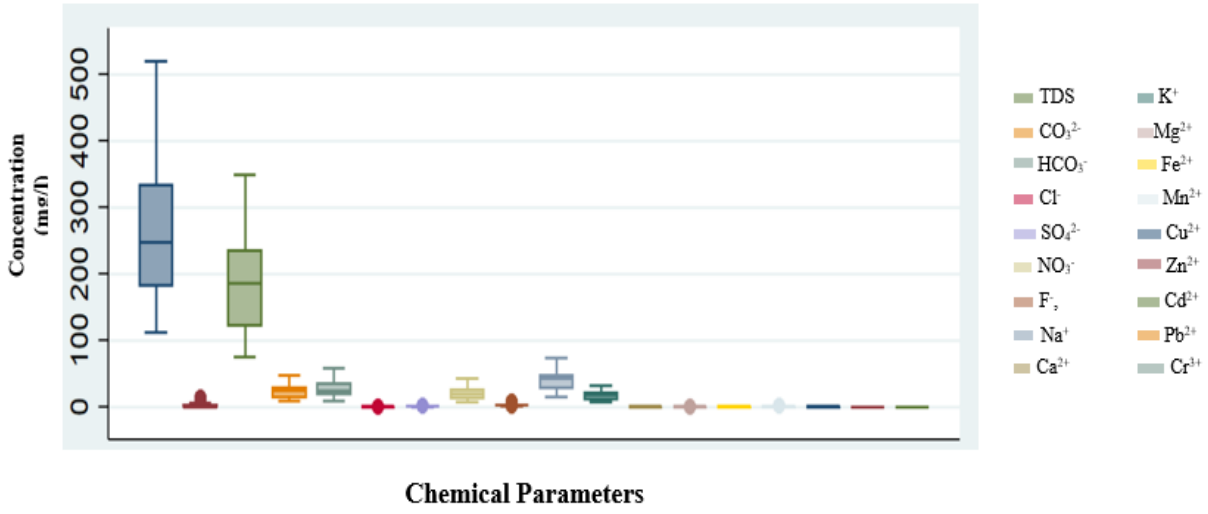

Figure 4.7: Ionic abundance of chemical parameters

4.2.2 Relationship of between chemical parameter within the basement aquifers

The statistical relationship between chemical parameters within basement aquifers was calculated using the Pearson correlation matrix (Table 4.4). The correction analysis displayed a moderate positive correlation at significance level 0.01 pH and CO_3^{2-}.

Table 4.4: Relationship between chemical parameters

	Temp	pH	EC	TDS	CO_3^{2-}	HCO_3^-	Cl^-	SO_4^{2-}	NO_3^-	F^-	Na^+	K^+	Ca^{2+}	Mg^{2+}	Fe^{2+}	Mn^{2+}	Cu^{2+}	Zn^{2+}	Cd^{2+}
Temp																			
pH	0.19																		
EC	0.14	0.1																	
TDS	0.13	0.14	.93**																
CO_3^{2-}	0.26	.58**	0.02	-0.2															
HCO_3^-	0.11	0.07	.99**	.95**	-0.1														
Cl^-	-0	-0	.88**	.89**	-0.2	.87**													
SO_4^{2-}	0.26	0.07	.74**	.57**	0.36	.64**	.48*												
NO_3^-	0.3	0.13	0.28	0.23	0.31	0.27	0.07	0.29											
F^-	-0.1	-0.2	-0	-0	0.08	-0.1	-0.1	0.17	-0										
Na^+	-0	0.01	.83**	.85**	-0.2	.82**	.97**	0.43	0.09	-0.1									
K^+	0.16	0.09	.76**	.58**	0.3	.68**	.64**	.79**	0.28	-0.2	.61**								
Ca^{2+}	0.22	0.16	.95**	.89**	0.09	.94**	.78**	.75**	0.24	0.07	.70**	.63**							
Mg^{2+}	0.1	0.04	.93**	.84**	0.03	.92**	.77**	.73**	0.39	-0.1	.71**	.83**	.82**						
Fe^{2+}	0.27	-0.1	0.3	0.28	-0.1	0.28	0.32	0.31	-0.2	0.19	0.26	0.11	.44*	0.06					
Mn^{2+}	0.31	0.25	0.03	0.07	0.24	0.04	-0.1	0.07	0.14	-0	-0.2	-0.1	0.24	-0.1	.50*				
Cu^{2+}	0.25	0.26	.47*	0.34	.52*	0.4	0.2	.62**	0.37	0.01	0.2	.48*	.52*	0.43	0.35	0.37			
Zn^{2+}	-0.1	-0	0.11	0.18	-0.2	0.15	0.21	-0.2	-0.1	0	0.24	0.05	0	0.17	-0.2	-0.2	-0.2		
Cd^{2+}	-0.3	0.06	-0.3	0.03	-.44*	-0.2	-0	.54*	-0.3	-0.1	-0.1	-0.48*	-0.2	-0.3	-0.2	0.2	-0.4	0.18	

Note:

** Correlation is significant at the 0.01 level (2-tailed).

* Correlation is significant at the 0.05 level (2-tailed).

The strongest positive correlation of EC also occurs with cation (Ca^{2+}, Mg^{2+}, Na^{+}, K^{+}) and anion (Cl^{-}, SO_4^{2-}). The strong positive correlation occurs between an anion (HCO_3^{-}) with cation (Ca^{2+}, Mg^{2+}, Na^{+}, K^{+}) and anion (Cl^{-}, SO_4^{2-}). Anion (Cl^{-}) is strongly positively correlated with cations (Na^{+}, Ca^{2+}, Mg^{2+} and K^{+}). Positive correlation of anion (SO_4^{2-}) occurs with cations (K^{+}, Ca^{2+}, Mg^{2+}) and trace metal (Cu^{2+}). Cation (Na^{+}) has correlation with cations (Mg^{2+}, Ca^{2+} and Ka^{+}) but cation (K^{+}) is positively correlated with cations (Mg^{2+} and Ca^{2+}). The strong positive correlation among cations occurs between Ca^{2+} and Mg^{2+}. At significant at the 0.05 level EC is the only physical chemical parameters showing weak positive correlation with trace element (Cu^{2+}). The weak positive correlation also occurs between anions Cl^{-} and SO_4^{2-}, as well as between anion (SO_4^{2-}) and heavy metal (Cd^{2+}). The cation (K^{+}) has weak positive correlation with trace metal (Cu^{2+}) and heavy metal (Cd^{2+}) but cation (Ca^{2+}) has a weak positive correlation with trace metal (Fe^{2+}, Cu^{2+}). The weak positive correlation among trace metals occurs between Fe^{2+} and Mn^{2+}. The correlation show that most dominant constituents are Ca^{2+}, Mg^{2+}, Na^{+}, HCO_3^{-}, SO_4^{2-} and Cl^{-}. Ca^{2+} is the most dominant cation, with HCO_3^{-} being the most dominant anion.

4.3 Spatial relationship of geological structures on groundwater geochemistry and groundwater flow within the deep basement aquifers

4.3.1 Hydrochemical variation within basement aquifers

The PCA was used understand sources of chemical parameters within the basement aquifers Five principal components with eigenvalues above 1, were extracted. (Table 4.5). PC1 registered positive loading in EC, TDS, HCO_3^{-}, Cl^{-}, SO_4^{2-}, Na^{+}, Ca^{2+} and Mg^{2+} which controlled 38.4% of the variation. PC2 register positive loading in SO_4^{2-}, strong negative loading in Cd^{2+} and controlled 14.3% of the variation. PC3 registered positive loading in Fe^{2+} and Mn^{2+} and controlled 11% of the variations. PC 4 registered positive loading in CO_3^{2-} and pH and controlled 10% of the variation. PC 5 registered a positive loading in F^{-} and controlled 6.66% of the variation. The five factors together controlled 80.31% of the variations, Table 4.5. The parameters which registered high positive loading in PC1 (EC, TDS, HCO_3^{-}, Cl^{-}, SO_4^{2-}, Na^{+}, Ca^{2+} and Mg^{2+}.

The PC1 shows the dissolution of the geological component from rock-water interaction, PC2 show the presence of deep-seated faults through the variation of SO_4^{2-} and Cd^{2+}.

PC3 indicate the presence of high evaporation with in the basement aquifers and regional groundwater flow with deep seated faults. PC 4 indicate the dissolution of carbonate mineral within basement aquifers and PC 5 shows little minor influence of water-rock interactions within deep aquifers. All these have been well shown in correction matrix of the PCA in table 4.6 and 4.7.

Table 4.5: Component matrix showing rotated factor loadings

Parameters	**Component**				
	1	2	3	4	5
Temp	0.03	0.37	0.51	0.1	-0.36
pH	0.06	-0.09	0.05	**0.87**	-0.18
EC	**0.97**	0.2	0.08	0.07	0.01
TDS	**0.96**	-0.07	0.1	0.07	-0.04
CO_3^{2-}	-0.1	0.51	0.05	**0.77**	0.14
HCO_3^-	**0.97**	0.11	0.08	0.02	-0.05
Cl^-	**0.95**	-0.07	-0	-0.1	-0.01
SO_4^{2-}	**0.61**	**0.63**	0.19	0.12	0.20
NO_3^-	0.17	0.48	-0	0.3	-0.28
F^-	-0.1	0.08	0.04	-0.1	**0.89**
Na^+	**0.91**	-0.05	-0.1	-0.1	-0.04
K^+	**0.7**	0.54	-0.1	0.11	-0.15
Ca^{2+}	**0.89**	0.17	0.3	0.14	0.10
Mg^{2+}	**0.89**	0.32	-0.1	0.06	-0.1
Fe^{2+}	0.29	-0.01	**0.78**	-0.2	0.29
Mn^{2+}	-0	-0.16	**0.82**	0.37	-0.03
Cu^{2+}	0.33	0.5	0.39	0.42	0.10
Zn^{2+}	0.25	-0.37	-0.5	0.09	0.07
Cd^{2+}	-0.1	**-0.89**	-0	0.06	-0.13
% of Variance	38.4	14.3	11	10	6.66
Cumulative %	38.4	52.6	63.6	73.6	80.31

Note: The bolded figures show the strong factor loadings in the principal components analysis.

Table 4.6: Relationship between chemical parameters showing distribution

	Temp	pH	EC	TDS	CO_3^{2-}	HCO_3^-	Cl^-	SO_4^{2-}	NO_3^-	F^-	Na^+	K^+	Ca^{2+}	Mg^{2+}	Fe^{2+}	Mn^{2+}	Cu^{2+}	Zn^{2+}	Cd^{2+}
Temp	1																		
pH	0.19	1																	
EC	0.14	0.1	1																
TDS	0.13	0.14	**0.93***	1															
CO_3^{2-}	0.26	**0.58***	0.02	-0.2	1														
HCO_3^-	0.11	0.07	**0.99***	**0.95***	-0.1	1													
Cl^-	-0.01	-0	**0.88***	**0.89***	-0.18	**0.87***	1												
SO_4^{2-}	0.26	0.07	**0.74***	**0.57***	0.36	**0.64***	0.48	1											
NO_3^-	0.3	0.13	0.28	0.23	0.31	0.27	0.07	0.29	1										
F^-	-0.11	-0.2	-0	-0	0.08	-0.1	-0.1	0.17	-0	1									
Na^+	-0.05	0.01	**0.83***	**0.85***	-0.19	**0.82***	**0.97***	0.43	0.09	-0.13	1								
K^+	0.16	0.09	**0.76***	**0.58***	0.3	**0.68***	**0.64***	**0.79***	0.28	-0.23	0.61	1							
Ca^{2+}	0.22	0.16	**0.95***	**0.89***	0.09	**0.94***	**0.78***	**0.75***	0.24	0.068	0.7	**0.63***	1						
Mg^{2+}	0.1	0.04	**0.93***	**0.84***	0.03	**0.92***	**0.77***	**0.73***	0.39	-0.11	0.71	**0.83***	**0.82***	1					
Fe^{2+}	0.27	-0.1	0.3	0.28	-0.08	0.28	0.32	0.31	-0.2	0.189	0.26	0.11	0.44	0.06	1				
Mn^{2+}	0.31	0.25	0.04	0.07	0.24	0.04	-0.1	0.07	0.14	-0.03	-0.24	-0.1	0.24	-0.1	**0.50***	1			
Cu^{2+}	0.25	0.26	0.47	0.34	**0.52***	0.4	0.2	**0.62***	0.37	0.007	0.2	0.48	**0.52***	0.43	0.35	-0.37	1		
Zn^{2+}	-0.12	-0	0.11	0.18	-0.15	0.15	0.21	-0.2	-0.1	-0	-0.24	0.05	0	0.17	-0.1	0.22	-0.23	1	
Cd^{2+}	-0.3	0.06	-0.3	0.03	-0.44	-0.2	-0	-0.5	-0.3	-0.12	-0.07	-0.5	-0.2	-0.3	-0.2	0.2	-0.43	0.18	1

*Means there is a strong relationship between the chemical parameters

Note: All units= mg/l except EC= µS/cm and Temp= °C

Table 4.7: The significant level in the chemical parameters

	Temp	pH	EC	TDS	CO_3^{2-}	HCO_3^-	Cl^-	SO_4^{2-}	NO_3^-	F^-	Na^+	K^+	Ca^{2+}	Mg^{2+}	Fe^{2+}	Mn^{2+}	Cu^{2+}	Zn^{2+}	Cd^{2+}
Temp																			
pH	0.21																		
EC	0.28	0.33																	
TDS	0.3	0.27	**0***																
CO_3^{2-}	0.13	**0***	0.46	0.26															
HCO_3^-	0.31	0.38	**0***	**0***	0.33														
Cl^-	0.49	0.47	**0***	**0***	0.22	**0***													
SO_4^{2-}	0.12	0.38	**0***	**0***	0.06	**0***	0.01												
NO_3^-	0.09	0.29	0.11	0.16	0.09	0.12	0.39	0.1											
F^-	0.33	0.15	0.44	0.44	0.36	0.38	0.36	0.23	0.45										
Na^+	0.42	0.48	**0***	**0***	0.21	**0***	**0***	0.03	0.35	0.3									
K^+	0.24	0.35	**0***	**0***	0.09	**0***	**0***	0	0.11	0.15	**0***								
Ca^{2+}	0.17	0.25	**0***	**0***	0.35	**0***	**0***	0	0.15	0.39	**0***	**0***							
Mg^{2+}	0.33	0.43	**0***	**0***	0.46	**0***	**0***	0	0.04	0.32	**0***	**0***	**0***						
Fe^{2+}	0.12	0.34	0.09	0.11	0.37	0.11	0.08	0.08	0.19	0.21	0.13	0.31	0.02	0.39					
Mn^{2+}	0.09	0.14	0.44	0.38	0.15	0.43	0.3	0.38	0.27	0.46	0.15	0.34	0.15	0.35	0.01				
Cu^{2+}	0.13	0.13	0.02	0.07	0.01	0.03	0.2	0	0.05	0.49	0.2	0.01	0.01	0.03	0.06	0.05			
Zn^{2+}	0.3	0.47	0.32	0.22	0.26	0.26	0.18	0.19	0.37	0.5	0.15	0.41	0.5	0.24	0.26	0.17	0.16		
Cd^{2+}	0.09	0.4	0.14	0.44	0.02	0.22	0.45	0.01	0.1	0.31	0.39	0.01	0.15	0.09	0.2	0.20	0.03	0.22	

* Correlation is significant at $\rho>0.5$

Note: All units= mg/l except EC= µS/cm and Temp= °C

4.3.2 Hydrochemical classification of basement aquifers

The hydrochemical classification of the basement data was done using the Hierarchical Cluster Analysis (HCA) using Ward linkage method based on the squared Euclidean distance between groups) on chemical variables. HCA applies the Euclidean separation technique as a similarity measure to distinguish between groundwater samples based on their hydrochemical characteristics. The dendrogram figure 4.8, obtained for both chemical parameters and general clustering of the groundwater samples in the study area.

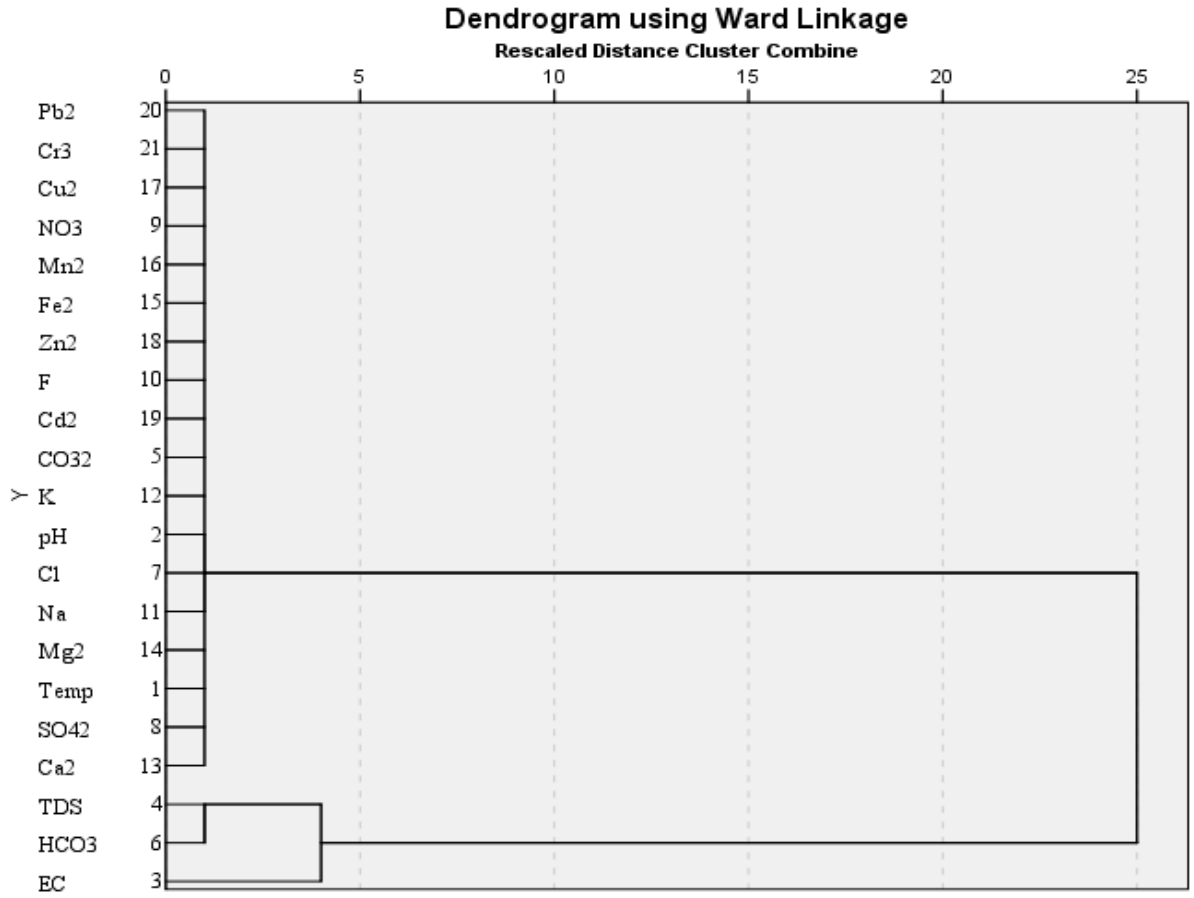

Figure 4.8: Dendrogram for hydrochemical variables within basement aquifers

Both chemical parameters and groundwater samples shows two clusters (C1 and C2). C1 has more chemical parameters and more groundwater sample site. C1 has Ca^{2+}, SO_4^{2-}, Temp, Mg^{2+}, Na^{+}, Cl^{-}, pH, K^{+}, with groundwater samples site of 13,8,1,14,11,7, 2,12,5,19,10,18,15,16,17,21,20 respectively. C2 has only three chemical parameters within three sample sites.

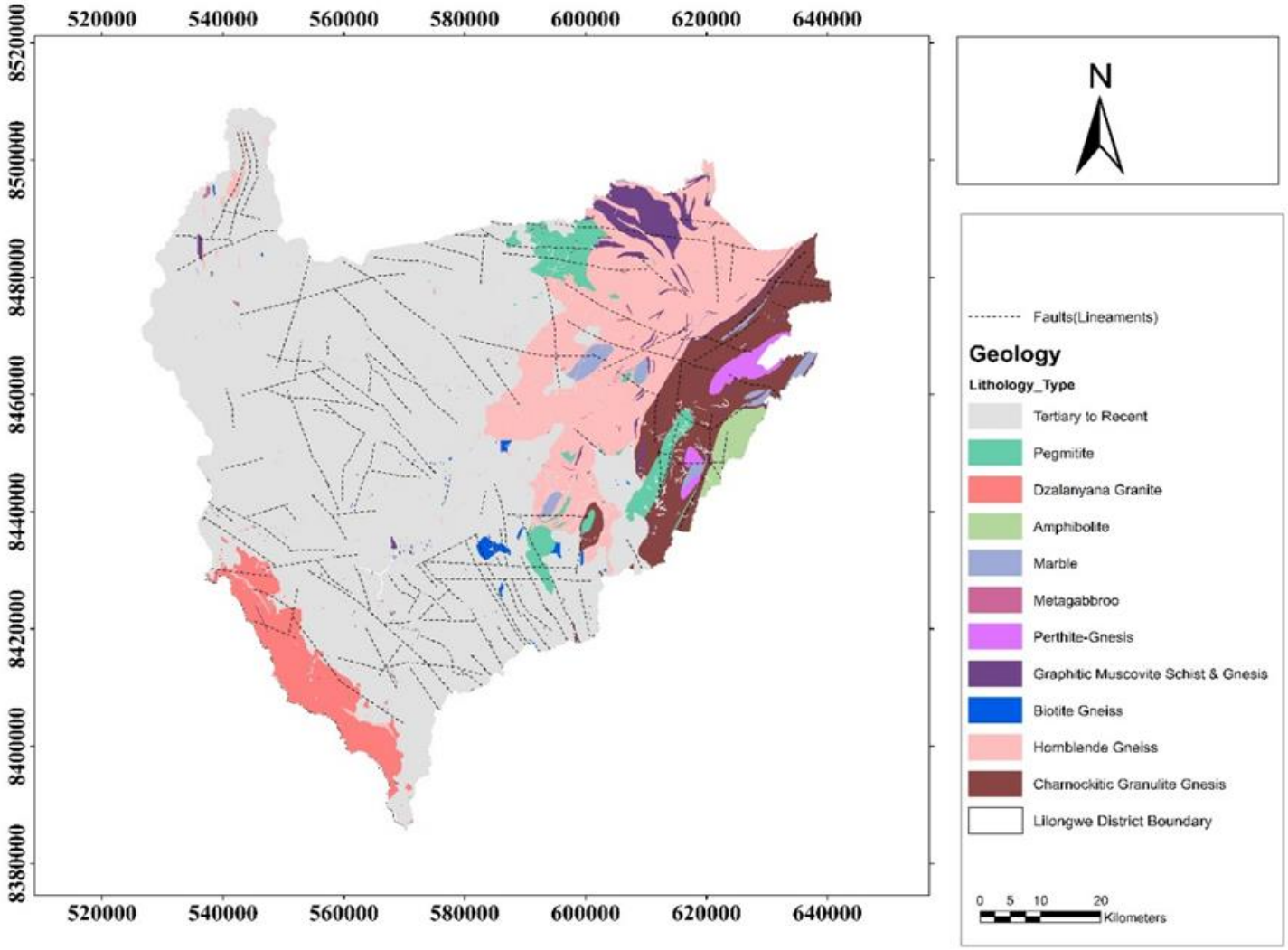

Figure: 4.9: Spatial occurrence of geological structures/ lineament within the study area

The clustering of TDS, HCO3- and EC shows that HCO3- is the only iron present in the deep aquifers influencing TDS and EC.

4.3.3 Spatial occurrence of geological structures/lineament within the study area

The structural interpretation through structural mapping, image processing and enhancement produce delineate lineaments and lithological contacts within the study area. The study area is mostly covered by the Archaean basement complex which was well displayed by the homogeneity in the aeromagnetic data. Aeromagnetic signatures showed differences in terms of lithology, differentiating between banded gneiss and granitic gneisses. Subtle variations in magnetic susceptibility also suggested different depths of burial of the basement geology below superficial cover. The lineaments are regional and were confirmed with high yielding boreholes along it showing the presence of regional aquifers with high groundwater potential. The results from the study area indicate the absence of dyke type of structures, the dyke could be too thin and therefore masked by the basement aeromagnetic signatures. The results show that the main faults and fracture directions are NNE-SSW, E-W, NE-SW and NW-SE occurring within the study area Figure 4.9.

4.4 Assessment of the groundwater quality for domestic and irrigation use

4.4.1 Domestic Use

The assessment of the groundwater quality for domestic use was compared with the chemical, physical and biological standards of WHO 2018 and MS733:2013. The results, Figure 4.10, shows that basement aquifers contain water that are within the standard limit of WHO 2018 and MS 733:2013. The basement aquifers indicate that 95% of them are within the MS733:2013 standard limit and does not contain faecal Streptococci in Appendix 4 B and Figure 4.11.

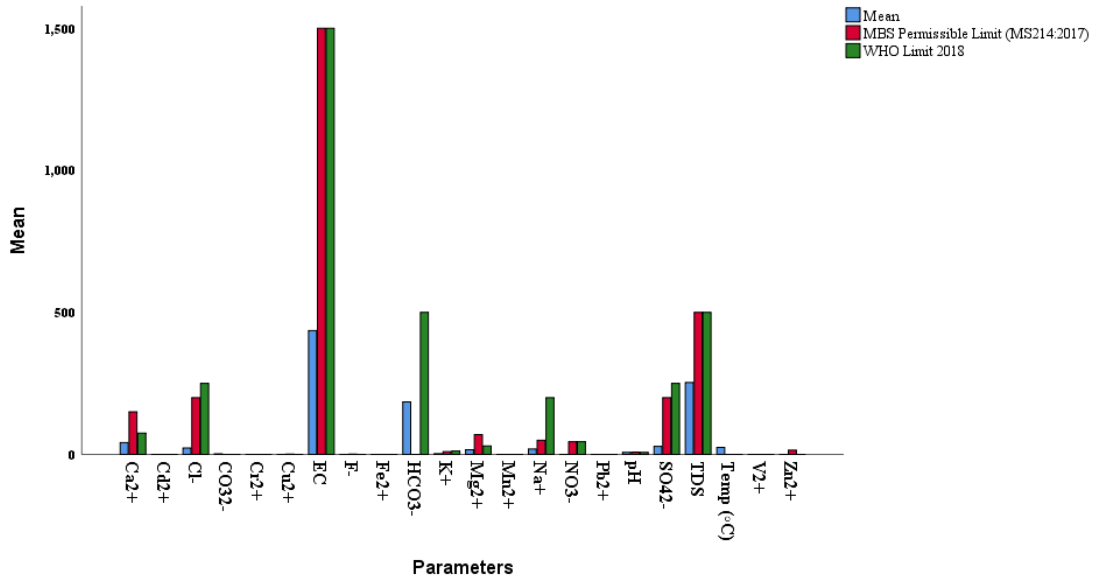

Figure 4.10: Groundwater quality within basement aquifers

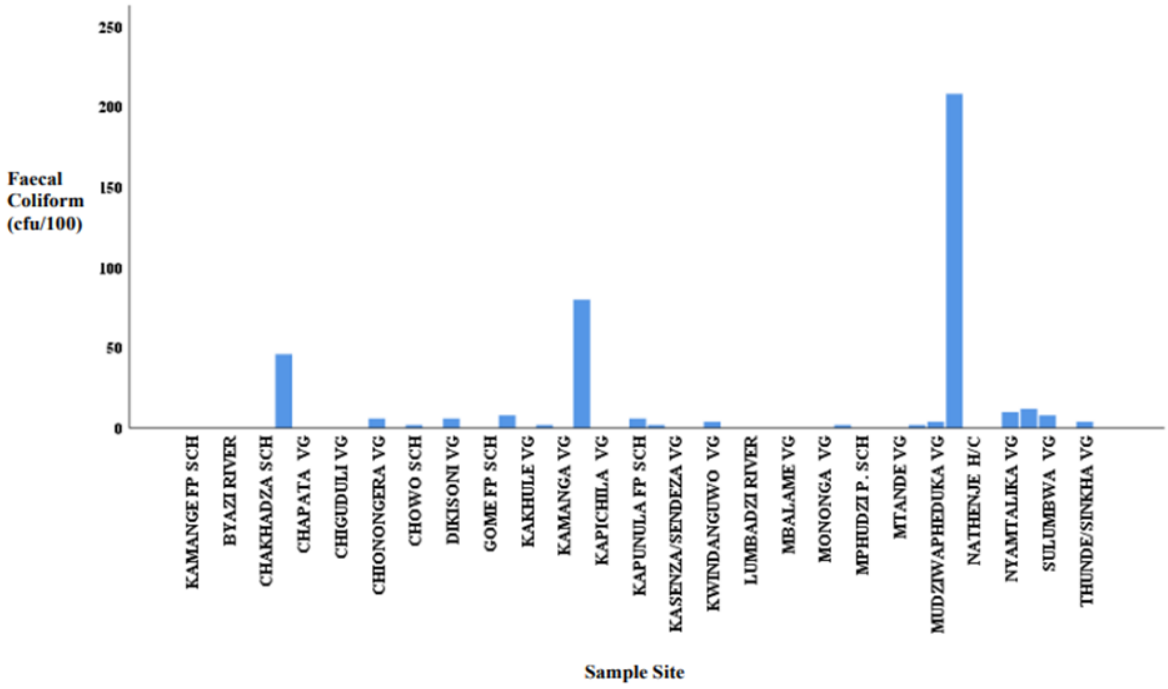

Figure 4.11: Faecal coliform within the basement aquifers

4.4.2 Irrigation purposes

The results for irrigation water quality using FAO 1994 irrigation water quality indices (WQI); Sodium Absorption Ratio (SAR), Permeability Index (PI), Sodium Percentage (%Na), Residual sodium carbonate (RSC), Magnesium Hazard (MH) or Magnesium Adsorption Ratio (MAR), Kelly Ratio and Corrosivity Ratio (CR) are presented in **Table 4.8** and **Appendix 5.**

Table 4.8: Statistical analysis of calculated irrigation water quality index

Parameter	SAR	PI	Na%	MH%	RSC	KR	CR	TDS	TH
Min	0.18	54.24	6.38	17.65	-0.40	0.08	0.24	112	2.38
Max	0.93	136.89	31.64	48.51	2.36	0.58	0.50	520	11.20
Mean	0.46	87.80	16.30	33.50	0.87	0.23	0.34	255	6.85
Std. Deviation	0.19	23	6.48	7.04	0.61	0.12	0.07	95	2.88

The results show that basement aquifers within the study area contains water that is suitable for irrigation use.

4.4.2.1 Classification and distribution of the groundwater salinity

The classification and distribution of the groundwater salinity (EC) using salinity classification shows that 19% of the boreholes have low salinity hazards are low, 71% of the boreholes have moderate salinity hazard and 10% of the boreholes have high salinity hazard (Figure 4.12).

The Wilcox Plot of EC against the percentage of sodium (Na) (Figure 4.13), classified groundwater within the study area to be of medium salinity and sodium, with few of low and high salinity as well as sodium concentration. The results show most samples fall within low and medium (C1 and C2), this indicates that these aquifers have no threats for irrigation use. The few samples falling in C3 have threats to irrigation use and can used with a caution.

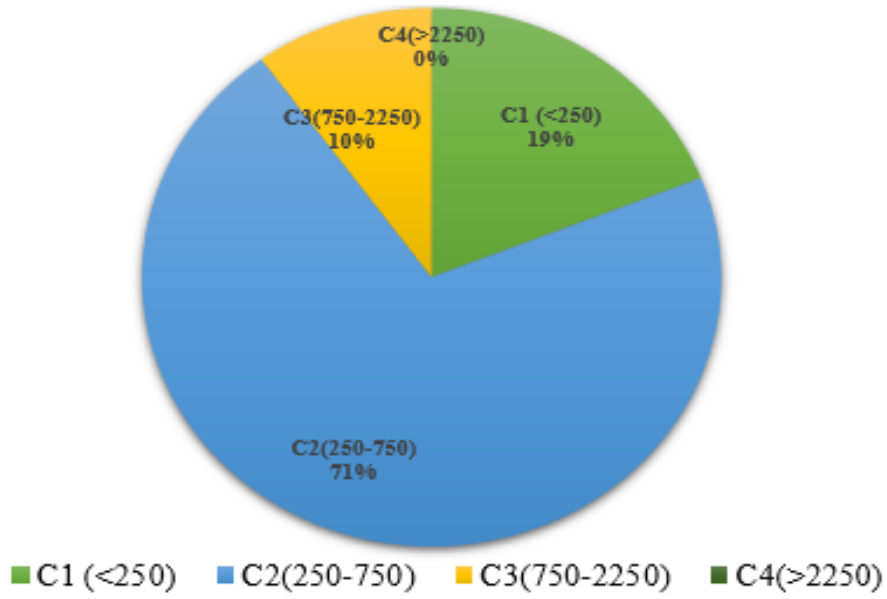

Figure 4.12: Percentage of Salinity Level within basement aquifers

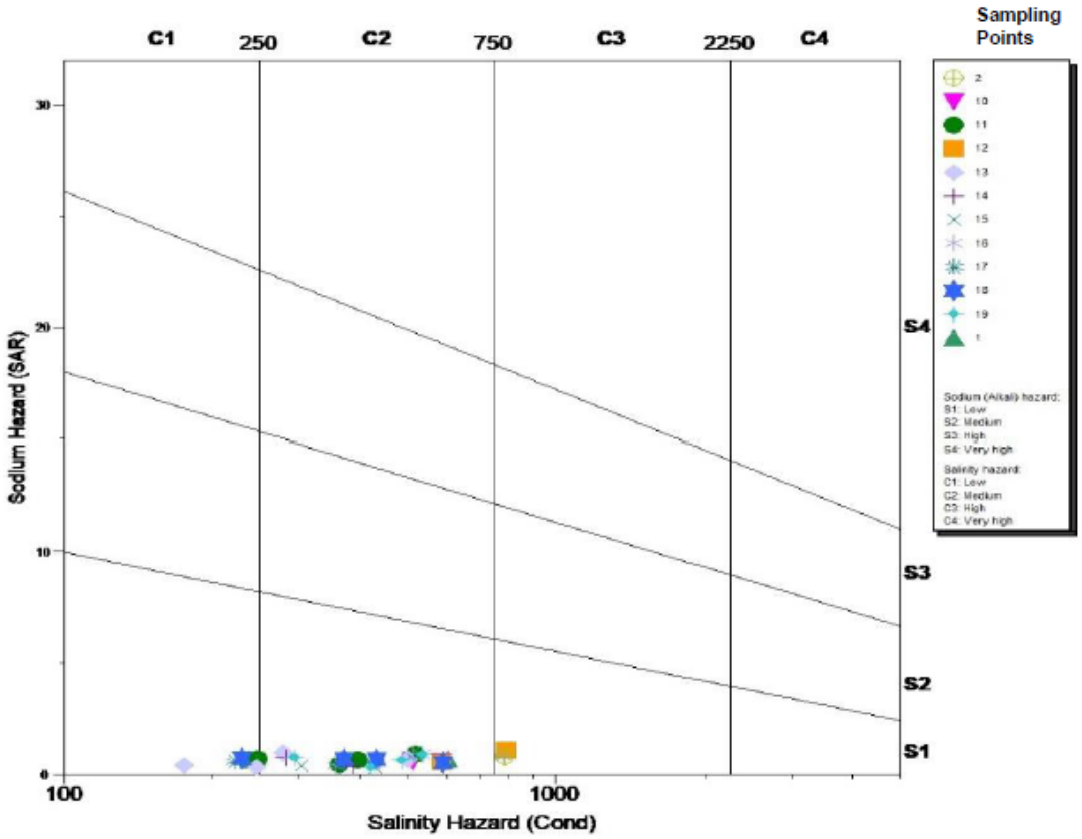

Figure 4.13: Classification of Sodium Hazard using Wilcox Diagram

CHAPTER 5: DISCUSSION

5.1 Characterization of basement aquifers

5.1.1 Aquifer type classification

It was observed that the comparison of the rest water level and the first water strike shows that water levels rise above the water strike. This shows aquifer conditions of confined to semi-confined aquifer, with the weathered aquifer being semi confined and the fractured deeper aquifer wholly confined (Woessner at al. 2023). Worthington 2022 stated that in the absence of any rainfall during the drilling period, this rise cannot be attributed to rainfall recharge but to confined aquifer conditions. The study classified aquifers based on the analysis of borehole yield data into two-aquifer group occurring in the study area and differs in the yields differ which vary significantly:

- Fracture aquifer
- Weathered aquifer

5.1.1.1 Fractured Basement Aquifers

The present study observed that fractured basement contains secondary porosity which enhance interconnectivity among fractures and other geological structures. These are groundwater flow conduits such as pegmatite veins and lithological contacts (Woessner at al. 2023). The study found out that there is high hydraulic conductivity in fractured under superficial, fracture under regolith and fractured out cropping most boreholes of the west as compared to the east of the study area, Figure 5.1. Yield in the west is high among the boreholes along the regional lineaments, on or close to geological contacts and the borehole yield, Figure 5.2, shows that 70% of yield in fractured aquifers is between 0.5 –7.0 l/s. Mkandawire 2004; Mapoma and Xie 2013, state that the yield indicate that fractured aquifers are highly variable and highly heterogeneous aquifer. The study also observed that fracture aquifer where groundwater circulates in fractures, fissures and joints in outcropping basement gneiss without significant cover have very low yield. These aquifers are found to the eastern part of the study area. Woessner at al. 2023 and Worthington 2022, state that these areas, runoff is more significant to the opposite of the area such as the west the study area, hence groundwater recharge is minimal.

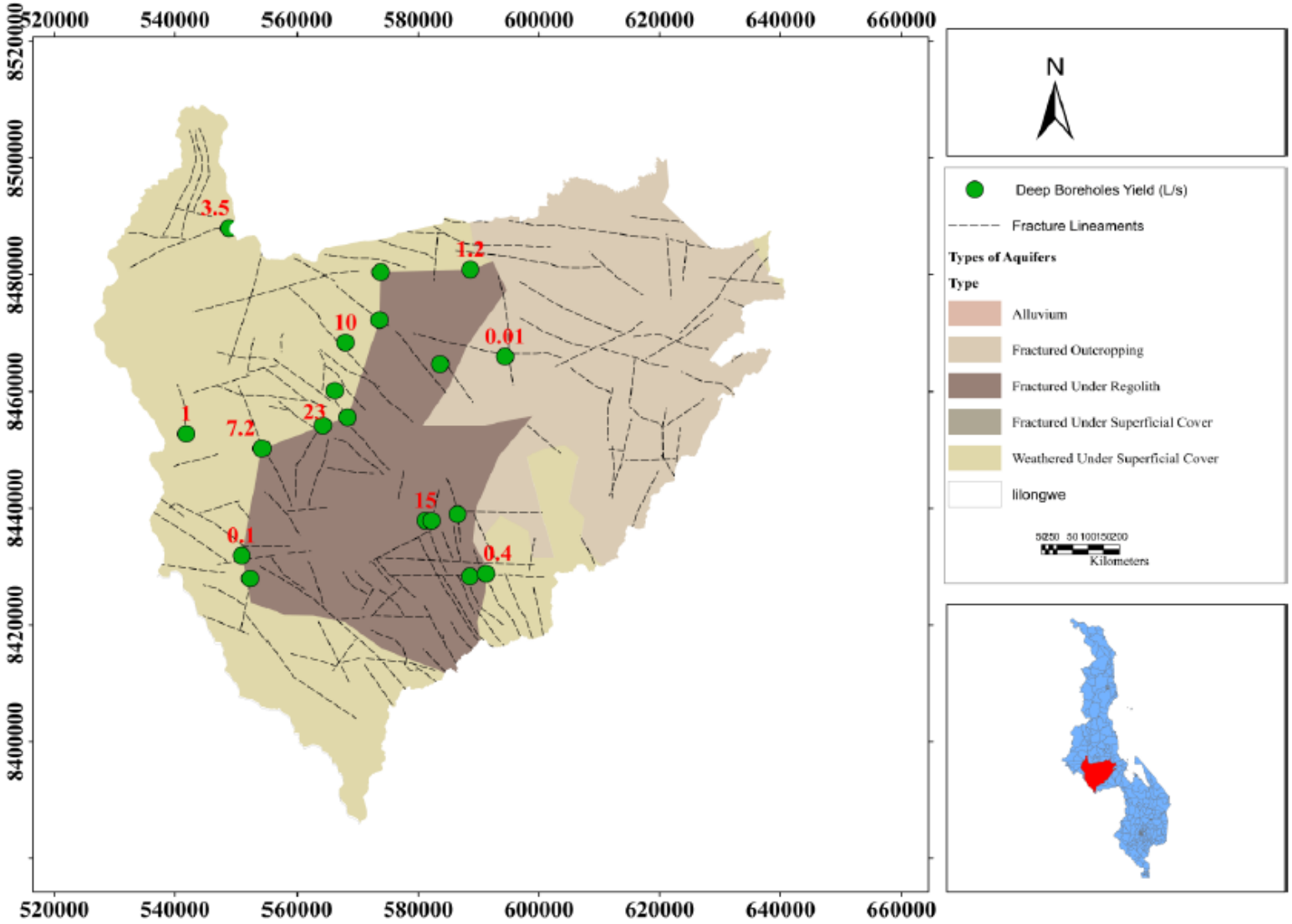

Figure 5.1: Types of aquifers and their yield (Red numbers)

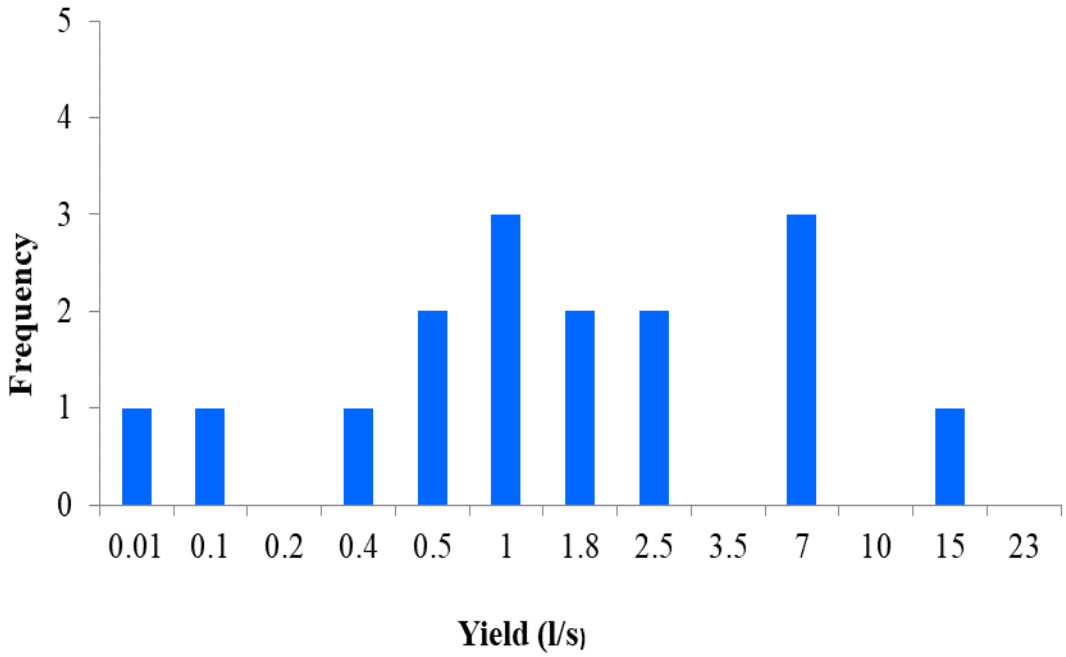

Figure 5.2: Yield in fractured rock zone

The study observed the presence of regolith fractures occurring within the weathered zone in the west and central part of the study area. Lachassagne et. 2021, state that the groundwater circulation in regolith is associated with fractures, fissures and joints with thick usually unsaturated to semi-saturated weathered regolith and significant superficial cover. The degree of fracturing is higher and deeper than fracture outcropping aquifers as the regolith stores more water, eventually percolating into the fractured zone.

5.1.1.2 Weathered Basement aquifers

The present study observed the presence of weathered basement is a layer of unconsolidated material which forms an extensive zone with a thin or thick aquifer in lithological logs. The groundwater circulates in intergranular pores created by deep weathering (Mapoma and Xie 2013). Due to superficial cover, infiltration is high, thus increasing rate of groundwater recharge. Depth of weathering is deep and fresh bedrock was usually intercepted below the weathered aquifer, with no further water strikes below the weathered aquifer (Mkandawire 2004; Mapoma and Xie 2013). The upper part has low permeability mostly associated with seepage, (Figure 5.1 and 5.3) and contains latosols and clay horizons.

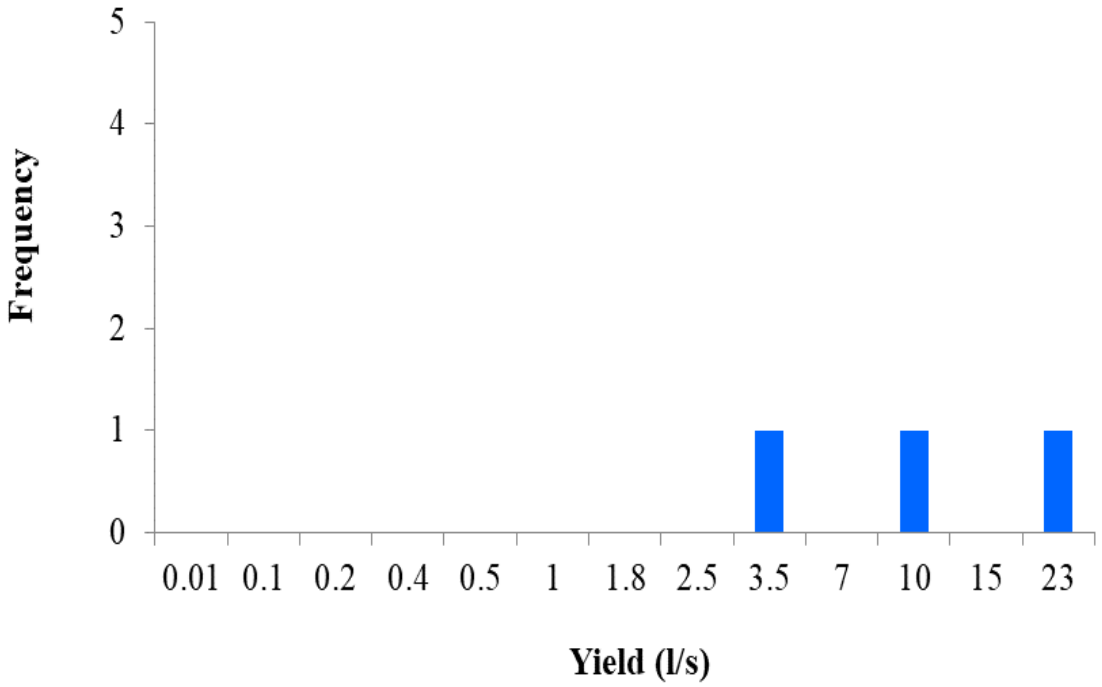

Figure 5 3: Yield in Weathered rock zone

These clay horizons, which form an aquitard, result in semi-confinement of both the weathered and fractured aquifer. Contrary to the studies by Lachassagne et al. 202, the present study found out that weathered aquifers contain high yield aquifers. It was observed that high yielding aquifers occurs within the saprolite and sapprock zone of the weathered basement, his also forms a transitional zone to the fractured zone and fresh basement rocks. The high yields occur at the base of the weathered rock, Figure 4.1 but depths of weathering have to be in excess of 40m. The frequency of high yield in the weathered aquifer is between 3.5 l/s to 23 l/s, Figure 5.4 which is occurring only in three deep boreholes within the study area. This indicate that low to medium variability and moderate heterogeneous (Worthington 2022 and Woessner at al. 2023).

5.1.2 Aquifer hydraulic characteristics

It was observed that high aquifer transmissivity (Figure 5.6) occurs in the central part going towards the western part of the study area which has both the weathered and fractured gneiss basement aquifers (Figure 5.1).

The graphical presentation (Figure 5.5), indicate 73% positive correlation coefficient between aquifer yield and aquifer transmissivity based on the calculated hydraulic parameters of deep boreholes (Table 4.2), within the study area. Sharp 2014, explains the higher the yield, the higher the transmissivity and conversely, the low the yield, the low the transmissivity explains the proportionality of yield to transmissity within the basement aquifers.

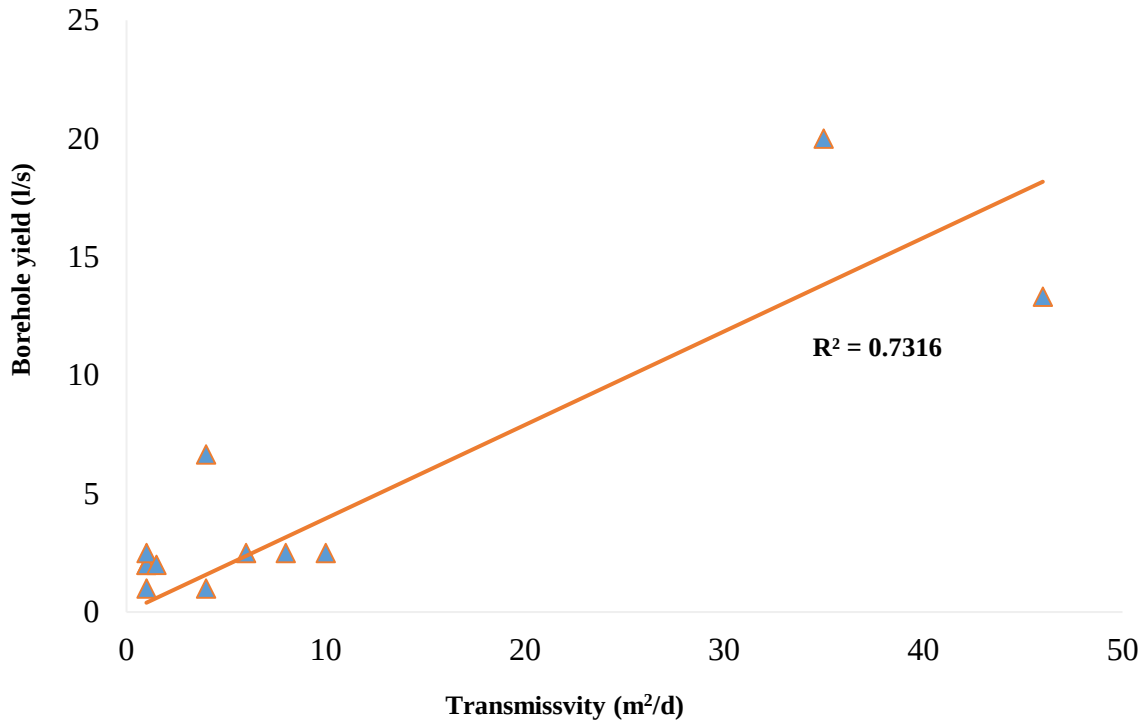

Figure 5.4: Plot of transmissivity against borehole yield

The present study found that the basement aquifers to the central, west and North West of the study area have high yields and high transmissivity. The area within these aquifers is dominated by fracturing and deep weathering which enhances interconnectivity of secondary porosity. Boreholes, E16, E9 and E21 in Figure 5.6 indicate medium to high aquifer potential with transmissivity of $4m^2/d$ to $8m^2/d$ and are associated with deep fracturing. High regional lineaments associated with deep weathering in boreholes E5, E13 and E15 of 40-60m deep have high permeability zones and have transmissivity of $10m^2/d$ to $60m^2/d$ with tested rates of 13 L/s to 20 L/s, (Figure 5.5).

Dewandel et.2012 and Woessner at al. 2023 state that high specific capacities and occurs within area of thick fractured aquifers, which is also associated with regional structures which form groundwater conduits with high permeability.

It was observed that boreholes were drilled in weathered aquifers, response in the aquifer test pumping shows a reflection of fractured aquifer. Woessner at al. 2023, explains that this indicates that fractured aquifer contributes to groundwater flow within the study area. The present study found out that high specific capacity is associated with boreholes with high transmissivity, whereas lowest specific capacity in boreholes is associated with lowest transmissivity, (Table 4.2), Figure 5.5. Sharp 2014, state that determination of groundwater potential through specific capacity by measuring borehole discharge rate per unit drawdown is associated with transmissivity. The higher the specific capacity, the higher the groundwater potential as high volume of groundwater can be pumped per meter of decline in water level.

5.1.3 Aquifer thickness

It was observed from the two maps were generated for the spatial distribution of the weathered and fractured zones aquifer thickness, (Figure 5.6) and (Figure 5.7). The maps show the weathered and fractured zones are thickest in the north and northwest of the study area, coinciding with areas of high groundwater recharge and superficial cover (Figure 5.1). The deep weathering and deep fracturing are associated with fracturing and faulting which correlates with high transmissivity E5 and E13, table 5.1 and Figure 5.5. According to Woessner at al. 2023, some lineaments/ faults are not groundwater conduits due to filling by hydrothermal fluids, clays or quartz and arguer and are impermeable. For instant E14 falls within a regional east -west lineament but has low yield and impermeable lineament. The groundwater flow within occurs along the regional lineament trends as such the groundwater flows in the east- west direction particularly NE to SW and has the thicker fracture zone, (Figure 5.1).

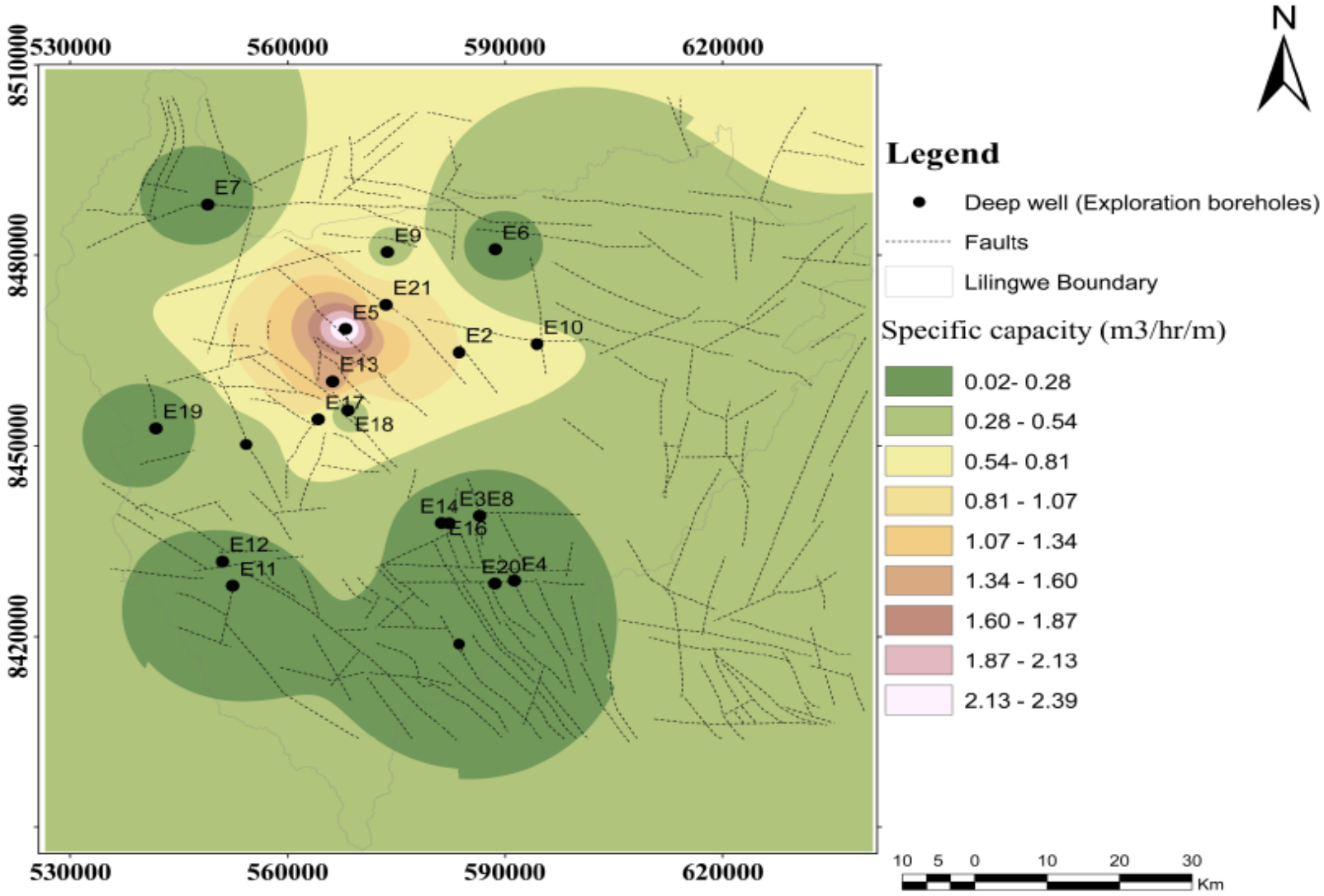

Figure 4.5: Spatial variation of aquifer transmissivity

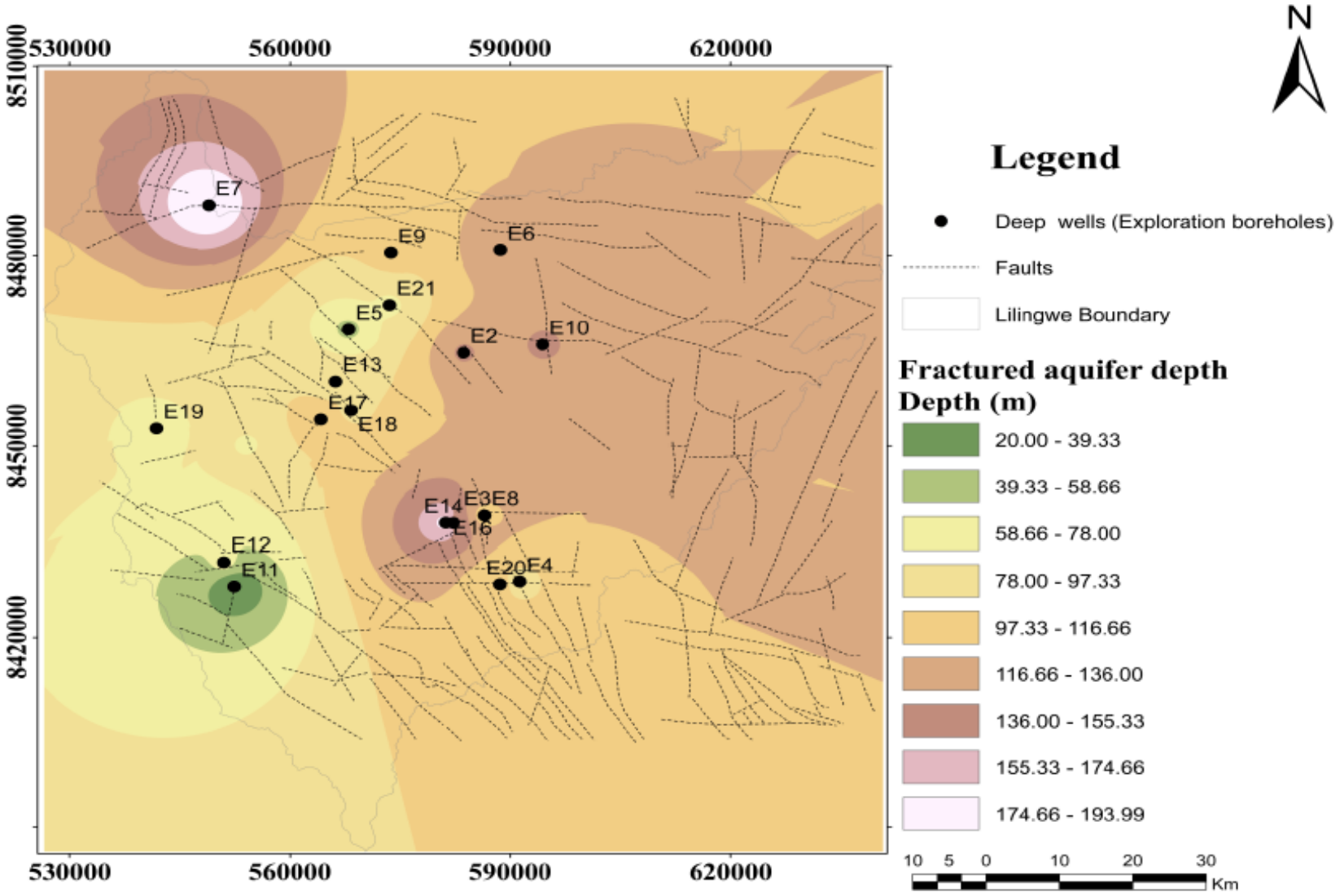

Figure 5.6: Spatial distribution of thickness of fractured aquifers

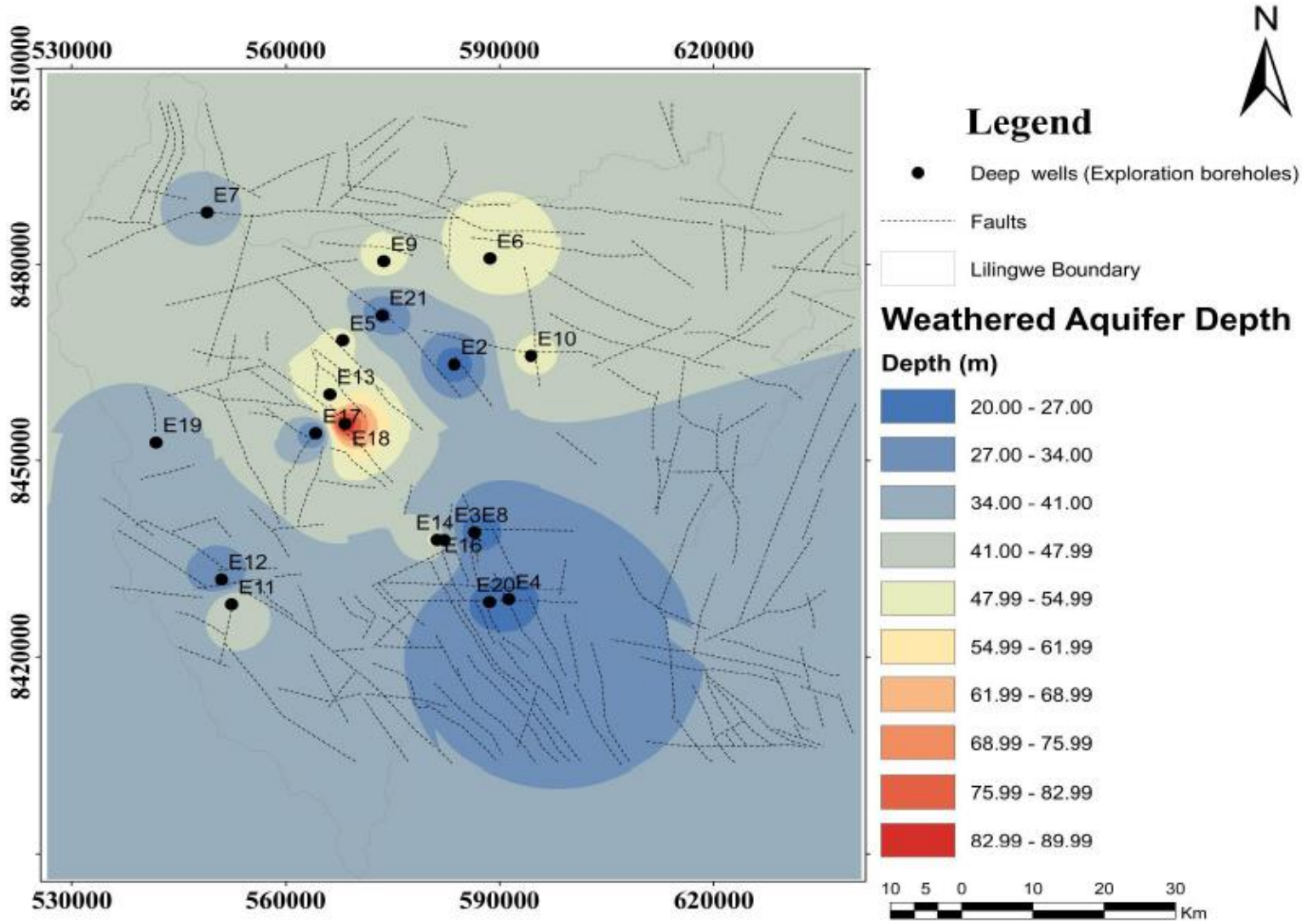

Figure 5.7: Spatial distribution of thickness of weathered aquifers

5.2 Delineation of the hydrogeochemistry of the aquifers within the basement complex rocks

5.2.1 Hydrochemistry classification using Piper plot and Durov plots

It was observed that the concentration of major cations shows the dominance of Ca^{2+} and mixture of (Ca^{2+} + Mg^{2+} + Na^{+} + K^{+}) in groundwater samples. The concentration of major anion is dominated by HCO_3^{-} + CO_3^{2-} with minor SO_4^{2-} , Figure 5.8. The basement aquifers is defined by Ca^{2+}-HCO_3^{-} concentration which indicate the influence of rainfall recharge and fresh groundwater associated with low TDS values. The presence of Na^{+} and SO_4^{2-}shows mixing of this fresh groundwater with relatively older water (Chegbeleh et al.2020).

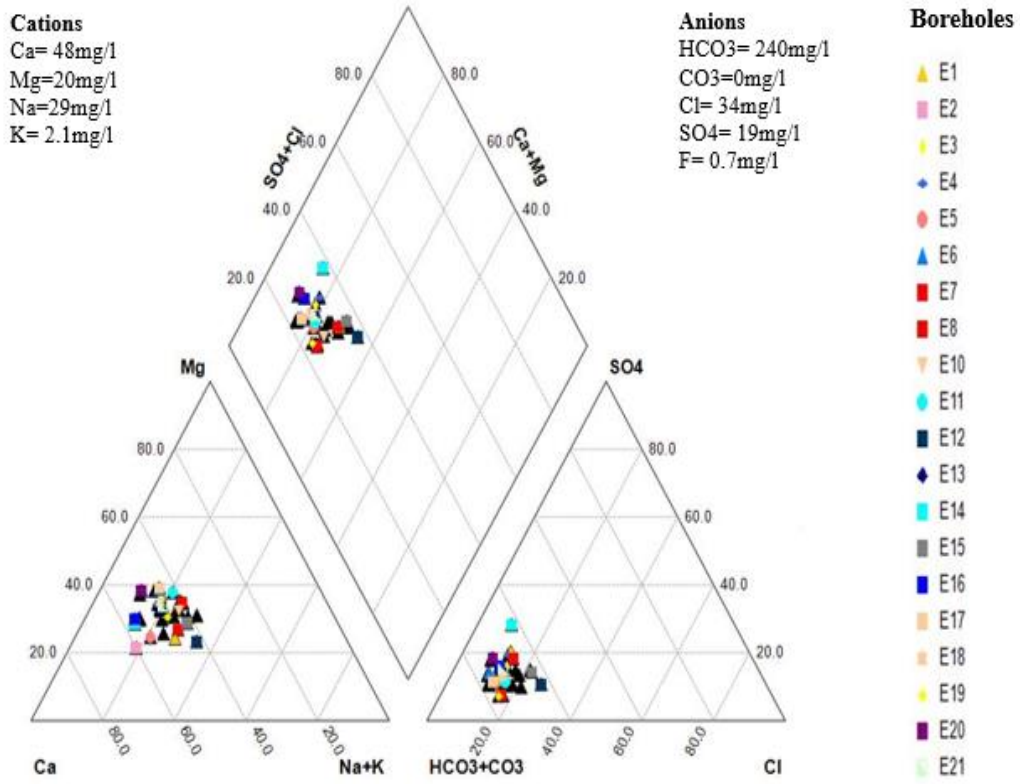

Figure 5.8: Piper plot of the basement aquifers in the study area

In the present study, the Durov plot, Figure 5.9, show the presence of simple dissolution or mixing within basement aquifers. The simple dissolution of minerals and mixing processes within the deep aquifers water is characterized by the concentration of Na-SO_4-Cl within the groundwater samples.

The plotting of the majority of ground water samples around the bicarbonate and calcium corners in the Durov plot indicated recently recharged groundwater (Apollaro et al. 2021).

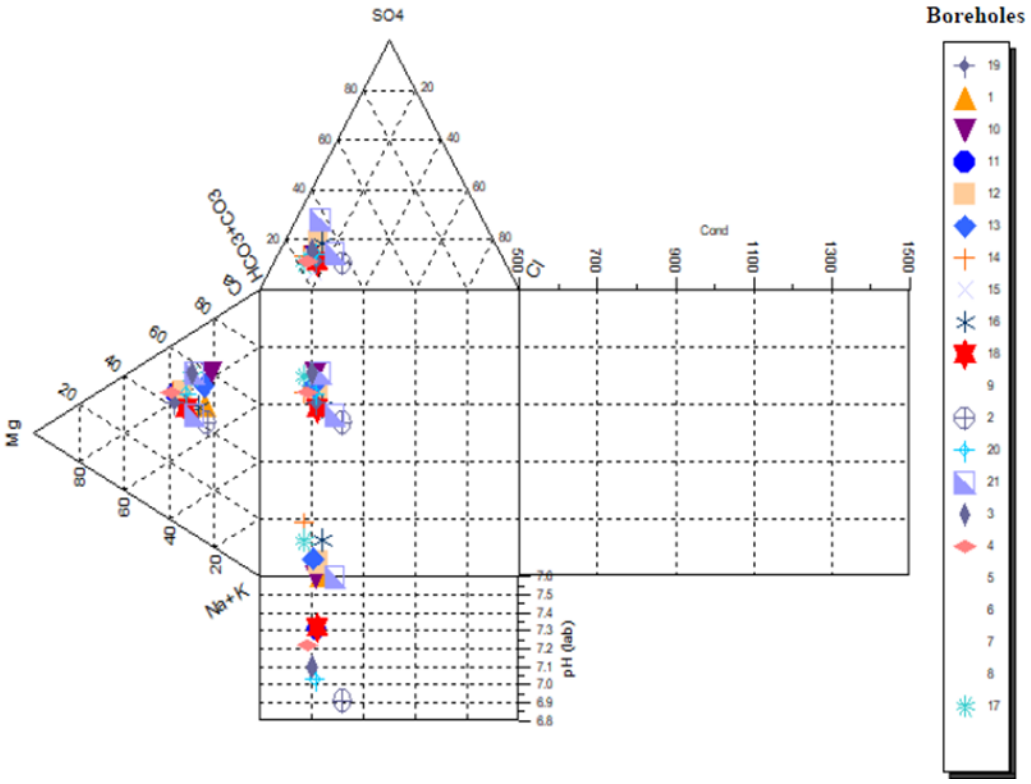

Figure 5.9: Durov plot of the basement aquifers in the study area

It was also observe that the clustering of anions is around HCO_3, Figure, 5.9. Chegbeleh et al 2020, Nyirenda et al 2020, this clustering show that some basement aquifers are associated with carbonate mineral weathering and this reveals the presence of alkaline type of water which is prominate in southern part of the study area

5.2.2 Chemical Dissolution within Basement aquifers

The study found that simple dissolution in basement aquifers is shown through low silicate weathering, carbonate dissolution and evaporite dissolution processes (Figure 5.10). The scatter plots indicate very few little weathering of metamorphic rocks mostly silicate weathering, carbonate dissolution and evaporite dissolution. Chegbeleh et al 2020 and Addison et al, reported of silicate weathering, carbonate dissolution and evaporite dissolution as process which led to simple dissolution process within the basement aquifers.

The study observed that the basement aquifers within the study area are associated with ionic exchange processes along the groundwater flow which drives the concentration of Na over Cl (Figure 5.11). The rising of salinity (Cl^-) concentration in few samples is due to the effect of high evaporation which may cause an increase in ionic concentration in groundwater due to deep weathering in some parts of the Lilongwe. Verspasiano et al 2021, described the rising as an effect of high evaporation caused by increased in ionic exchange within basement aquifers.

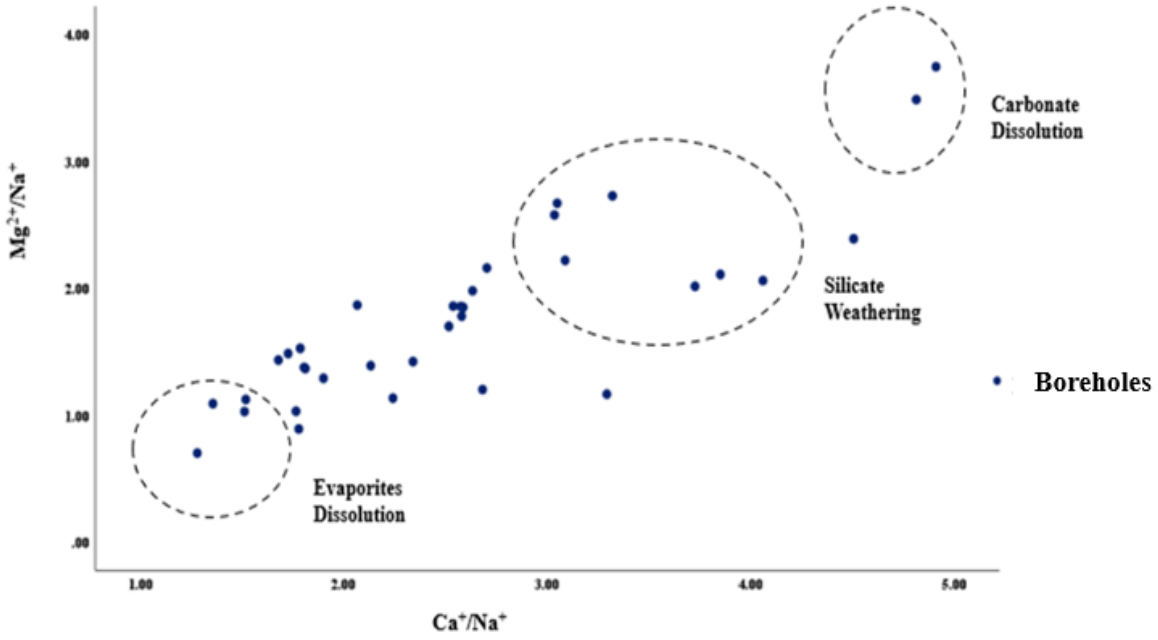

A

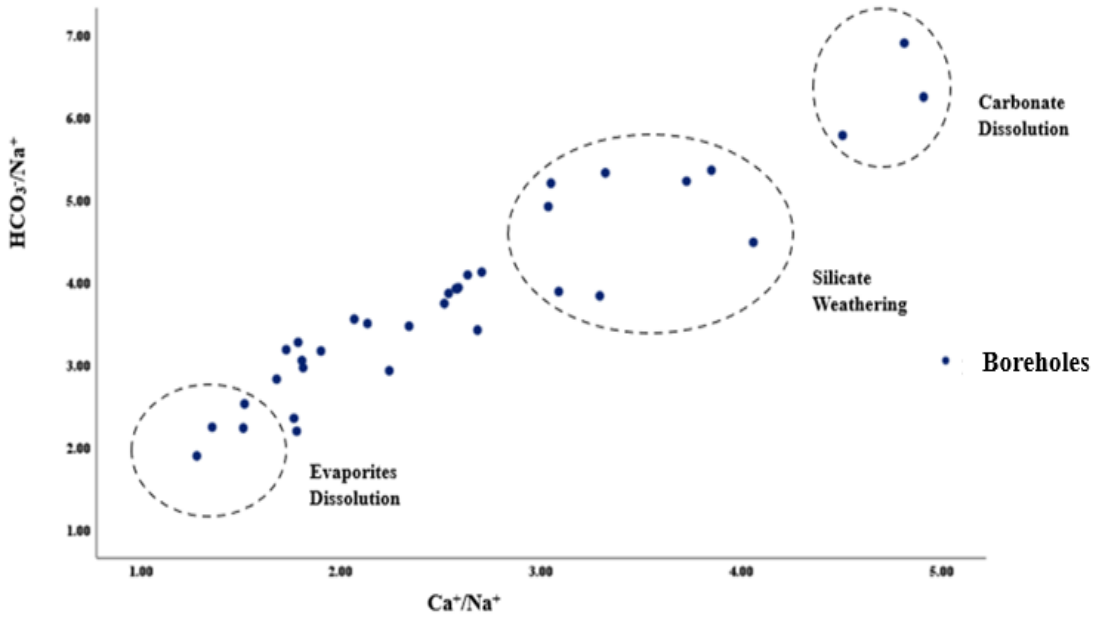

B

Figure 5.10: Ionic ratio plot A: Ca^{2+}/Na^{+} versus Mg^{2+}/Na^{+} and B: Ca^{2+}/Na^{+} versus Na^{+}/HCO_3^{-}

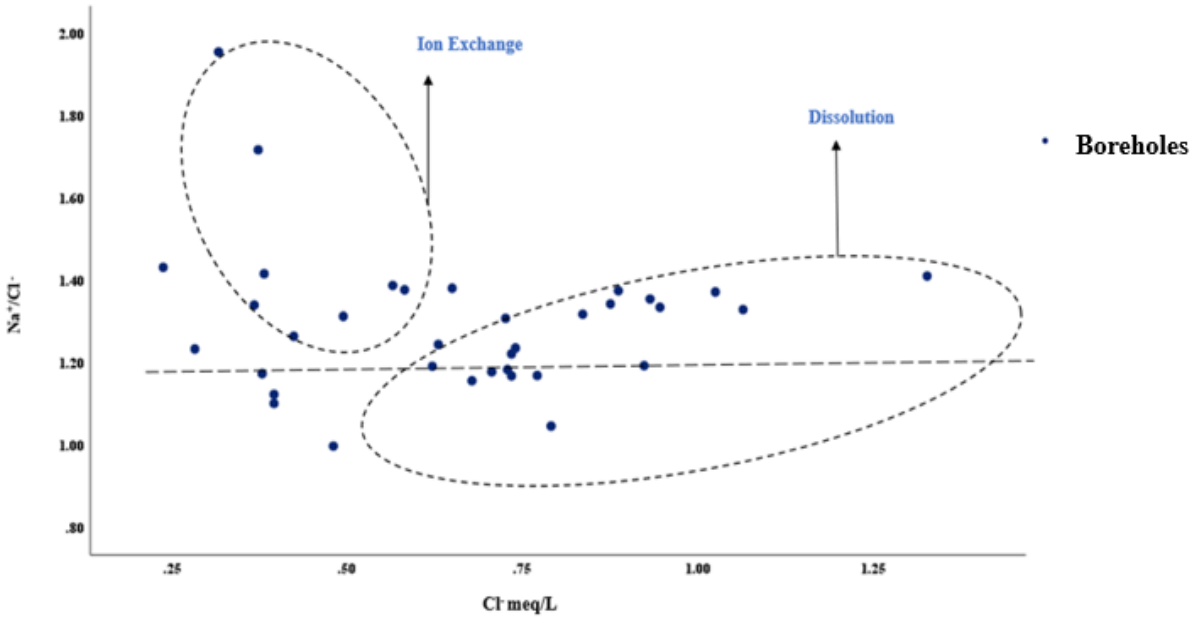

Figure 5. 11: Scatter plot (Na^{+}/Cl^{-} vs Cl^{-})

5.3 Evaluation of spatial relationship of geological structures on groundwater geochemistry and groundwater flow

5.3.1 Spatial distribution of groundwater type and groundwater flow within the basement aquifers in relation to fracturing.

The present study found that the basement aquifers within are characterized with Ca-HCO_3, Ca+Mg-SO_4, Na+K-HCO_3 and Ca-SO_4 groundwater types, Figure 5.12. The Ca-HCO_3 is the dominant groundwater type which shows the presence of recently recharged groundwater and this is consistent with low TDS of <1,000mg/l in the groundwater within the aquifers. It observed that the spatial trend of the groundwater types follows the trend of regional lineaments orientation. Ca-SO_4 and Ca-Mg-SO_4 groundwater type is only present in the central and northern part of the study area. Na+K-HCO_3 groundwater type occurs to the northern and southern part of the study area, Figure 5.12. Ca-HCO_3 varies across the study area. Ca-HCO_3 is spatial varying along the regional fault which is trending SE to NW which is along the regional groundwater flow within the study area. According to Bank and Joloza 2020, Flores et al 2023, the top and shallow weathered aquifer is characterized by Ca-HCO_3. Flores et al 2023 explained that the deep fractured aquifer is characterized by Na+K-HCO_3, Ca-SO_4 and Ca-Mg-SO_4 water. Verspasiano et al 2021 state that dominance of Ca-HCO_3 indicates that the area is an active groundwater recharge zone.

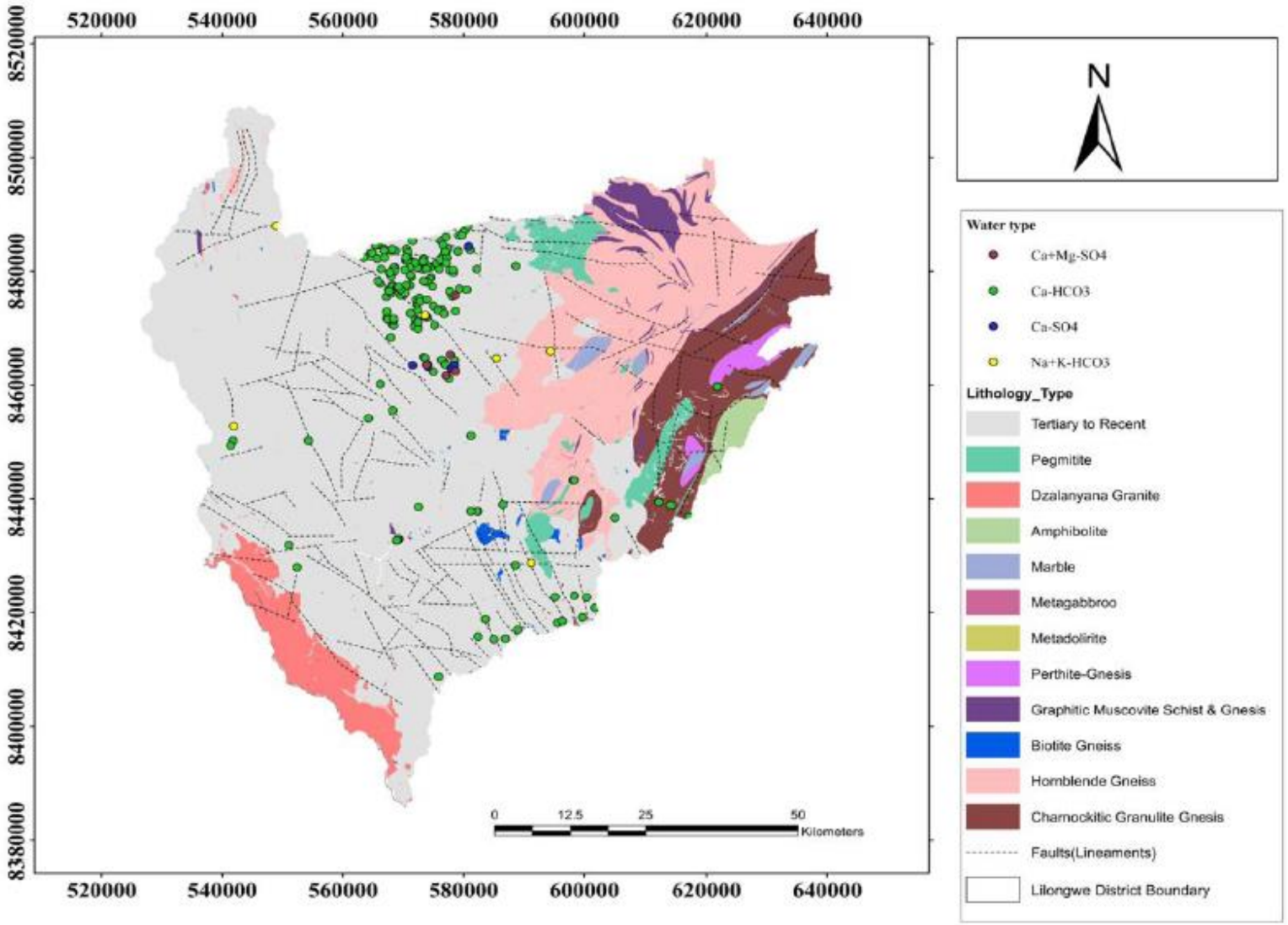

Figure 5.12: Spatial variation of groundwater types within geological structures/ lineament in the study area

The presence of Ca-HCO_3 water across the study area show that there is high recharge in basement aquifers through faults hence presence of fresh groundwater. Chegbeleh et al 2020 state that the presence of Ca-SO_4 and Ca-Mg-SO_4 groundwater type shows that there is a mixing of fresh recently recharge groundwater with older and more saline groundwater. The presence study found the groundwater flow with the basement is characterized by local, intermediate and regional groundwater flow systems occurring within deep fractures. Ca-HCO_3 show the presence of local flow systems occurring mostly within the weathered zone and have fresh groundwater (Verspasiano et al. 2021). Flores et al 2023 state that the presence of Na+K-HCO_3 shows the presence of alkali groundwater relates to the northern and southern part of the study area which is mostly fractured and weathered. This indicates the presence of intermediate groundwater flow system between weathered and fractured zones and is associated with a mixture of fresh and saline groundwater. Chegbeleh et al 2020; Verspasiano et al. 2021, Flores et al 2023, Joloza and Banks 2020, Ca-SO_4 and Ca+ Mg-SO_4 indicate the presence of regional groundwater flow system which is deep and is controlled with deep regional fractured basement aquifer. This has a long residence time within aquifers.

5.3.2 Ionization in relation to geological structures within basement aquifers

The present study found the dominance of Na^+ and SO_4^{2-} in the basement aquifers mostly in deep well samples. Verspasiano et al. 2021, state that this dominance shows the presence of deep fractured aquifer which reflects deep percolation associated regional to intermediate flow systems. It was also observed that the dominance of Ca^{2+}, Mg^{2+} and HCO_3^- is common among the shallow well samples. Pradhan et al. 2022 and Sikakwe & Eyong 2022, state this dominance to be associated with shallow fractures within the weathered and shallower groundwater flow. The present study show that dominance of Na-SO_4 occurs in the central part of the study area associated with numerous fractures and has high transmissivity and yield Figure 5.5 and Figure 5.12. Chegbeleh et al 2020, state that Na-SO4 is usual associated with deep fracturing and high regional groundwater from which is influence the high transmissivity and high production of the aquifer. The scatter plot of chemical elements shows that the relationships among major ions within the basement aquifers has high contribution of Ca^{2+}, Figure 5.13 A, B and C. The relationship between alkali metals (Ca^{2+} + Mg^{2+}) vs Total Cations, (Na^++ Ka^+) vs Total Cations, alkali metals and Ca^{2+} vs Mg^{2+}; shows a relative high contribution of Ca2+ in basement aquifers.

This high contribution Ca^{2+} ions in the basement aquifer system are influenced by the high percolation of recent water within the system through the deep lying fractures which are conduits to groundwater flow (Sunkari et al. 2022).

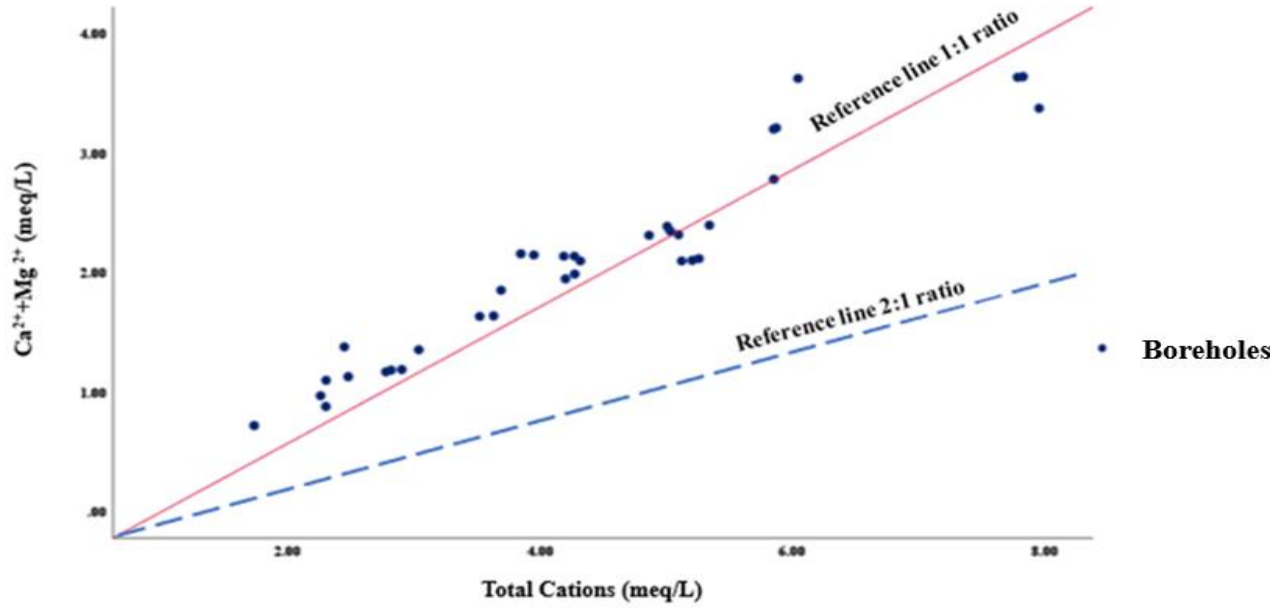

Figure 5.13: A: (Ca^{2+} + Mg^{2+}) vs Total Cations

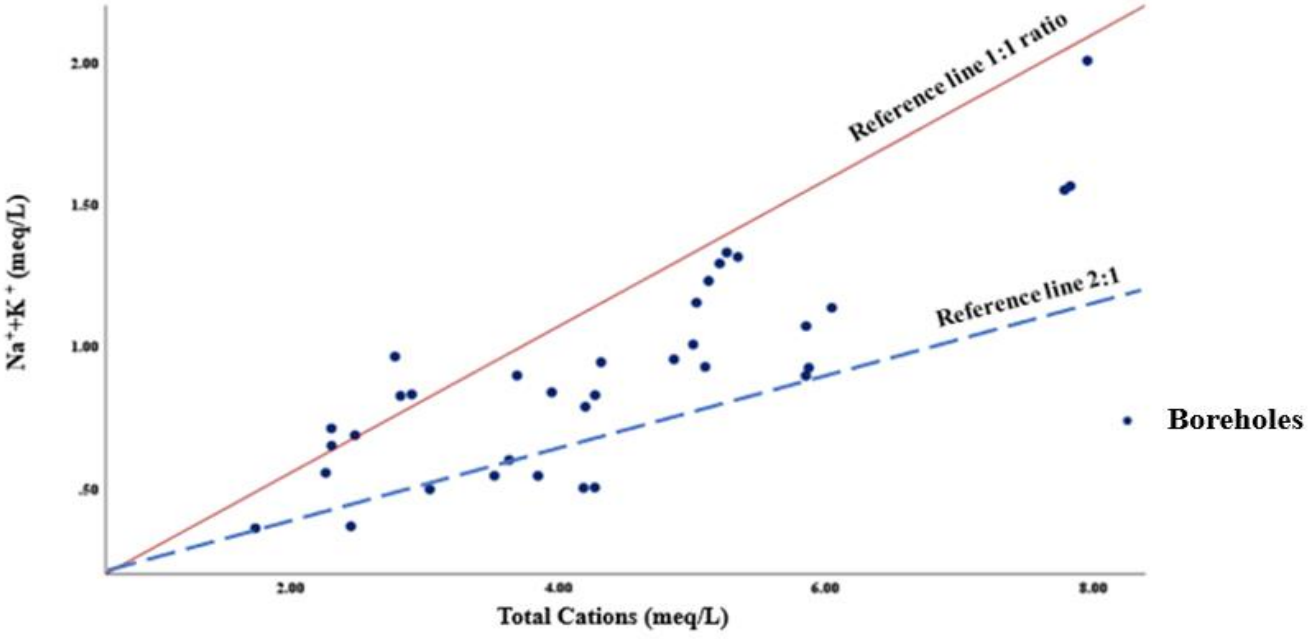

Figure 5.13: B: (Na^{+}+ Ka^{+}) vs Total Cations

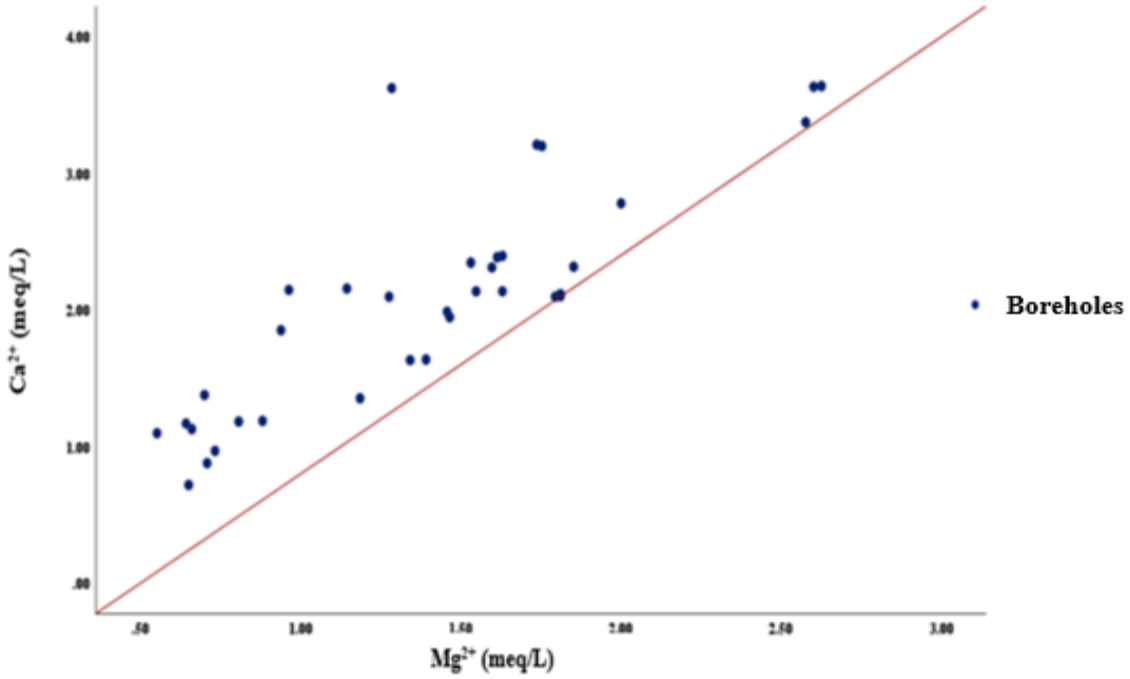

Figure 5.13: C: Cations vs Cations (Ca^{2+} vs Mg^{2+})

Blanchette et al. 2013 and Aisha et al.2022, state that the presence of this fresh or recently recharge water which has little residence time attribute to the high Ca^{2+} which has not undergone full chemical evolution from Ca^{2+} dominant (fresh water) to Na^{+} dominant (old water).

5.3.1 Groundwater chemistry control mechanism within the basement aquifers.

It was observed that the natural controlling mechanism of groundwater within the study area is through evaporation and precipitation dominance, Figure 5.14. According to Pradhan et al. 2022 suggested that this is an influence by high supply of ions from the atmosphere which explains the factor of high groundwater recharge through rainfall through surface lineaments within the basement rocks.

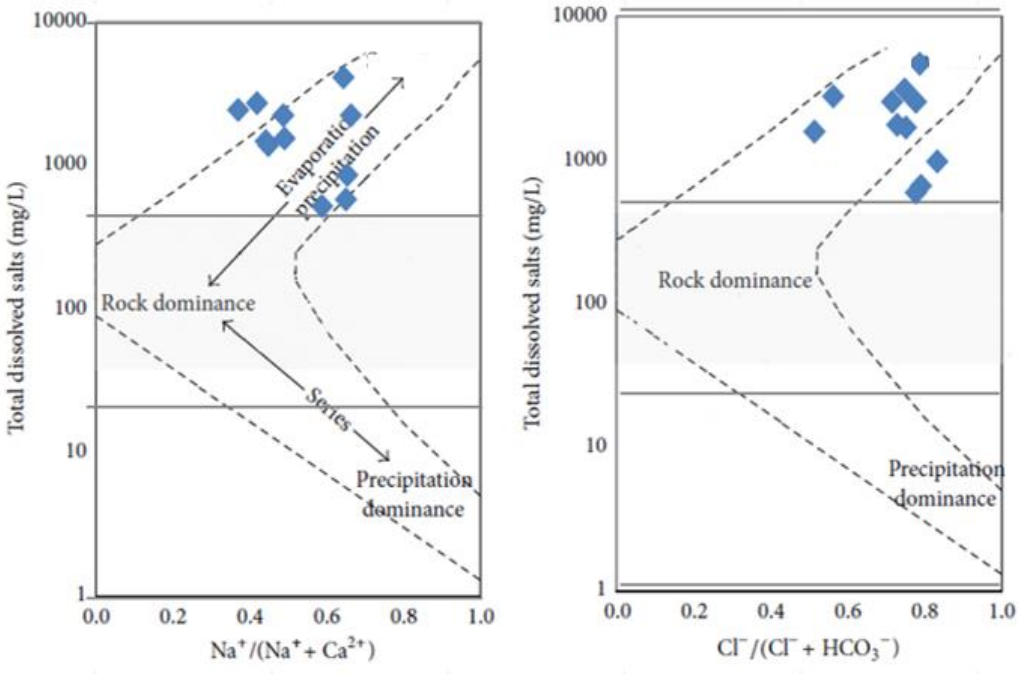

Figure 5.14: Gibbs plot showing geochemical evolution within basement aquifers

5.4 Groundwater quality assessment

5.4.1 Domestic Use

All chemical constituents within basement aquifers shows that the groundwater is within the recommended World Health Organization standards (WHO, 2018) and Malawi Bureau of Standards (MBS, 2017) standards for groundwater quality standard.

5.4.2 Irrigation use

All chemical constituents within basement aquifers shows that the groundwater is within the FAO 1994 irrigation water index good for irrigation purposes.

CHAPTER 6: CONCLUSION AND RECOMMENDATIONS

6.1. Conclusion

In the present study, basement aquifers were characterized into fractured aquifers and weathered aquifer. Fractured aquifers have a character of low to high yield and transmissivity of low to medium. Weathered aquifers have a character yield of very high yield and very high transmissivity. Low yield and low transmissivity occur in the east of the study area and are associated with aquifers occurring in outcropping fractures. The medium to high yield and medium transmissivity occurs to the west and are associated with aquifers occurring in the regolith fractures which are below weathered zone and superficial cover. High yield and very high transmissivity occur to west and central part of the study area and are associated with deep weathering areas. The deep weathering is also associated with the deep regional fault zones.

Basement aquifers are defined by concentration of Ca^{2+} and HCO_3^- which indicate the influence of recharge through rainfall and fresh groundwater associated with low TDS values. Presence of Na^+ and SO_4^{2-}shows mixing of this fresh groundwater with relatively older water. There is a presence of simple dissolution or mixing within basement aquifers. Simple dissolution of minerals and mixing processes within the deep aquifers water is indicated by the concentration of Na-SO4-Cl within the groundwater samples. Significant factors controlling the aquifers chemistry within basement aquifers starts with precipitation of the oversaturated minerals with increasing TDS, ion exchange and simple dissolution.

Deep fractures are spatially related to the dominance of Na^+ and SO_4^{2-} in groundwater samples which shows the presence of deep percolation and dominance of Ca^{2+}, Mg^{2+} and HCO_3^- in groundwater samples relates to shallow fractures. Deep fractures influence percolation and are associated regional to intermediate flow systems. The shallow fractures are associated with shallower groundwater flow. Basement aquifers are characterized with Ca-HCO_3, Ca-SO_4, Na+K-HCO_3^- and Ca-SO_4 groundwater types. The most dominant groundwater type in the study area is Ca-HCO_3 water which shows the presence of recently recharged groundwater. The groundwater flow within the study area is associated with regional fractures. The prominent groundwater flow is characterized by local, intermediate and regional groundwater flow systems.

Local flow systems occur mostly within the weathered zone and have fresh groundwater characterized by Ca-HCO_3 water type from recently recharge groundwater. Intermediate system occurs in both the weathered and fractured zones is associated with Na+K-HCO_3^-. These are controlled by weathering and fracturing within the weathered zone. Regional groundwater flow system is deep, mainly controlled with deep regional fractured basement aquifer. This has a long residence groundwater type and has Ca+ Mg-SO_4 and Ca-SO_4 water type.

All groundwater chemical parameters were within the recommended standard of MBS 2017 and WHO 2018 standard for domestic use. The basement aquifers are within the FAO 1994 irrigation water index requirement for irrigation use.

6.2 Recommendations

In regards with to the findings from this study, the recommendations are made towards improving understanding on groundwater resource management and development within basement aquifers of Lilongwe:

a) Groundwater development of large volume should target the fractured aquifer which have high storativity.
b) Frequently groundwater monitoring is required to understand the rate of recharge and discharge within the basement aquifers to check the rate of dissolution.
c) Groundwater resource management should focus much on understanding of the regional groundwater flow so that deep aquifers are fully utilized.
d) Deep are shallow aquifers can be utilized for domestic and irrigation use since it contains good water
e) Further studies need to improve understanding of the hydraulic connection between the regolith and the underlying fractured bedrock.
f) Most groundwater development within the area should target the fractured aquifer under weathered regolith and superficial cover.

6.3 Further research

There is a need to conduct further studies within basement aquifers of Lilongwe on the following areas;

a) Most studies are need in understanding the isotopic composition within deep aquifers.
b) More studies on deep aquifers should focus in understand the hydrogeochemistry pattern from recharge to discharge areas.

REFERENCES

Addison, M., Rivett, M., Phiri, P., Mblame,E.,Banda,M.,Phiri, O., Lakudzala, W. & Kalin, R., 2020, 'Identify Groundwater Flouride Source in a Weathered Basement Aquifer in central Malawi: Human health and Policy Implications,' *Applied Sciences* 10(14), 5006, viewed 21 September 2022, from https//doi:10.3390/app10145006.

Aghazadeh, N., Chitsazan, M. & Golestan, Y., 2016, 'Hydrochemistry and quality assessment of groundwater in the Ardabil area, Iran', *Applied Water Science* 7(7), 3599–3616, viewed August 2021, from https://doi.org/10.1007/s13201-016-0498-9.

Ahmad, A. & Al-Ghouti, H., 2020, 'Approaches to achieve sustainable use and management of groundwater resources in Qatar: A review', *Groundwater for sustainable development 11*, 100367, viewed October 2020, from https://doi.org/10.1016/j.gsd.2020.100367.

Aisha, K., Abu, E. & Ahmad, K., 2022, 'Hydrogeochemical processes of groundwater from basement complex rock in Keffi, Central Nigeria', *British Journal of Enviromental Sciences* 10(5), pp 34-48, viewed 28 September 2023, from https://doi.org/10.37745/bjes.2013vo10n5pp3448.

Alilouch, R., Morabiti, K. & El Mrih, A., 2017, 'The Contribution to hydrogeological and hydrochemical knowledge of the aquifers in the East side of Bouhachem area(Tetouan, Morocco)', *Journal of Material and Environmental Sciences* 8(12),4510-4522, viewed 05 November 2020, from http://www.jmaterenvironsci.com.

APHA, 2017, *Standard Methods for Examination of Water and Wastewater*, 23rd Edition, American Public Health Association (APHA), American Water Works Association, Water Environment Federation, Washington, D.C.

Apollaro, C., Fuoco, L., Calabrese, L., Marini, G., Vepsasiano, G.& Muto, F., 2021, 'Geochemical Modelling of Water-Rock Interaction Processes in the Pollino National Park', *Hindawi Geofluids* 2021, viewed 11 Jan 2021, from https://doi.org/10.1155/2021/6655711.

Aral, M. M. & Taylor, S. W., 2011, *Groundwater Quantity and Quality Management*, Reston, Virginia, American Society of Civil Engineers, viewed 23May 2020, from www.pubs.asce.org.

Banks, E. & Joloza, A., 2019, 'Hydrogeochemistry Characterization of groundwater in major aquifers in Malawi', Paper presented at 2nd SADC Groundwater Conference,Johannesburg, South Africa, 4th - 6th September, 2019.

Bianchi, M., Palamakumbura, R., MacDonald, A. & Macdonald, D., 2020, 'Assessing regional variation in yield from weathered basement aquifers in West Africa and modelling their future groundwater development and sustainability', *Hydrogeology Journal*(2023)31, 257–274, viewed 11october 2020, from https://doi.org/10.1007/s10040-023-02594-w.

Blanchette, D., Lefebvre, R., Nastev, M. & Cloutier, V., 2013, 'Groundwater Quality, Geochemical Processes and Groundwater Evolution in the Chateauguay River Watershed, Quebec, Canada. Canadian Water Resources', *Canadian Water Resources Journal* 35(4), 503-526, viewed 10 August 2020, from https://doi.org/10.4296/cwrj3504503.

Bu. J, Liu. W. & Ling. K., 2020, 'Comparative Study of Hydrochemical Classification Based on Different Hierarchical Cluster Analysis Methods' International Journal of Enviromental Research and Public Health 2020,17, 9515, viewed September 2023, from dio:10.3390/ijerph17249515.

Carrard, N., Foster, T.& Willetts, J.,2019, 'Groundwater as a Source of Drinking Water in outheast Asia and the Pacific: A Multi-Country Review of Current Reliance and Resource Concerns', *Water 2019* 11(8), 1605, viewed 11 October 2020, From doi.org/10.3390/w11081605.

Carter, S., and Bennet, D., 1973, *The Geology and Mineral Resources of Malawi*, Bull. No. 6, Geological Surveys Department, Malawi, Malawi Government Printer, Zomba.

Chegbeleh, L., Akurugu, B. & Yidana, S., 2020, 'Assessment of Groundwater Quality in the Talensi District, Northern Ghana', *The Scientific World Journal* 2020, 24, viewed 10 April 2020, from https://doi.org/10.1155/2020/8450860.

Chen, J., Huang, Q., Yaling Lin, Y., Fang, Y., Qian, H., Liu R. & Hongyun, M., 2019, 'Hydrogeochemical Characteristics and Quality Assessment of Groundwater in an Irrigated Region, Northwest China', *Water 2019* 11(1), 96, viewed 10July 2020, from https://doi.org/10.3390/w11010096.

Chilton, P. & Foster, D., 1995, 'Hydrogeological Characterisation and Water-Supply Potential of Basement Aquifers in Tropical Africa', *Hydrogeology Journal* 3(1), 36-40.

Council for Geoscience, 2018, *Malawi Hydrogeological and Water Quality Atlas*, Ministry of Water and Sanitation, Lilongwe, Malawi.

Department of Climate Change and Meteorological Services, 2022, *Annual season report 2022*, Ministry of Natural Resources and Climate Change, Malawi.

Dewandel, B., Maréchal, C., Bour, O., Ladouche, B., Ahmed, S., Chandra, S. & Pauwels, H., 2012, 'Upscaling and regionalizing hydraulic conductiv ity and efficient porosity at watershed scale in crystalline aquifers,*'Journal of Hydrology* 416-417, 83–97, viewed 14 April 2022, from https://doi.org/10.1016/j.jhydrol.2011.11.038.

Eid, H., Elbagory, M., Tamma, A., Gad, M., Elsayed, S., Hussein, H., Moghanm, S., Omara, A.E.-D., Kovács, A. & Péter, S., 2023, 'Evaluation of Groundwater Quality for Irrigation in Deep Aquifers Using Multiple Graphical and Indexing Approaches Supported with Machine Learning Models and GIS Techniques, Souf Valley, Algeria', *Water 2023* 15(1),182, viewed 10 January 2023, from https://doi.org/10.3390/ w1501018.

Fetter, C. W., 2018, *Applied Hydrogeology*, 4th edition, Waveland Press Inc, Long Grove, Illinois, USA.

Flores, Y., Eid, M., Sz ″ucs, P., Sz″ocs, T., Fancsik, T., Szanyi, J., Kovács, B., Markos, G., Újlaki, P., Tóth, P., 2023, 'Integration of Geological, Geochemical Modelling and Hydrodynamic Condition for Understanding the Geometry and Flow Pattern of the Aquifer System, Southern Nyírség–Hajdúság, Hungary. *Water 2023*, 15, 2888, viewed 22 September 2023, from https://doi.org/10.3390/w15162888.

González, J., Comte, J., Legchenko, A., Ofterdinger, U.& Healy, D., 2021, Quantification of groundwater storage heterogeneity in weathered/fractured basement rock aquifers using electrical resistivity tomography: Sensitivity and uncertainty associated with petrophysical modelling, *Journal of Hydrology* 593, 125637, viewed February 2021, from https://doi.org/10.1016/j.jhydrol.2020.125637.

Government of Malawi (GOM), 2007, *National Water Policy*, 2nd edition, Ministry of Irrigation and Water Development, Lilongwe, Malawi.

Government of Malawi (GOM), 2017, *National Water Resources Master Plan: Final Report 2*, December 2014, National Water Development, Ministry of Agriculture, Irrigation and Water Development, Lilongwe, Malawi.

Guo, H., Li, M., Wang, L., Yunlong Wang, Y., Zang, X., Zhao, X., Wang, H. & Zhu, J., 2021, 'Evaluation of Groundwater Suitability for Irrigation and Drinking Purposes in an Agricultural Region of the North China Plain,*'Water 2021*13(23),3426, viewed 07January 2022, from https://doi.org/10.3390/w13233426.

Han, D., 2010, *Concise Hydrology*, 1st edition, University of Bristol, BS8 1TR, Dawei Han &Ventus Publishing Aps, UK.

Hao, Q., Xiao, Y., Chen, K., Zhu, Y. & Li, J., 2020, 'Comprehensive Understanding of Groundwater Geochemistry and Suitability for Sustainable Drinking Purposes in Confined Aquifers of the Wuyi Region, Central North China Plain', *Water 2020* 12(11), 3052, viewed 31 October 2021, from https://doi.org/10.3390/w12113052.

Hodges, M., Biggs, J., Goda, K. & Aspinall, W., 2015, 'Assessing Infrequent Large Earthquakes Using Geomorphology and Geodesy,*'Natural Hazards*76(3),1781-1806, viewed 11 August 2020, from DOI 10.1007/s11069-014-1572-y.

Hussien, B. & Faiyad, A.,2016, 'Modeling the Hydrogeochemical Processes and Source of Ions in the Groundwater of Aquifers within Kasra-Nukhaib Region (West Iraq),*'International Journal of Geosciences*7(10), 1156-1181, viewed 10 January 2020, from doi: 10.4236/ijg.2016.710087.

Jafary F. & Bradley, C., 2018, 'Groundwater Irrigation Management and the Existing Challenges from the Farmers; Perspective in Central Iran', *Land 2018* 7(1), 15, viewed 11 January 2020, from https://doi.org/10.3390/land7010015.

Japan International Corporation Agency (JICA), 2017, *Malawi National Water Resources Master Plan*, Ministry of Water and Sanitation, Lilongwe, Malawi.

Johnson, K.H., 2016, 'Groundwater contaminant plume maps and volumes, 100-K and 100–N Areas, Hanford Site, Washington', *U.S. Geological Survey Open-File Report 2016–1161*, 64, viewed 11March 2021, from http://dx.doi.org/10.3133/ofr20161161.

Kang, M., Ayars, J. & Jackson, R., 2019, 'Deep groundwater quality in the southwestern United States', *Environmental Research Letters*14(3), viewed 18 March 2020, from https//doi: 10.1088/1748-9326/aae93c.

Kalantar, B(ed.)., 2021, 'Groundwater Management and Resources,' IntechOpen, viewed 23 June 2022, from DOI: 10.5772/intechopen.87804.

Kalin, R., Rivett, M.,Phiri, P., Mblame,E.,Banda,M.,Phiri, O., Lakudzala, W. & Addison, M., 2020, 'Identify Groundwater Flouride Source in a Weathered Basement Aquifer in central Malawi: Human health and Policy Implications,' *Applied Sciences*10(14), 5006, viewed 20 September 2022, from https//doi:10.3390/app10145006.

Kaur, T., Bhardwaj, R. & Arora, S., 2016, 'Assessment of groundwater quality for drinking and irrigation purposes using hydrochemical studies in Malwa region,southwestern part of Punjab, India,' *Applied Water Science 2017* 7(10), 3301–3316, 11 March 2020, from http://doi10.1007/s13201-016-0476-2.

Kaonga, C., Kosamu, B. & Tenthani, C., 2015, 'Climate Variation based on Temperature and Solar Radiation data over aperiod of 29 years in Lilongwe City Malawi,' *African Journal of Environmental Science and Technology* 9(4),346-353, viewed 20 August 2020, from https://doi.org/10.5897/AJEST2014.1840.

Khatri, N. & Tyagi, S., 2015, 'Influences of natural and anthropogenic factors on surface and groundwater quality in rural and urban areas', *Frontiers in Life Science* 8(1), 23-39, 18 November 2020, from https://doi.org/10.1080/21553769.2014.933716.

Khogali, A., Birkle, P., Al-Shaibani, A.,Keller M., Tawabini, B. & Makkawi, M., 'Geochemical Assessment of Potential Sources for Nitrate in the Wasia Aquifer', Al Kharj Area, Central Saudi Arabia*, Water 2020*12(5),1479, viewed 12February 2021, from https://doi.org/10.3390/w12051479.

Konikow, L.& Bredehoeft, J., 2020, Groundwater Resources Development: Effects and sustainability, Published by the Groundwater Project, Guelph, Ontario, Canada, 2020.

Lachassagne, P., Dewandel, B., Wyns, R., 2021, Review: 'Hydrogeology of weathered crystalline/hard-rock aquifers—guidelines for the operational survey and management of their groundwater resources', *Hydrogeology Journal* 29, viewed 22 May 2022, 2561–2594, from https//dio.org/10.1007/s10040-021-02339-7.

Leedy, P. D. & Ormrod, J. E., 2015, Practical Research: Planning and Design, 11th edition, Edinburgh Gate, Pearson.

Li, X., Wu, H., Qian, H. & Gao, Y., 2018, 'Groundwater Chemistry Regulated by Hydrochemical Processes and Geological Structures: A Case Study in Tongchuan, China', *Water 2018* 10(3), 338, viewed 12January 2020, from https://doi.org/10.3390/w10030338.

Lilongwe City Council, 2010, Final Report Summary: The Study on Urban Development Master Plan, September 2010, Government of Malawi, Ministry of Local Government and Rural Development.

Lilongwe Water Board, 2015, 'Lumbadzi Groundwater Development. Volume 1 Part 1', *Detailed Design Report*, December 2015, Lilongwe, Malawi.

Liu, X., Li, L.& Hul, A., 2013. 'Hydrochemical Characterization of a Groundwater Aquifer and its Water Quality in Relation to Irrigation in the Jinghuiqu Irrigation District of China', *Water Environmental Research* 85(3), 245-258.

Lohr, S., 2022, *Sampling Design and Analysis*, CRC Press, New York.

Luo, W., Gao, X., & Zhang, X., 2018, 'Geochemical processes controlling the groundwater chemistry and fluoride contamination in the Yuncheng Basin, China An area with complex hydrogeochemical conditions', *PLoS ONE* 13(7), 137-161, viewed 12 May 2020, from https://doi.org/10.1371/journal.

Makungo, R., Odiyo, J & Ndiritu, J., 2020, 'Hydraulic characteristics of a fractured crystalline basement aquifer in Nzhelele area, Limpopo Province, South Africa', *Cogent Engineering*8(1), 1928387, viewed 28 January 2021, from https://doi.org/10.1080/23311916.2021.1928387.

Malawi Bureau of Standards (MBS), 2017, *Catalogue of Malawi Standards,Malawi Burea of Standards,* Blanytre, Malawi.

Narsimha , A., Sudarshan, V. & Swathi, P., 2013, 'Groundwater and its assessment for irrigation purpose in Hanmakonda Area, Warangal District, Andhra Pradesh, India,' *International Journal of Research in Chemistry and Environment* 3(2), 196–200, viewed 26 November 2020, from http://ijrce.org/download.php?file=19.

National Statistical Office, 2019, *Malawi 2018 Population and Housing Census: Main Report, National Statistical Office,* Zomba, viewed 13 March 2021, from *https://malawi.unfpa.org/en/resources/malawi-2018-population-and-housing-census-main-report.*

National Statistical Office, 2020*, Fifth Integrated Household Survey 2019-2020,* The World Bank. Washington, D.C., viewed 11May 2021, from https://microdata.worldbank.org/index.php/catalog/3818.

Nyirenda, T., Mapoma, H., Msiska, A., Dzonzi-Undi, J. & Jumbo, S., 2015, 'Hydrogeochemical Assessment of Groundwater Quality in Salima and Nkhotakota Districts, Malawi',*International Journal of Science and Research* 4(9),1568-1576, viewed 07 April 2021, from www.ijsr.net.

Olea-Olea, S., Escolero, O.,Mahlknecht, J.,Ortega,L.,Taran, Y., Moran-Zenteno, D., Zamora-Martinez, O. & Tadeo-Leon, J, 2020, 'Water-rock interaction and mixing processes of complex urban groundwater flow system subject to intensive exploitation: The case of Mexico City', *Jounal of South American Earth Sciences* 103, 102719, viewed 08 July 2021, from https://doi.org/10.1016/j.jsames.2020.102719.

Poeter, E., Fan, Y., Cherry, J., Wood, W. & Douglas, M., 2020., Groundwater in Our Water Cycle: Getting to know Earth's most Important Fresh Water Source, The Groundwater Project, Guelph, Ontario, Canada.

Pradhan, R., Behera, A., Kumar, S., Kumar, P. and Biswal, T., 2022, Recharge and geochemical evolution of groundwater in fractured basement aquifer (Nw India): Insights from enviromental Isotopes (^{18}O, ^{17}O and ^{2}H) and hydrogeochemical studies, *Water 2022*, 14, 315, Viewed 10th October 2022, from https://doi.org/10.3390/w14030315.

SADC-GMI, 2019, Gap Analysis and Action Plan – Scoping Report: *Malawi, SADC GMI Report*, Bloemfontein, South Africa.

Rawat, S., Singh, K. & Gautam, K., 2018, 'Assessment of groundwater quality for irrigation use: A peninsular case study,' *Applied Water Science*8, 233, viewed 15 May 2020, from https://doi.org/10.1007/s13201-018-0866-8.

Sharp, J., 2014, Fractured Rock Hydrogeology, Taylor & Francis Editors, London, UK.

Siebert, S., Burke, J., Faures, J.,Frenken, K., Hoogeveen, J., Doll, P. & Portmann, F., 2010,'Groundwater use for irrigation – a global inventory', *Hydrology and Earth System Sciences*14(10), 1863-1880.

Sidibé, A., Lin, X. & Koné, S., 2019, 'Assessing Groundwater Mineralization Process, Quality, and Isotopic Recharge Origin in the Sahel Region in Africa', *Water 2019*11(40), 789, viewed 23 August 2020, from https://doi.org/10.3390/w11040789.

Sajil Kumar, P. & James, E., 2016, 'Identification of hydrogeochemical processes in the Coimbatore district, Tamil Nadu, India', *Hydrological Sciences Journal* 61 (4), 719-731, 24 February 2021, from https://doi.org/10.1080/02626667.2015.1022551.

Sikakwe, G. & Eyong. G., 2022, 'Groundwater flow and geochemical processes affecting its quality in the basement (Oban Massif) and sedimentary (Mamfe Embayment) environments, southeastern Nigeria', *Journal of African Earth Sciences*, 188, 2022, 104467, viewed 21 September 2023, from https://doi.org/10.1016/j.jafrearsci.2022.104467.

Sunkari, E., Seidu, J. & Ewusi, A., 2022, 'Hydrogeochemical evolution and assessment of groundwater quality in the Togo and Dahomeyan aquifers, Greater Accra Region, Ghana,' *Environmental Research* 208, viewed 25 May 2022, from https//doi.org/10.1016/j.envres.2022.112679.

Tikhomirov, V., 2016, *Hydrogeochemistry Fundamentals and Advances*, 3rd edition, Scrivener Publishing, Massechusetts.

UN-HABITAT, 2011, *Lilongwe Urban Profile*, United Nations Settlement Programme, Regional and Technical Coorporation Division, Nairobi, Kenya, viewed 18 December 2020, from http://www.unhabitat.org.

Vespasiano, G., Muto, F. & Apollaro, C., 2021, 'Geochemical, geological and groundwater quality characterization of a complex geological framework: The case study of the Coreca Area (Calabria, South Italy)', *Geosciences 2021*, 11, 121, viewed 20 September 2023, from https://doi.org/10.3390/ geosciences11030121.

Wali, S.,Alias, N & Harun, S., 2020, 'Hydrogeochemical evaluation and mechanisms controlling groundwater in diferent geologic environments, Western Sokoto Basin, Northwestern Nigeria', *SN Applied Sciences* 2, 1808, viewed 27 February 2021, from https://doi.org/10.1007/s42452-020-03589-y.

Wanda, E., Gulula, L. & Phiri, A., 2013, 'Hydrochemical assessment of groundwater used for irrigation in Rumphi and Karonga districts, Northern Malawi', *Physics and Chemistry of the Earths parts A/B/C* 66, 51-59, 20 November 2020, from https://doi.org/10.1016/j.pce.2013.09.001.

World Bank, 2017, *Annual report 2017(Lilongwe Water and Sanitation Project)*, The World Bank.1818 H Street, NW, Washington, D.C., USA.

World Bank, 2019, *Malawi Watershed Services Improvement Project*, The World Bank, 818 H Street, NW, Washington, D.C., USA

World Health Organization, *2018 Guidelines for Drinking-water Quality*, Fourth Edition, World Health Organisation 2018.

Worthington, S., 2022, 'Estimating Effective Porosity in Bedrock Aquifers', *The National Groundwater Association*, 60 (2), viewed 20 september 2023, from https://dio.org/10.1111/gwat.13171.

Zelterman, D., 2015, *Applied Multivariate Statistics with R*, Springer International Publishing, New Haven, CT, USA.

Zhu, H.,Zhou, J.,Song, T.,Feng, H.,Liu, Z.,Liu, H. & Ren, X., 2020, 'Influences of natural and anthropogenic processes on the groundwater quality in the Dagujia River Basin in Yantai, China',

Journal of Water Supply 69(2),184-196, viewed 18 January 2021, from https://doi.org/10.2166/aqua.2019.113.

APPENDICES:

Appendix 1: Research Ethics and Regulatory Approval and Permit by MZUNIREC

MZUZU UNIVERSITY

DIRECTORATE OF RESEARCH

Mzuzu University
Private Bag 201
Luwinga
Mzuzu 2
MALAWI
TEL: 01 320 722
FAX: 01 320 648

MZUZU UNIVERSITY RESEARCH ETHICS COMMITTEE (MZUNIREC)

Ref No: MZUNIREC/DOR/22/01 **26th Jan., 2022**

Mr. Daniel Kilembe,
Mzuzu University,
P/Bag 201,
Mzuzu.
Email: dkilembe@gmail.com

Dear Mr. Kilembe,

RESEARCH ETHICS AND REGULATORY APPROVAL AND PERMIT FOR PROTOCOL REF NO: MZUNIREC/DOR/22/01: CHARACTERIZATION AND HYDROGEOCHEMISTRY OF AQUIFERS SYSTEMS IN CRYSTALLINE BASEMENT WITHIN LILONGWE RIVER BASIN, MALAWI

Having satisfied all the relevant ethical and regulatory requirements, I am pleased to inform you that the above referred research protocol has officially been approved. You are now permitted to proceed with its implementation. Should there be any amendments to the approved protocol in the course of implementing it, you shall be required to seek approval of such amendments before implementation of the same.

This approval is valid for one year from the date of issuance of this approval. If the study goes beyond one year, an annual approval for continuation shall be required to be sought from the Mzuzu University Research Ethics Committee (MZUNIREC) in a format that is available at the Secretariat. Once the study is finalised, you are required to furnish the Committee with a final report of the study. The Committee reserves the right to carry out compliance inspection of this approved protocol at any time as may be deemed by it. As such, you are expected to properly maintain all study documents including consent forms.

Committee Address:
Secretariat, Mzuzu University Research Ethics Committee, P/Bag 201, Luwinga, Mzuzu 2; E-mail address: mzunirec@mzuni.ac.mw

Wishing you a successful implementation of your study.

Yours Sincerely,

Gift Mbwele

MZUZU UNIVERSITY RESEARCH ETHICS ADMINISTRATOR

For: CHAIRMAN OF MZUNIREC

Appendix 2: Authorization letter from Lilongwe Water Board

LILONGWE WATER BOARD

'Potable water all the time for all'

HEAD OFFICE
Madzi House, Area 3
Off - Likuni Road
Lilongwe, MALAWI

Your Ref
Our Ref: MW-LWSP-52121-CS-OCBS

P.O. Box 96, LILONGWE.
Phone: (+265) 01 750 366 Head Office
(+265) 01 753 630 Faults Desk
Fax: (+265) 01 752 294 / 01 757 343

27th November, 2020

Daniel Fred Kilembe
Mzuzu University,
Private Bag 201,
Luwinga.
Mzuzu 2, Malawi.
ur@mzuni.ac.mw

Dear Sir,

PERMISSION FOR MR. DANIEL KILEMBE TO USE DATA COLLECTED UNDER CONSULTANCY SERVICES FOR ASSESSMENT AND MAPPING OF GROUNDWATER SOURCES FOR LILONGWE CITY FOR HIS MASTER'S DEGREE STUDY

Reference is made to your letter dated 11th September 2020 and recommendation letter by GMS/HydroConsult JV on 26th October 2020, requesting permission to use data collected during *'Consultancy Services for Groundwater Mapping and Assessment for Lilongwe City'*, on your thesis/dissertation, *'Characterization and Hydrogeochemistry of Aquifers Systems in Crystalline Basement of Lilongwe Plain in Linthipe River Basin'*.

Permission to use the data is granted only for the purposes of your study research thesis. Lilongwe Water Board remains the custodian of the data.

Yours faithfully,

Ephraim BANDA

PROJECT IMPLEMENTATION UNIT MANAGER

All correspondence should be addressed to the Chief Executive Officer

Appendix 3: Sampling Points

Sampling Location from Afridev Pumped Borehole

Sample ID	UTMX	UTMY	Point Name	TA
BH1	565359	8435321	Mphudzi Primary School	Masumbankhunda
BH2	552483	8431158	Dambuleni Village	Masumbankhunda
BH3	571108	8422847	Dikisoni Village	Masula
BH4	581359	8424632	Mtande Village	Chiseka
BH5	586224	8434648	Sulumbwa Village	Chadza
BH6	545423	8482395	Kachipinda Village	Khongoni
BH7	546941	8486359	Mtayamatalala Village	Khongoni
BH8	548212	8490429	Mpaka Village	Khongoni
BH9	543956	8485276	Kamange Primary School	Khongoni
BH10	542971	8479007	Mswati Village	Khongoni
BH11	549323	8482119	Kazilele Primary School	Kabudula
BH12	562052	8476211	Kasenza Village	Kabudula
BH13	566458	8469766	Kamanga Village	Kabudula
BH14	573833	8461999	Chaombwa 1 Village	Kabudula
BH15	553950	8485308	Kakhule Village	Kabudula
BH16	554537	8446998	Kalonga Village	Kalolo
BH17	553960	8458401	Kapichila Village	Kalolo
BH18	543239	8455970	Kapanula Primary School	Kalolo
BH19	541758	8450047	Chileka Community Day School	Kalolo
BH20	542216	8442837	Nyamtalika Village	Kalolo
BH21	550021	8448672	Mkomba Village	Kalolo

Sample ID	UTMX	UTMY	Point Name	TA
BH26	558631	8460350	Thumba Village	Kabudula
BH27	573546	8459171	Sankhani Village	Njewa
BH28	577719	8454930	Mudziwapheduka Village	Njewa
BH29	585510	8442968	Chapata Village	Kalumbu
BH30	590825	8435877	Chadza Health Center	Chadza
BH31	597988	8442585	Nathenje Health Center	Chadza
BH32	605508	8438671	Nyaka Village	Kalumbu
BH33	619570	8448662	Chionongera Village	Mazengera
BH34	618307	8455369	Chowo Primary school	Chitekwere
BH35	611107	8454761	Thunde/Sinkha Village	Mazengera
BH36	604189	8455250	Kapichila Village	Mazengera
BH37	597911	8459614	Chimutu Village	Chimutu
BH38	601003	8462189	Kampala Village	Chimutu
BH39	595692	8471913	Nankhonde Primary School	Chimutu
BH40	588803	8474559	Chithumba Village	Chitukula
BH41	591910	8478585	Fusani Village	Mkukula
BH42	585047	8483916	Tovi Village	Mkukula
BH43	582726	8482157	Mononga Village	Mkukula
BH44	579915	8490362	Chakhadza School	Mponela
BH45	600157	8490723	Chiguduli School	Msakambewa
BH46	590788	8486649	Mbalame Village	Mkukula

BH22	574114	8450225	Chaphinja Village	Mbwatalika
BH23	567002	8445910	Kwindanguwo Village	Mbwatalika
BH24	562834	8449984	Kasanja Village	Malili
BH25	563921	8456789	Gome Primary School	Mbwatalika

BH47	585866	8477490	Lumbadzi	Mkukula
BH48	588695	8482795	Airport	Mkukula
BH49	586639	8467980	Magwelo School	Chitukula
BH50	581842	8463257	Area 25 Town	Chitukula

Sampling Location from Deep wells (Exploration Boreholes)

Sample ID	UTMX	UTMY	Elevation	Borehole Depth	Aquifer Host Rock
E1	582392	8437824	1162	90	Biotite Gneiss
E2	585455	8464692	1176	180	Biotite Gneiss
E3	586508	8438985	1105	200	Graphitic Gneiss
E4	591247	8428764	1138	200	Graphitic Gneiss
E5	567970	8468369	1140	200	Biotite Gneiss
E6	588649	8480894	1121	200	Biotite Gneiss
E7	548925	8487982	1176	262	Biotite Gneiss
E8	583648	8418870	1210	185	Biotite Gneiss
E9	573786	8480461	1219	200	Granite
E10	552431	8427961	1165	250	Graphitic Gneiss
E11	552431	8427961	1165	195	Amphibolite
E12	551036	8431845	1188	200	Amphibolite
E13	566202	8460155	1130	200	Granite
E14	582225	8437824	1126	195	Amphibolite
E15	554284	8450227	1176	200	Granite
E16	581196	8437828	1081	245	Biotite Gneiss
E17	564226	8454148	1144	200	Granite
E18	568303	8455562	1124	299	Biotite Gneiss
E19	541844	8452726	1149	200	Biotite Gneiss
E20	588584	8428313	1161	200	Graphitic Gneiss
E21	573593	8472233	1156	200	Granite

Appendix 4: Calibration Curves

Calibration Curve (10ml Standard Solution)

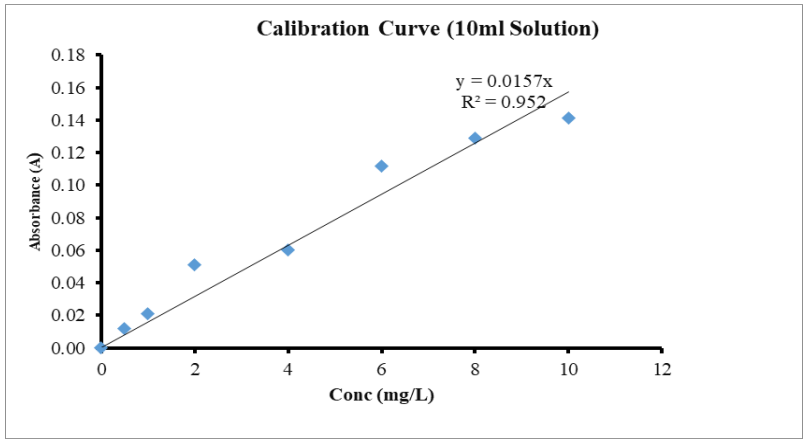

Calibration Curve (15ml Standard Solution)

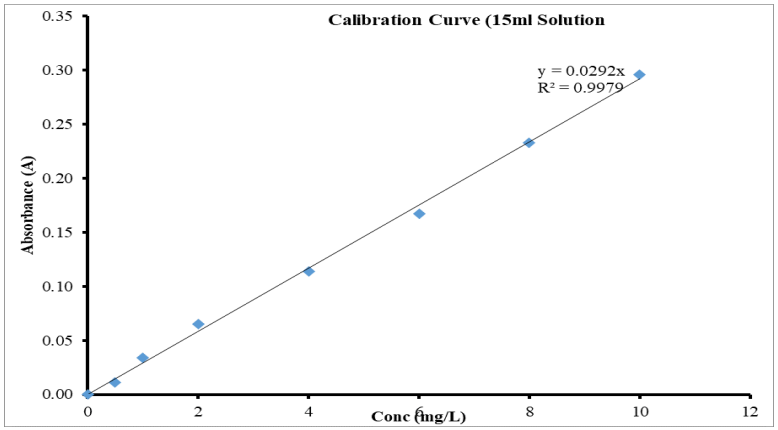

Calibration Curve (20ml Standard Solution)

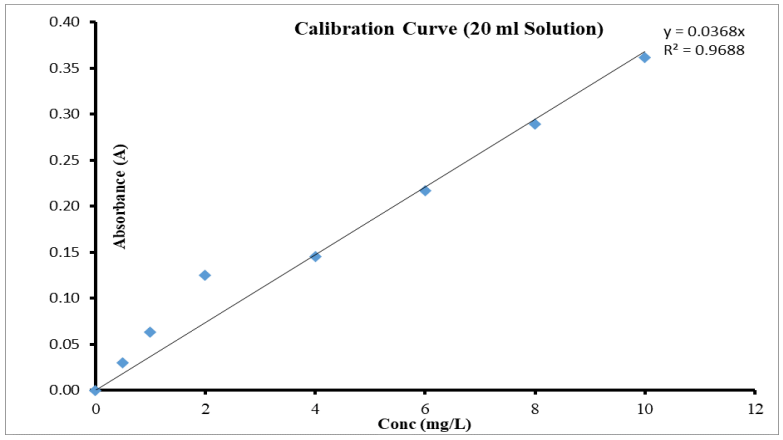

Calibration Curve (Manual Standard Solution)

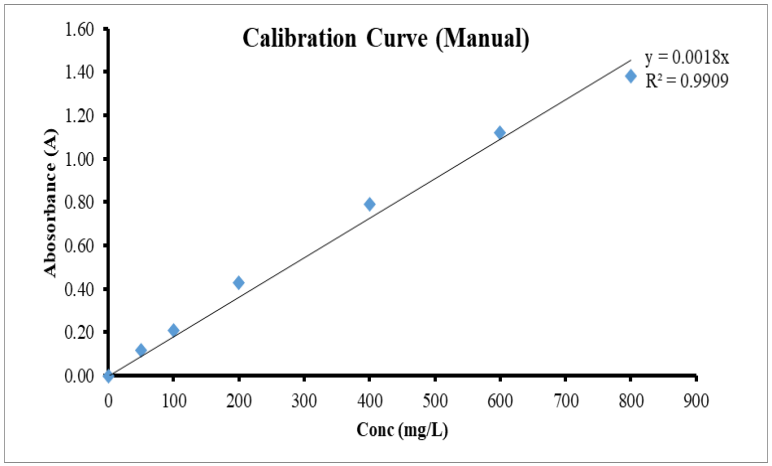

Appendix 5: Table 3. 4: Formula's for calculating irrigation water indices (Base on FAO 1994 Irrigation Water Quality Index)

Irrigation Water Index	Formula	Reference(s)
Sodium Absorption Ratio (SAR	$SAR = \frac{Na^+}{\sqrt{\frac{(Ca^{2+}+Mg^{2+})}{2}}}$ where Na^+, Ca^{2+} and Mg^{2+} are in meq/l.	(Kaur et al. 2016)
Permeability Index (PI)	$PI = \left[\frac{Na^+ + \sqrt{HCO_3^-}}{Ca^{2+} + Mg^{2+} + Na^+}\right] \times 100$	(Narsimha et al.2013)
Sodium Percentage (%Na)	$\%Na = \left[\frac{Na^+}{Ca^{2+}+Mg^{2+}+Na^+ +K^+}\right] \times 100$ ():	(Narsimha et al. 2013)
Residual sodium carbonate (RSC)	$RSC = \left[\left(HCO_3^- + CO_3^{2-}\right) - \left(Ca^{2+} + Mg^{2+}\right)\right]$	(Narsimha et al. 2013)
Magnesium Hazard (MH) or Magnesium Adsorption Ratio (MAR)	$MAR = \left[\frac{Mg^{2+}}{Ca^{2+} + Mg^{2+}}\right] \times 100$	(Narsimha et al. (2013)
Kelly Ratio	$KR = \frac{Na^+}{Ca^{2+} + Mg^{2+}}$	(Rawat et al.2018)
Corrosivity Ratio (CR)	$CR = \frac{\left(\frac{Cl^-}{35.5} + 2\left(\frac{SO_4^{2-}}{96}\right)\right)}{\left(2\left(\frac{HCO_3^- + CO_3^{2-}}{100}\right)\right)}$	(Kaur et al.2016)
Total Hardness (TH)	$TH = 2.5 \times Ca^{2+} + 4.1 \times Mg^{2+}$	(Rawat et al.2018)

Note: All the ion concentrations in SAR, RSC and Kelly Ratio are expressed in meq/l

Appendix 6: Aquifer Parameters from Deep wells

Easting	Northing	Elevation(m)	Depth	First Significant Water Strike(m)	Yield at water strike(l/s)	SWL(m)	Final Yield(l/s)	Confinement(m)	Aquifer Type
554284	8450227	1176	200	21	0.05	5	7.2	16	Fractured Biotite Gneiss
582225	8437824	1126	200	26	0.21	25	0.2	1	Weathered Pegmatite
564226	8454148	1144	200	25	0.011	24	0.5	1	Fractured Granite
581189	8437858	1081	245	155	10.2	6	15	149	Fractured Biotite Gneiss
568303	8455562	1124	299	34	0.001	10	2.5	24	Fractured Biotite Gneiss
583648	8464692	1176	185	15	0.08	12	1.25	3	Fractured Biotite Gneiss
586508	8438985	1105	200	15	0.8	8	1.8	7	Fractured Graphitic Gneiss
591247	8428764	1138	200	25	0.206	20	0.4	1	Fractured Biotite Gneiss
567970	8468369	1140	200	28	0.52	7	10	21	Fractured Biotite Gneiss
588649	8480894	1121	200	48	0.003	22	1.2	26	Fractured Biotite Gneiss
548925	8487982	1176	262	60	2.6	5	3.5	55	Weathered Biotite Gneiss
586508	8438985	1210	185	25	0.46	12	2.5	13	Fractured Biotite Gneiss
573786	8480461	1219	200	33	0.328	20	7.2	13	Fractured Granite
594395	8465981	1186	200	50	0.01	22	0.01	28	Fractured Biotite Gneiss
552431	8427961	1165	250	34	0.008	15	1.1	19	Fractured Biotite Gneiss
566202	8460155	1130	200	30	1	8	23	22	Weathered Biotite Gneiss
551036	8431845	1188	200	82	0.1	15	0.1	67	Fractured Amphibolite
588584	8428313	1161	200	37	0.82	13	1.8	24	Fractured Graphitic Gneiss
573593	8472233	1156	200	26	0.001	10	4	16	Fractured Biotite Gneiss
541844	8452726	1149	200	16	1	11	1	5	Weathered Biotite Gneiss

Appendix 7: Results of Water Quality Indices within the study Area

Parameters	Range	Classification	Results	Percentage
SAR (mg/l)	<10	Excellent	E1, E2, E3, E4, E5, E6, E7, E8, E9, E10, E11, E12, E13, E14, E15, E16, E17, E18, E19, E20, E21	100%
	10–18	Good	None or zero	0
	18–26	Doubtful	None or zero	0
	>26	Unsuitable	None or zero	0
PI	>75%	Good and suitable for Irrigation	E1, E5, E6, E7, E8, E11, E12, E14, E15, E16, E17, E18, E19	62%
	25-75%	Good and suitable for Irrigation	E2, E3, E4, E9, E10, E13, E20, E21	38%
	<25%	Unsuitable for Irrigation	None or zero	0
RSC (meq/l)	< 5	Safe	E1, E2, E3, E4, E5, E6, E7, E8, E9, E10, E11, E12, E13, E14, E15, E16, E17, E18, E19, E20, E21	100%
	5–10	Marginal	None or zero	0
	>10	Unsatisfactory	None or zero	0
Na%(mg/l)	<20	Excellent	E3, E4, E5, E6, E9, E10, E11, E12, E13, E14, E16, E17, E18, E19, E20, E21	76%
	20–40	Good	E1, E2, E7, E8, E15	24%
	40–80	fair/permissible	None or zero	0
	>80	Poor	None or zero	0
KR	< 1	Suitable	E1, E2, E3, E4, E5, E6, E7, E8, E9, E10, E11, E12, E13,	100%

			E14, E15, E16, E17, E18, E19, E20, E21	
	>1	Excess level	None or zero	
MAR (mg/l)	< 50	Excellent	E1, E2, E3, E4, E5, E6, E7, E8, E9, E10, E11, E12, E13, E14, E15, E16, E17, E18, E19, E20, E21	100%
	>50	Harmful for soil	None or zero	0
TDS (mg/l)	0–1000	Freshwater	E1, E2, E3, E4, E5, E6, E7, E8, E9, E10, E11, E12, E13, E14, E15, E16, E17, E18, E19, E20, E21	100%
TH (mg/l)	0–75	Soft	E1, E2, E3, E4, E5, E6, E7, E8, E9, E10, E11, E12, E13, E14, E15, E16, E17, E18, E19, E20, E21	100%
	75–150	Moderately hard	None or zero	0
	150–300	Hard	None or zero	0